

**Modelling the nitrogen and phosphorus leaching to
groundwater and surface water with ANIMO 3.5**

**P. Groenendijk
J.G. Kroes**

20 JUL 2000

Report 144

Winand Staring Centre, Wageningen (The Netherlands), 1999

978105

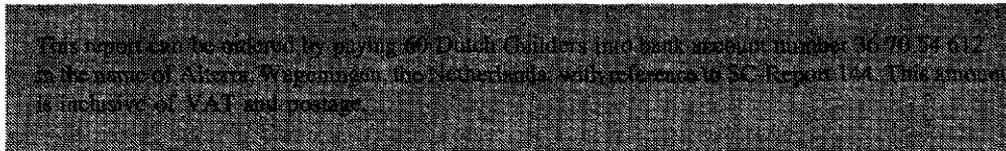
ABSTRACT

P. Groenendijk and J.G. Kroes, 1999. *Modelling the nitrogen and phosphorus leaching to groundwater and surface water with ANIMO 3.5*. Wageningen (The Netherlands), Winand Staring Centre. Report 144. 138 pp.; 50 Figs; 13 Tables; 77 Refs.

The fertilization reduction policy intended to pursue environmental objects and regional watermanagement strategies to raise groundwater levels justify a thorough evaluation of the effectivity of measures and reconnaissance of adverse impacts. A concise description is presented of the model formulations as has been implemented in version 3.5 of the ANIMO model. The model aims at the evaluation and prediction of nutrient leaching to ground water and surface water systems under the influence of fertilization, soil properties, soil tillage, cropping pattern and hydrological conditions. Some model validations at field scale are discussed briefly and three examples of recent regional model applications are presented.

Keywords: environmental protection, groundwater pollution, nutrient leaching, simulation model, surface water pollution

ISSN 0927-4537



©1999 Winand Staring Centre for Integrated Land, Soil and Water Research
P.O. Box 125, NL-6700 AC Wageningen (The Netherlands)
Phone: 31 (317) 474200; fax: 31 (317) 424812; e-mail: postkamer@sc.dlo.nl

No part of this publication may be reproduced or published in any form or by any means, or stored in a data base or retrieval system, without the written permission of the Winand Staring Centre.

The Winand Staring Centre assumes no liability for any losses resulting from the use of this report.
Project 81060 [rep144.pdf /Gro/12-1999]

Contents

	page
Preface	9
Summary	11
1 INTRODUCTION	13
2 PROCESS FORMULATIONS	15
2.1 Hydrological schematization for local and regional applications	15
2.1.1 System definition	15
2.1.2 A regional approach for lateral flow towards surface-waters	16
2.1.2.1 Lower boundary	16
2.1.2.2 Lateral boundary fluxes in a single drainage system	17
2.1.2.3 Lateral boundary fluxes in a multiple drainage system	20
2.1.3 Upper soil storage and surface runoff	24
2.2 Mass conservation and transport equation (CTE)	26
2.2.1 General equations	26
2.2.2 Relations between CTE's of dissolved substances	27
2.2.3 Numerical approach	29
2.2.4 Numerical analysis	33
2.3 Organic cycle	36
2.3.1 Additions to the soil system	39
2.3.2 Transformations	40
2.3.3 Transport of organic substances	42
2.4 Nitrogen cycle	43
2.4.1 Ammonium sorption	43
2.4.2 Fertilization, volatilization and tillage	45
2.4.3 Crop uptake	46
2.4.4 Mineralization and immobilization	56
2.4.5 Nitrification and denitrification	57
2.4.6 Transport of nitrogen substances	58
2.5 Phosphorus cycle	59
2.5.1 Phosphate sorption and precipitation	59
2.5.2 Fertilization and tillage	64
2.5.3 Crop uptake	65
2.5.4 Mineralization and immobilization	68
2.5.5 Transport of phosphorous substances	68
2.6 Environmental influences on transformation rates	68
2.6.1 Aeration	69
2.6.2 Temperature	76
2.6.3 pH	77
2.6.4 Soil moisture content	78
2.7 Initial conditions	78
2.7.1 Soil organic matter	78
2.7.2 Root residues and produced dry matter	79

2.7.3 Nitrogen	79
2.7.4 Phosphorus	80
2.8 Boundary conditions	81
3 CONCISE PROGRAMME DESCRIPTION	83
3.1 General data flow	83
3.2 Model structure	84
3.3 Inputs and outputs	85
4 VALIDATION AT FIELD SCALE	89
4.1 Introduction	89
4.2 Forage maize and catch crops on a sandy soil	91
4.2.1 Introduction	91
4.2.2 Method	91
4.2.3 Results	92
4.3 Non-grazed grassland on a sandy soil	94
4.3.1 Introduction	94
4.3.2 Method	95
4.3.3 Results	95
4.4 Winter wheat on silty loam soil	97
4.4.1 Introduction	97
4.4.2 Method	97
4.4.3 Results	98
4.5 Grazed grassland on clay soil	100
4.5.1 Introduction	100
4.5.2 Method	101
4.5.2 Results	101
4.6 Phosphorus leaching from grassland on a sandy soil	102
4.6.1 Introduction	102
4.6.2 Method	103
4.6.3 Results	103
4.7 Flower bulb soils	105
4.7.1 Introduction	105
4.7.2 Method	105
4.7.3 Results	107
5 REGIONAL MODEL APPLICATIONS	109
5.1 Introduction	109
5.2 Leaching of nitrogen and phosphorus from rural areas to surface waters in The Netherlands	110
5.2.1 Introduction	110
5.2.2 Methodology	111
5.2.3 Results	112
5.3 Simulation of phosphate leaching in catchments with phosphate saturated soils	117
5.3.1 Introduction	117
5.3.2 Methodology	117
5.3.3 Results	117

5.4 Beerze Reusel catchment	119
5.4.1 Introduction	119
5.4.2 Methodology	119
5.4.3 Results	121
References	125
Annexes	
1 List of symbols	132
2 The coefficients $\xi_1(t)$ and $\xi_2(t)$, $\zeta_1(t)$ and $\zeta_2(t)$ in the equations to compute the resulting and the average concentration (Par. 2.2.3)	137

Preface

This report gives an account of the ANIMO model version 3.5. Earlier versions of this model were developed since 1985 and were reported in internal notes of the DLO Winand Staring Centre only. The main part of this report comprises a brief description of the model formulations, some field validations and some regional applications. Currently, the ANIMO model serves as one of the parent models for the development of the Dutch consensus leaching model STONE. STONE is regarded as the consensus nutrient emission model for all governmental departments involved in environmental policy making (National institute for health and the environment; Institute for Inland water management and waste water treatment; Agricultural Research Department) and will operate at a national and regional scale for global problems. For field scale studies and for specific regional environmental problems however, the ANIMO model will still be available in future.

DLO research programme 317 'Nutrient dynamics and management' takes the responsibility for the maintenance of the model and software implementation. For questions about the model formulations the reader is referred to the main author (p.groenendijk@alterra.wag-ur.nl). Information on the programme code is obtainable by contacting ing. J. Roelsma (j.roelsma@alterra.wag-ur.nl).

Summary

The ANIMO model aims to quantify the relation between fertilization level, soil management and the leaching of nutrients to groundwater and surface water systems for a wide range of soil types and different hydrological conditions. The model is a functional model incorporating simplified formulations of processes. The organic matter cycle plays an important role for quantifying the long term effects of land use changes and fertilization strategies. Attention has been paid to describe the most relevant processes governing the organic cycle.

A concise description of the process formulations implemented in version 3.5 of the ANIMO model is given. These include:

- Addition of organic materials and nutrients to the soil system by fertilization, root residues and harvest losses and the redistribution of these materials by tillage.
- Accumulation and decomposition of soil organic matter in relation to the quality and composition of different organic materials.
- Crop uptake of nitrogen and phosphorus in relation to the nutrient status of arable crops and grassland. Dry matter production of grassland is simulated by a dynamic sub-model.
- Sorption of ammonium and non-linear time-dependent sorption of phosphate to the solid soil phase.
- Nitrification and denitrification as a function of the oxygen demand of transformation processes and the diffusive properties of the soil.
- Volatilization of ammonium and atmospheric supply by dry and wet deposition.
- Influence of environmental factors (pH, temperature, aeration and drought condition) on the transformation rates.
- Leaching of different nitrogen and phosphorus species: ammonium, nitrate, dissolved organic nitrogen, mineral phosphate and dissolved organic phosphorus.

The model generates material balances as well as time series of all relevant state variables for a user defined number of soil layers and a user defined time interval.

The performance of the model with respect to nitrate leaching, phosphate leaching and crop uptake has been validated for a number of field plots. Field validations of the nitrogen related model outputs are presented in this report for:

- plots with forage maize and nitrogen catch crops on a sandy soil;
- a non-grazed grassland plot on a sandy soil;
- a winter wheat plot on an silty loam soil;
- a grazed grassland plot on a clay soil.

Field validations of phosphorus leaching have been conducted at:

- a phosphate saturated grassland plot on a wet sandy soil;
- a phosphate saturated flower bulb plot on a calcareous weakly humous sandy soil.

It has been concluded that the model performance is acceptable, but some processes requires further study and other sources of validation data (e.g. nutrient uptake by arable crops, influence of preferential flow on water fluxes and solute migration, assessment of initial phosphate distribution).

The model has been applied at regional scale in a number of research projects aiming to analyse the effects of different scenarios of fertilizer management on nitrogen and phosphorus leaching. The impacts of a prohibition of groundwater withdrawal for sprinkling of grassland and the regional environmental impacts of waterconservation management leading to swamp conditions in future nature areas on the nutrient discharges to groundwater and surface water have been analyzed in the Beerze Reusel catchment in the Southern part of The Netherlands. A complete stop of sprinkling, whilst equal fertilization doses are applied, will lead to an increase of the average nitrate concentration in groundwater in areas characterized by a relative high sprinkling requirement. The raise of water tables due to the nature oriented water management will lead to a considerable increase of P-discharge in the future nature areas.

In the framework of National Policy Documents on Water Management, the model was applied to estimate the effects of fertilizer reduction on the nutrient leaching from rural areas into regional surface water. The fertilization scenario aiming at a balance between nutrient application, crop uptake and acceptable environmental losses resulted to a long term reduction with respect to the nitrogen load on surface waters reduction of about 50% relative to the leaching to be expected for the continuation of the 1993-fertilizer applications. For the assumed fertilization doses which aim at a balance between fertilization and crop uptake, no reduction of phosphate leaching is expected. The model has also been used in regional research projects studying the relation between the phosphate saturation degree of sandy soils and phosphate surpluses on the load on surface water systems (Central and Southern sand district). For the scenario assuming a $40 \text{ kg ha}^{-1} \text{ a}^{-1}$ P-surplus, the long term load on surface waters increased in time, whereas for the $10 \text{ kg ha}^{-1} \text{ a}^{-1}$ P-surplus scenario no further increase is expected after 20 years. A tentative assessment was made of the effects of a chemical treatment of strongly P-saturated soils to reduce the phosphate leaching. It was concluded that in case of a larger P-surplus ($40 \text{ kg ha}^{-1} \text{ a}^{-1}$), the positive effects of chemical treatment are diminished by an increased P leaching from other soils.

Although the data acquisition requires considerable efforts and required skills to apply the model instrument is high, the model has proven to be a useful tool in scenario analysis and decision making.

1 INTRODUCTION

Management of land and water resources has resulted in an increased need for information on the environmental impacts of fertilization strategies, land use changes and water management policies. Application of animal manure and artificial fertilizers to mineral soils has resulted in an increased leaching of nutrients to groundwater and surface water systems. In many cases the sorption capacity of iron and aluminium minerals has been utilized to fix phosphates to such a degree that leaching of soluble phosphate to surface waters can be expected. Legislation measures to control fertilizer applications are currently considered at regional, national and international levels. Most of the measures are based on rough risk assessments with regard to nitrate leaching. It is not always clear what the short and long term effects of regulative measures will be. There is a need to quantify the sources of nutrients which contaminate groundwater systems and lead to eutrophication of surface waters. Quantification and evaluation of strategies requires various climatic conditions, soil types, water management alternatives, cropping patterns and agricultural technologies.

A thorough understanding of the transfer and transformation principles which lead to contamination and eutrophication requires a comprehensive knowledge of processes governing the changes in the soil-water-plant system. Due to the development of simulation models, the interactions of different processes as influenced by farming strategies and soil and water management can be studied. A simulation model enables the integration of knowledge of different disciplines and the analysis of short and long term impacts of changes in farming strategy, climate and water management on the environment. The aim of the ANIMO model is to derive cause-effect relationships between fertilization rate, cropping pattern and water management and the nutrients losses leaving the agricultural system. The model results act generally as useful guides to support management decisions of soil and water resources.

The first version of the model originates from 1985 (Berghuijs-van Dijk *et al.*, 1985) and did not comprise a phosphate module. During the last few years, special attention has been paid to the formulation of a submodel for transformation processes which influence phosphate mobility and solute concentrations in soils. These processes have been observed to proceed as a series of kinetic reactions. Model analyses have shown that even when the use of manure is reduced to very low levels, it may last more than a number of decades before the release of accumulated phosphate reduces to acceptable levels. Desorption of phosphates, even when far-reaching measures are implemented, may cause an exceedance of water quality standards for long periods.

The ANIMO model is a software package developed by the DLO-Winand Staring Centre. It aims to be used for field and regional assessments with respect to groundwater and surface water pollution by soluble nitrogen and phosphorus species, originating from soil with agricultural land use. The model has been tested and the overall performance has been validated for a number of field plots. A sensitivity analysis of the model parameters and a tentative uncertainty analysis have been carried out by Groenenberg *et al.*, (1999).

In the future, the model will be used as a parent model to derive simplified versions in the framework of the national consensus model for all governmental departments involved in environmental policy making.

The underlying report aims to give an account of the process descriptions implemented in the animo model provides a description of the processes formulated in the ANIMO and to give some insight in the capabilities and the performance of the model. Chapter two provides a brief description of the present version (3.5), as it has been used in the national Water Reconnaissance Survey in 1995/1996 (Boers *et al.*, 1997). A more detailed description of the formulations, backgrounds of the theories and ideas for future developments can be found in Rijtema *et al.*, (1999). Chapter three summarizes how to use the model and chapter four provides a short description of model validations at field scale. Chapter five gives some recent model applications at regional scale.

For user guidelines and modellers instructions, the reader is referred to Kroes and Roelsma (1998). More detailed information on the results of different research projects for which the model was used can be found in a number of reports and publications (Drent *et al.*, 1988; Kroes *et al.*, 1990; Van der Bolt *et al.*, 1990; Hendriks *et al.*, 1994; Schoumans and Kruijne, 1995; Hack-ten Broeke and Dijkstra, 1995; Van der Bolt *et al.*, 1996b; Groenendijk and Van der Bolt, 1996; Kroes *et al.*, 1996; Kruijne *et al.*, 1996; Boers *et al.*, 1997).

2 PROCESS FORMULATIONS

2.1 Hydrological schematization for local and regional applications

2.1.1 System definition

Water discharge to groundwater and surface water is schematized by a pseudo-two dimensional flow in a vertical soil column with unit surface. This soil column is schematized into a number of model compartments thicknesses related to the physical dispersion which can be expected. The boundary at the top of this column is the soil surface. The bottom boundary can be located in the unsaturated or in the saturated zone of the soil. The lateral boundary may be formed by one or more drainage systems. The position of the bottom and the lateral boundaries depends on the scale and type of the application.

Hydrological data (e.g. water fluxes and moisture contents of the distinct soil layers) are supplied by an external field plot model (SWAP; Van Dam *et al.*, 1997) or regional groundwater flow model (SIMGRO; Querner and Van Bakel, 1989). The vertical schematization resulting from the spatial discretization as applied in the water quantity model forms part of the input of the model (Fig. 1).

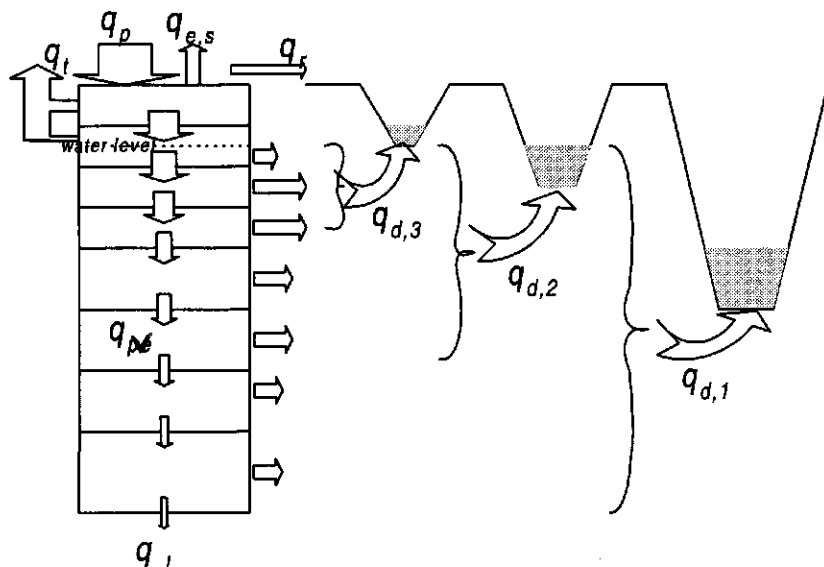


Fig. 1 Definition of a soil profile and the main terms of the water balance (q is a water flux in $m^3 m^{-2} d^{-1}$; q_p is precipitation, q_t is transpiration, $q_{e,s}$ is soil evaporation, q_s is surface runoff, q_v is vertical percolation, q_l is leaching, $q_{d,1}$, $q_{d,2}$, $q_{d,3}$ is drainage to first, second and third order drainage system)

A water quantity model (e.g. SWAP) should simulate all relevant terms of the water balance. Such a complete water balance for a soil-water-crop system can be formulated

as:

$$\frac{\Delta V}{\Delta t} = q_p + q_s - q_{e,s} - q_{e,p} - q_{e,i} - q_t - q_r - q_l - q_{d,1} - q_{d,2} - q_{d,3} \quad (1)$$

where:

ΔV :	change in areic water volume during a time step ($\text{m}^3 \text{m}^{-2}$)
Δt :	time increment (d)
q_p :	precipitation flux ($\text{m}^3 \text{m}^{-2} \text{d}^{-1}$)
q_s :	seepage flux ($\text{m}^3 \text{m}^{-2} \text{d}^{-1}$)
$q_{e,s}$:	soil evaporation flux ($\text{m}^3 \text{m}^{-2} \text{d}^{-1}$)
$q_{e,p}$:	ponding evaporation flux ($\text{m}^3 \text{m}^{-2} \text{d}^{-1}$)
$q_{e,i}$:	interception evaporation flux ($\text{m}^3 \text{m}^{-2} \text{d}^{-1}$)
q_t :	transpiration flux ($\text{m}^3 \text{m}^{-2} \text{d}^{-1}$)
q_r :	surface runoff ($\text{m}^3 \text{m}^{-2} \text{d}^{-1}$)
q_l :	leaching across the bottom boundary flux ($\text{m}^3 \text{m}^{-2} \text{d}^{-1}$)
$q_{d,1} \ q_{d,2} \ q_{d,3}$:	drainage flux to 1 st , 2 nd and 3 rd order drainage systems ($\text{m}^3 \text{m}^{-2} \text{d}^{-1}$)

The nett incoming flux across the top boundary results from the precipitation minus the interception and evaporation from the bare soil and the ponding layer, and minus the surface runoff. The nett incoming flux across the lateral boundary of the profile results as the difference between infiltration from and drainage towards surface-water system(s). The nett incoming flux across the lower boundary results from the difference in seepage from and leaching towards deeper soil layers below the profile. Some models for water transport in the unsaturated and saturated zone have options to simulate water fluxes to/from surface-water systems. In many water quantity models this is not taken into account and therefore the model ANIMO has an option to simulate water flow to/from surface-water systems. This option is based on a regional approach for the surface-water system(s) which will be discussed in the next paragraph.

2.1.2 A regional approach for lateral flow towards surface-waters

For solute transport it is essential to take the discharge to drainage systems into account since it reduces the load on groundwater systems and it may contribute considerably to the solute balance of a soil system. The residence time of soil water is strongly influenced by the spacing and the basis of the drainage systems.

2.1.2.1 Lower boundary

Groundwater flow can be divided into a local and a regional flow (Fig. 2). The regional flow is not important for the transport of substances from the soil surface to a neighbouring surface-water system. The local flow however is the essential transport route towards the surface-water system. To catch this local flow the position of the model profile should be such that it accounts for most of the streamlines discharging to the surface water. In the ANIMO model this is achieved by a rule of thumb stating the maximum depth of the local flow should be less than 1/4 of the

drain distance. If for example the distance between ditches is 20 m; the position of the lower boundary should be at 5 m below the soil surface. Then, the model profile will cover more than 85% of the local flow.

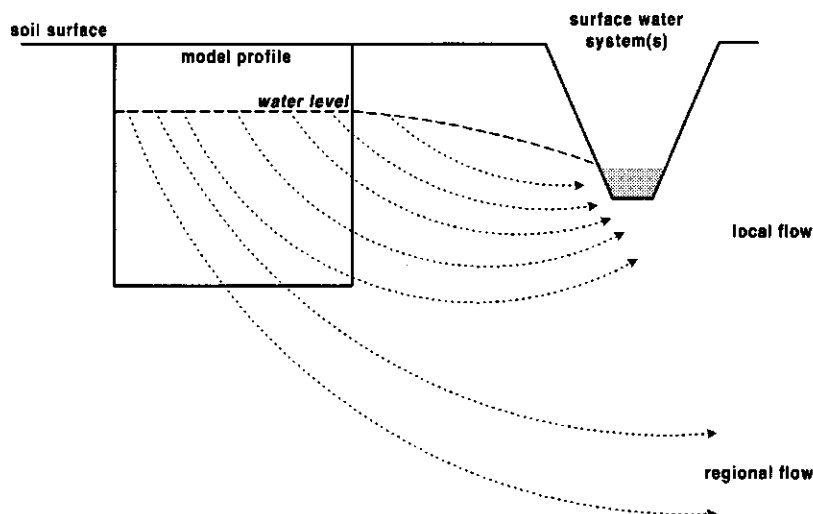


Fig. 2 Schematization of local and regional groundwater flow and the position of a 1-dimensional model profile to simulate lateral flow to surface-water system(s)

Once the regional and local flow have been segregated by the position of the lower boundary, the lateral boundary can be used to simulate discharge to drainage systems. Given water discharges and drain distances are used to simulate residence times of water and solute in the saturated part of the soil profile.

2.1.2.2 Lateral boundary fluxes in a single drainage system

In humid climates like The Netherlands, with relatively low rainfall intensities stretched out over long periods, most drainage problems can be solved by using approaches valid for steady state flow between parallel drains with equal distance, size and drainage level. A general equation to quantify a drainage flux in such a situation is:

$$q_d = \frac{h - h_d}{\Upsilon_d} \quad (2)$$

where:

- q_d : drainage flux ($\text{m}^3 \text{m}^{-2} \text{d}^{-1}$)
- Υ_d : drainage resistance of an open field drain or a tile drainage system (d)
- h_d : drainage level (m)
- h : phreatic groundwater level (m)

With the assumption that the given drainage flux q_d is determined by the precipitation excess, it will now be explained how this drainage flux can be appointed to the lateral boundary of a one dimensional model profile.

In a homogenous layer of constant thickness where radial flow in the surroundings of the drains can be neglected, drainage water flow can be described with a stream function (Fig. 3). For a two-dimensional transect between parallel perfect drains the stream function can be given as a function of depth and distance (Ernst, 1973):

$$\Psi(x,z) = -\frac{q_{net}}{H}x(H-z) \quad (3)$$

where:

- $\Psi(x,z)$: stream function as a function of depth z and distance x ($\text{m}^3 \text{m}^{-1} \text{d}^{-1}$)
- q_{net} : precipitation excess ($\text{m}^3 \text{m}^{-2} \text{d}^{-1}$)
- z : depth below the soil surface (m)
- x : distance relative to the water divide between 2 drains (m)
- H : thickness of aquifer (m)

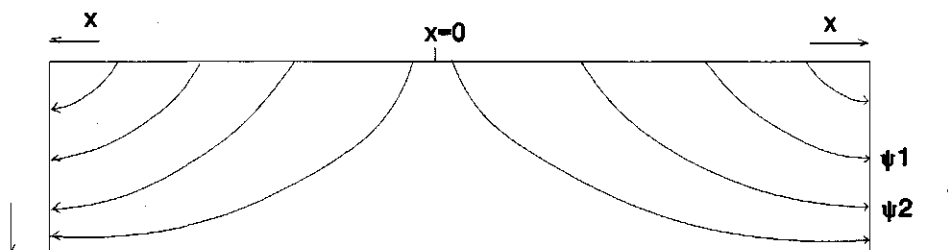


Fig. 3 Streamlines as calculated from the streamfunction ψ (after Ernst, 1973)

The vertical water fluxes q_z and the horizontal flux q_x are obtained by taking partial derivatives of the streamfunction Ψ . For q_z holds:

$$q_z = \Psi_x(x,z) = -\frac{\partial \Psi}{\partial x}(x,z) = \frac{q_{net}}{H}(H-z) \quad (4)$$

The horizontal flux q_x is given by:

$$q_x = \Psi_z(x,z) = -\frac{\partial \Psi}{\partial z}(x,z) = \frac{q_{net}}{H}x \quad (5)$$

In the vertical column representing the soil system, the drainage rate k_d ($\text{m}^3 \text{m}^{-3} \text{d}^{-1}$) is defined as the derivate of the vertical flux to z :

$$k_d = - \frac{dq_z}{dz} \quad (6)$$

From the continuity equation it follows that the drainage rate is also related to the gradient of the horizontal flux:

$$k_d = \frac{dq_x}{dx} = \frac{q_{net}}{H} \quad (7)$$

This formulation is introduced in the general mass balance equation by means of the sink term R_x (paragraph 2.8).

The vertical flux q_z in the one-dimensional model system can be formulated as a linear relation with depth according to:

$$q_z = q_d \left(1 - \frac{z}{H}\right) \quad (8)$$

By means of the approach given above for saturated flow towards drainage systems a pseudo two-dimensional transport is considered. In the one-dimensional model system the water flux q_d is divided proportional to the thickness of the model compartments between the phreatic groundwater level and the lower boundary of the model profile. The sum of model compartments from which water fluxes to and from a drainage system are simulated is called a 'model discharge layer'. The effect of pseudo two-dimensional transport on the residence time of water particles discharging to a drainage system will be explained by looking at a 'model discharge layer' into more detail. A 'model discharge layer' and its water fluxes in a discharging situation are shown in Figure 4a. For a system with one surface-water system the vertical water flux is given as a linear function with depth (Fig. 4b).

The residence time of water particles in the one-dimensional profile is obtained by integrating the vertical water flux over depth:

$$t_{res} = \int_{z_1}^{z_2} \frac{\varepsilon dz}{q_z} \quad (9)$$

where is t_{res} is the residence time (d) within one simulated time step for water particles moving from depth z_1 (m) to depth z_2 (m), ε is porosity ($m^3 m^{-3}$). A combination of the previous two equations results in the following formulation for the residence time:

$$t_{res} = \frac{\varepsilon H}{q_d} \ln \frac{q_{z2}}{q_{z1}} \quad (10)$$

where:

$q_{z,1}$ and $q_{z,2}$: vertical water fluxes at depths z_1 and z_2 ($\text{m}^3 \text{m}^{-2} \text{d}^{-1}$)

H : thickness of the aquifer (m)

This solution implies that the residence time of the water particles flowing vertically downward increases logarithmic with depth (Fig. 4c). The hydrological model schematization results in a similar expression for the relation between residence time variation and depth in the soil profile as given by Ernst (1973).

Summarizing the following assumptions have been made:

- Dupuit-assumption: pressure head, groundwater level and equivalent thickness of 'model discharge layer', in the horizontal plane, are assumed to be equal;
- symmetric groundwater flow;
- equivalent thickness of 'model discharge layer' should be less than 25% of the distance between the drains. If the equivalent thickness is larger than 25% of the drain distance, than the lower boundary of the 'model discharge layer' is adjusted until this conditions is met.
- radial flow near the drains is neglected.

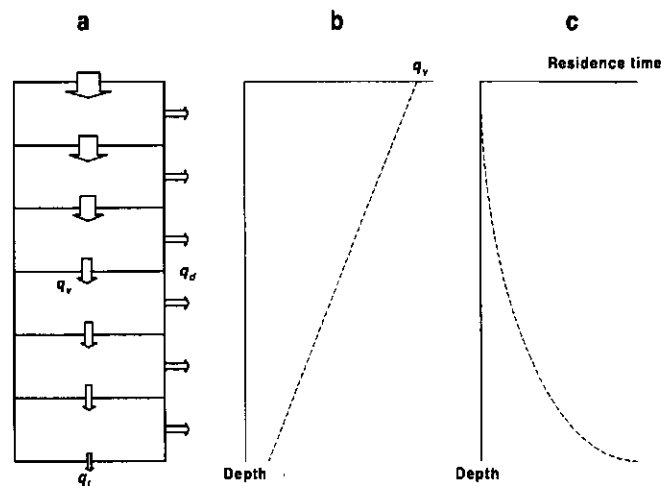


Fig. 4 Model discharge layers and water fluxes in a discharging situation. a) Model discharge layer with vertical flux q_z , leaching flux q_l and drainage flux q_d ; b) Vertical flux q_z as function of depth; c) Residence time as function of depth

2.1.2.3 Lateral boundary fluxes in a multiple drainage system

Regional water discharges generally give a non-linear relation between measured discharges and groundwater tables. This drainage concept is illustrated in Figure 5, depicting a linear reservoir model with outlets at different heights.

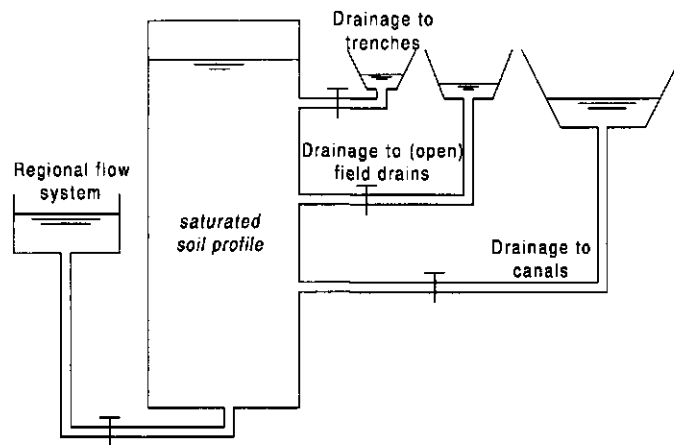


Fig. 5 Schematic representation of the regional drainage concept

The general shape of such a so-called q/h -relation is given in Figure 6a. The relation can be schematized by distinguishing discharges with a low and discharges with a high intensity. High discharge intensities with shallow groundwater tables are mainly caused by shallow drains, such as open field drains and tile drains, with relatively short residence times, whereas low discharge intensities with deep groundwater tables are the result of drainage canals at larger distance, resulting in large residence times.

In the model schematization the q/h -relation is dissected into a number of linear relations (Fig. 6b), each of them representing a certain type of drainage system. From these schematized q/h -relations drainage resistances are derived and used as input for the calculation of the drainage quantities per time step and per surface-water system, as depending on the depth of the groundwater table and the surface-water level. Total regional discharge is calculated by the expression:

$$q_{d,r} = \sum_{i=1}^n q_{d,i} = \sum_{i=1}^n \frac{h - h_{d,i}}{\Upsilon_i} \quad (11)$$

where:

- $q_{d,r}$: regional drainage flux ($\text{m}^3 \text{m}^{-2} \text{d}^{-1}$)
- $q_{d,i}$: water flux flowing to drain of order i ($\text{m}^3 \text{m}^{-2} \text{d}^{-1}$)
- i : order of the drainage system (-)
- n : total number of drain systems present (-)
- Υ_i : drainage resistance of system i (d)
- h : height of the phreatic groundwater level midway between drains (m)
- $h_{d,i}$: height of the water level in drain system i (m)

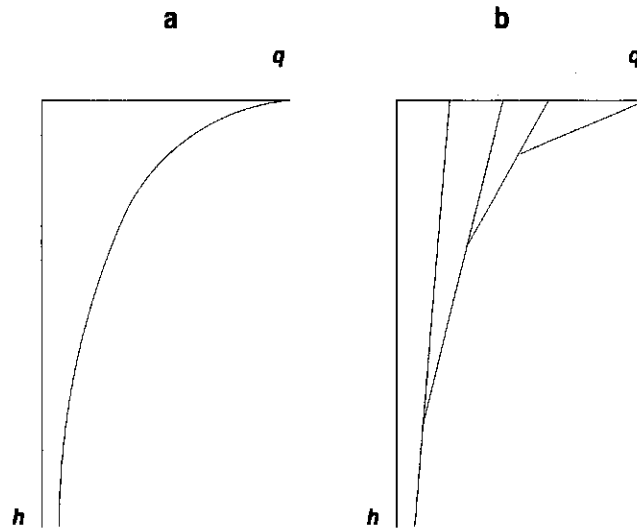


Fig. 6 Relations between groundwater level (h) and regional discharge (q). a) Measured q/h -relation (after: Ernst, 1978); b) Schematized q/h -relation with 4 drainage systems

Drains continuously containing water will have an infiltration function when the phreatic groundwater level is below the water level in the drainage system under consideration. When the phreatic groundwater level falls below the pressure head of the aquifer, leaching conditions are changing into seepage conditions.

In analogy with the situation with only one surface-water or drainage system, so-called 'model discharge layers' are identified from which water is discharged to corresponding drainage systems.

In the current version of the ANIMO model, the differences in residence time of the water particles discharging to the corresponding drainage systems have been taken into account by assuming the thickness of the discharging layers ('model discharge layers') proportional to the drainage discharges towards the corresponding drains, or:

$$(kH)_{i-1} : (kH)_i = L_{i-1} q_{i-1} : L_i q_i \quad (12)$$

where:

- kH_i : the transmissivity of 'model discharge layer' i
- L_i : drain distance (m)
- q_i : drainage flux towards drainage system i ($m^3 m^{-2} d^{-1}$)

The product of L_i and q_i equals the drain discharge flow. It should be noted that according to the superposition principle, drains of a certain order also function as drains of the superposed orders.

The size of the discharging soil layers or 'model discharge layers' can now be estimated, since the sum of the thicknesses of the 'model discharge layers' is determined by groundwater level and lower boundary of the model profile. In most cases, this surface is located at the hydrological base. The depth of the bottom of the second and higher order systems follows from the ratios between the transmissivity of the considered layer and the total transmissivity. The ratios between the transmissivities can be calculated from the proportion between the discharges. In the ANIMO model the ratio between the transmissivities is computed from the proportion between discharges:

$$\frac{(kH)_i}{(kH)_1} = \frac{\sum_{j=i}^n \left(\frac{q_j}{\sum_{k=1}^j \frac{1}{L_k}} \right)}{\sum_{j=1}^n \left(\frac{q_j}{\sum_{k=1}^j \frac{1}{L_k}} \right)} \quad (13)$$

When the proportion between transmissivities has been assessed, the bottom of each layer can be computed. Figure 7 denotes the calculation method for soil profiles with heterogeneous conductivity distribution with depth.

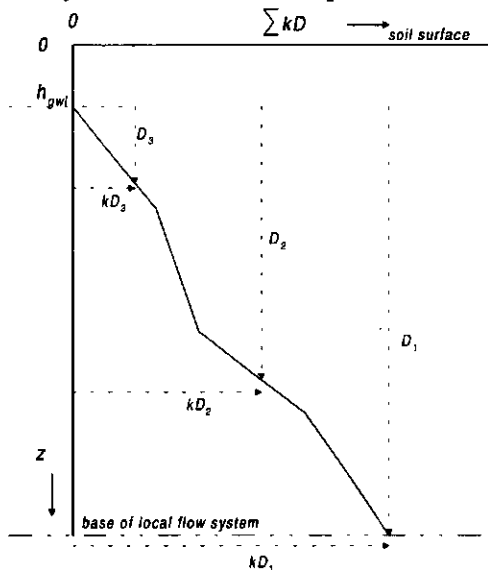


Fig. 7 Bottom of model discharge layers as a function of transmissivities in a heterogeneous soil profile

The depth of the bottom of a certain discharge layer (H_2 , H_3) can be obtained by interpolation in the cumulative kH -relation with depth.

2.1.3 Upper soil storage and surface runoff

Animal manure and fertilizers can be applied to a field plot at any time. Most of the added nutrients will be transported into the soil profile via percolating rain water. It thus depends on the rainfall pattern whether and when the fertilization will be effective for plant roots. To account for this phenomenon, an imaginary storage reservoir has been introduced at the soil surface in which all additions are immediately dissolved. In the model schematization, the solute migration within this reservoir is described as a piston flow. The total quantity of added material in stock will be depleted after a precipitation volume which equals the reservoir volume. The store of materials in this artificial reservoir is evaluated each time interval by means of book keeping. When the front of the piston flow breaks through at the bottom of the reservoir within a certain time interval, the average input concentration to the first soil compartment is calculated as a time weighted average of old and new concentrations in the surface reservoir. The release rate can be manipulated by the choice of an appropriate thickness Z_{surf} of the reservoir. The release fraction within a time increment after a rain shower is calculated according to:

$$\frac{M_{\Delta t}}{M} = \frac{q_p \Delta t}{Z_{surf}} \quad (14)$$

where:

- M : quantity of material added to the surface reservoir (kg m^{-2})
- $M_{\Delta t}$: quantity of material released from the reservoir to the first layer (kg m^{-2})
- Z_{surf} : depth of surface reservoir (m)
- $q_p \Delta t$: cumulative rainfall volume since the addition of material (m)

The remaining store of nutrients not yet released is evaluated each time interval by means of book keeping. The total quantity of manure material in stock will be depleted after a precipitation volume which equals the reservoir volume.

Surface runoff may occur in situations where the precipitation intensity exceeds the infiltration rate of the soil and in situations where the precipitation excess causes the groundwater level to rise above the soil surface. In both cases the overland flow transports solutes to the surface water that originates from one of the three following pathways: direct precipitation, overland flow and interflow.

Diffusion and dispersion of solutes from the soil to the runoff water has been taken into account, by supposing a part of the surface runoff flowing through the first model compartment. This may be of special importance in situations where a substance is added to the top to the soil and the substance will only enter the soil with a precipitation excess that follows the application time. During such events the runoff water may contain high doses of the substance applied.

The runoff solute flux as determined by a hydrological model is subdivided into three fractions. The load on surface water equals the sum of three different fluxes:

$$J_{s,r} = q_r \{ f_0 c_0 + f_1 c_1 + (1 - f_0 - f_1) c_p \} \quad (15)$$

where:

$J_{s,r}$: runoff solute flux ($\text{kg m}^{-2} \text{d}^{-1}$)

q_r : runoff water flux ($\text{m}^3 \text{m}^{-2} \text{d}^{-1}$)

c_o : solute concentration in the upper soil layer (kg m^{-3})

c_l : solute concentration in the surface reservoir (kg m^{-3})

c_p : solute concentration in rain water (kg m^{-3})

f_o : fraction of the runoff that passes the surface reservoir (-)

f_l : fraction of the runoff that passes the first model compartment (-)

The solute transport to surface water systems described by surface runoff sub-model is illustrated in Figure 8.

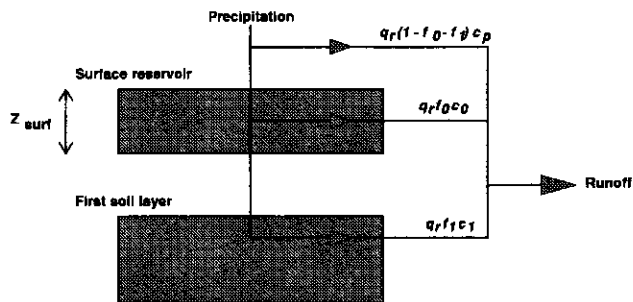


Fig. 8 Schematization of surface water contamination by surface runoff

2.2 Mass conservation and transport equation (CTE)

2.2.1 General equations

A mathematical description of transport processes in a soil system must obey the law of conservation of matter and energy. For a substance in a soil system this law can be written in words:

$$\text{accumulation} = \text{inflow} - \text{outflow} - \text{sinks} - \text{sources} \quad (16)$$

Accumulation is the storage change of a substance and can take place in the liquid phase as well as in the solid phase. Inflow and outflow of a substance occurs as a solute flux across the boundaries of the system. The general formulation of the mass conservation and transport equation reads as follows:

$$\frac{\partial c^*}{\partial t} = - \frac{\partial J_s}{\partial z} + R_p - R_d - R_u - R_x \quad (17)$$

where:

- c^* : mass concentration of a substance in the soil (kg m^{-3})
- J_s : vertical solute flux ($\text{kg m}^{-2} \text{d}^{-1}$)
- R_p : source term for production ($\text{kg m}^{-3} \text{d}^{-1}$)
- R_d : sink term for decomposition ($\text{kg m}^{-3} \text{d}^{-1}$)
- R_u : sink term for crop uptake ($\text{kg m}^{-3} \text{d}^{-1}$)
- R_x : sink term for lateral outflow or infiltration ($\text{kg m}^{-3} \text{d}^{-1}$)

The mass concentration of a substance in a soil system equals the sum of the concentrations present in the liquid phase and in the solid phases:

$$c^* = \theta c + \rho_d X_e + \rho_d X_n + \rho_d X_p \quad (18)$$

where:

- θ : volume moisture fraction ($\text{m}^3 \text{m}^{-3}$)
- c : mass concentration in the liquid phase (kg m^{-3})
- ρ_d : dry bulk density (kg m^{-3})
- X_e : content sorbed to the solid phase in equilibrium with c (kg kg^{-1})
- X_n : content of non-equilibrium sorption phase (kg kg^{-1})
- X_p : content of the substance involved in precipitation reaction (kg kg^{-1})

The solute flux through the soil system is the sum of a convective flux and a flux caused by molecular diffusion and dispersional mixing:

$$J_s = qc - \theta D_{dd} \frac{\partial c}{\partial z} \quad (19)$$

where:

q : vertical water flux ($\text{m}^3 \text{m}^{-2} \text{d}^{-1}$)
 D_{dd} : apparent dispersion coefficient ($\text{m}^2 \text{d}^{-1}$) which is the sum of the coefficients for dispersion and diffusion of a solute in the liquid phase ($D_{dd} = D_{dis} + D_{diff}$).

By combining the continuity equation and the flux density equation a general convection-dispersion equation (CD-equation) is obtained:

$$\frac{\partial(\theta c)}{\partial t} + \rho_d \frac{\partial X_e}{\partial t} + \rho_d \frac{\partial X_n}{\partial t} + \rho_d \frac{\partial X_p}{\partial t} = - \frac{\partial}{\partial z} (qc - \theta D_{dd} \frac{\partial c}{\partial z}) + R_p - R_d - R_u - R_x \quad (20)$$

From this equation the concentration c has to be found. Due to the second order partial differential there are only a few analytical solutions available for a limited set of boundary conditions. Therefore this type of CD-equations is mostly solved by numerical approximation methods such as finite differences. The CD-equation is then rewritten as an equation with differences instead of partial differentials. A numerical solution scheme (explicit/implicit) is used to solve sets of (linear) difference equations. Examples of models that use this approach are LEACHM (Wagenet and Hutson, 1992), DAISY (Hansen *et al.*, 1990), WAVE (Vancllooster *et al.*, 1994). The numerical approximations preferably use a solution scheme which eliminates or minimizes the numerical dispersion and then reintroduce a physical dispersion.

The ANIMO model utilizes a semi-analytical solution of the CD-equation. The semi-analytical approach is well known in modelling point sources of groundwater contamination (Davis and Salama, 1994) and modelling pollutant transport in surface water systems (Todini, 1996).

2.2.2 Relations between CTE's of dissolved substances

The ANIMO-model distinguishes five leaching substances: three soluble nitrogen substances (nitrate-N, ammonium-N, dissolved organic-N) and two soluble phosphorus substances (mineral-P and dissolved organic-P). The concentration of each of these soluble species is solved using the general mass conservation and transport equation (CTE) for each timestep (Table 1 and Table 2).

Table 1 Conservation and transport equations governing the leaching of nitrogen compounds

Substance	Conservation	Vertical transport	Lateral outflow	Crop uptake	Decomposition	Production
Dissolved organic nitrogen:	$\frac{\partial \theta c_{ON}}{\partial t}$	$= -\frac{\partial J_{s,ON}}{\partial z}$	$-R_{x,ON}$		$-R_{d,ON}$	$+R_{p,ON}$
Ammonium:	$\frac{\partial \theta c_{NH4}}{\partial t} + \rho_d \frac{\partial X_{e,NH4}}{\partial t}$	$= -\frac{\partial J_{s,NH4}}{\partial z}$	$-R_{x,NH4}$	$-R_{u,NH4}$	$-R_{d,NH4}$	$+R_{p,NH4}$
Nitrate:	$\frac{\partial \theta c_{NO3}}{\partial t}$	$= -\frac{\partial J_{s,NO3}}{\partial z}$	$-R_{x,NO3}$	$-R_{u,NO3}$	$-R_{d,NO3}$	$+R_{x,NO3}$

Table 2 Conservation and transport equations governing the leaching of phosphorus compounds

Substance	Conservation	Vertical transport	Lateral outflow	Crop uptake	Decomposition	Production
Dissolved organic phosphorus:	$\frac{\partial \theta c_{OP}}{\partial t}$	$= -\frac{\partial J_{s,OP}}{\partial z}$			$-R_{d,OP}$	$+R_{p,OP}$
Dissolved mineral phosphorus:	$\frac{\partial \theta c_{PO4}}{\partial t} + \rho_d \frac{\partial X_{e,PO4}}{\partial t}$ $\rho_d \frac{\partial X_{n,PO4}}{\partial t} + \rho_d \frac{\partial X_{p,PO4}}{\partial t}$	$= -\frac{\partial J_{s,PO4}}{\partial z}$	$-R_{x,PO4}$	$-R_{u,PO4}$	$-R_{d,PO4}$	$+R_{p,PO4}$

Since many of the processes of the carbon, nitrogen and phosphorus cycle are interrelated it is important to use an appropriate computation scheme. The calculation sequence to solve the CTE within each timestep for all soluble substances is indicated in Figure 9. From this figure it can be seen that each solution of the CTE implies leaching of a soluble substance.

The CTE is first solved for the dissolved organic substances. Decomposition of organic matter results in mineralization of ammonium (Fig.9, left). The decomposition of ammonium resulting from the next solution of the CTE is caused by nitrification and produces nitrate. Solving the CTE for nitrate results in denitrification and the production of the nitrogen gas N_2 . For phosphorus (Fig. 9, right) the sequence is

analogous: firstly computing of organic-P rates, and secondly simulation of conservation and transport of the mineral -P components.

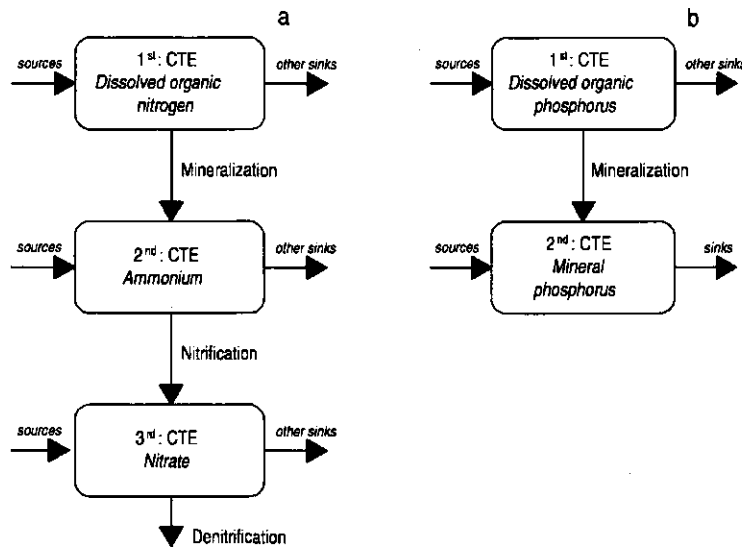


Fig. 9 Calculation sequence to solve the CTE of the dissolved nitrogen (a) and phosphorus (b) substances.

2.2.3 Numerical approach

Water balance

The spatial differential terms in Eq. 20 are developed as finite increments. The soil layers with thickness Δz are assumed to exhibit a uniform substance concentration within the layer and to be perfectly mixed over the entire thickness. The incoming flux $q_{i-1/2}$, the outgoing flux $q_{i+1/2}$ and the lateral transpiration flux q_{tr} are calculated from a water balance model. The transpiration flux q_{tr} has been related to the transpiration rate u_{tr} (d^{-1}) as follows:

$$q_{tr} = \int_z^{z+\Delta z} u_{tr} dz \quad (21)$$

A schematization of the fluxes has been depicted in Figure 10.

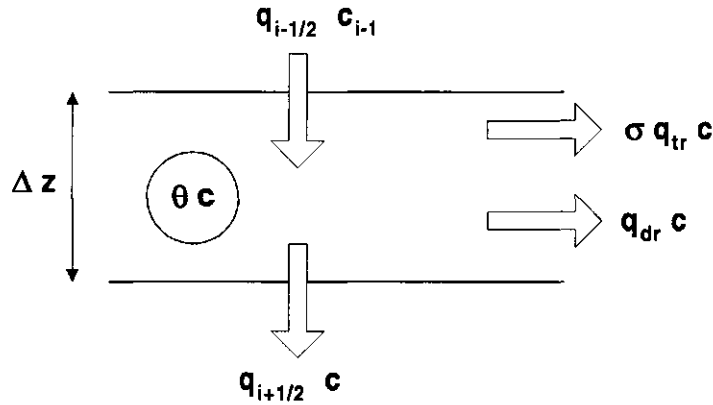


Fig. 10 Schematization of water and solute flows ($q_{i-1/2}c_{i-1}$ = inflow; $q_{i+1/2}c$ = outflow; $\sigma q_{tr}c$ = plant uptake; $q_{dr}c$ = outflow to drains; θc = dissolved amount) in a perfectly mixed soil layer

The concentration in the inflowing water is defined as c_{i-1} , so the chemical's influx is calculated as $q_{i-1/2} c_{i-1}$. The solute outflux consist of the plant uptake stream $\sigma q_{tr} c$ and the flux to downstream layers $q_{i+1/2} c$. The value of c_{i-1} is determined as the time averaged concentration in the adjacent upstream soil layer. Since the water volume is completely mixed, the chemical's concentration in the outflowing water equals the concentration within the layer.

When appropriate layer thicknesses are chosen, the mathematical dispersion can be used to simulate natural dispersion. The justification of this assumption is given by the numerical analysis presented in Paragraph 2.2.4. The analysis has been performed under steady state hydrological conditions and assumed zero decomposition en transformation rates.

Conservation in aqueous phase and equilibrium sorption

Since the incoming and outgoing fluxes are constant with time during a time interval, the soil moisture content varies linear with time according to: $\theta(t) = \theta(t_0) + \varphi t$, where $\theta(t_0)$ is the moisture fraction at the beginning of the timestep t_0 and φ is the moisture change with time. This variable is calculated from data supplied by hydrological models. The rate of change of the amount within the aqueous phase:

$$\frac{\partial \theta c}{\partial t} = (\theta(t_0) + \varphi t) \frac{\partial c}{\partial t} + \varphi c \quad (22)$$

The expression of the equilibrium sorption can be incorporated into the conservation equation by elaborating the differential quotient $\partial X_d / \partial t$:

$$\rho_d \frac{\partial X_e}{\partial t} = \rho_d \left(\frac{dX_e}{dc} \right) \frac{\partial c}{\partial t} = \rho_d K_d(c) \frac{\partial c}{\partial t} \quad (23)$$

where $K_d(c)$ is the differential sorption coefficient. The differential adsorption coefficient is approximated by the average value $K_d(c)$. This value is assessed by

calculating the slope of the chord of the adsorption isotherm:

$$\bar{K}_d(c) = \frac{1}{c(t) - c(t_0)} \int_{t_0}^t \left(\frac{dX_e}{dc} \right) dc = \frac{X_e(t) - X_e(t_0)}{c(t) - c(t_0)} \quad (24)$$

Although $K_d(c)$ is a function of the concentration, its average value is considered to be constant during the timestep.

Vertical transport

The second order partial differential equation is simplified to a first order equation by eliminating the dispersion/diffusion term. The remaining first order differential equation can be solved analytically. Diffusion/dispersion is then introduced by choosing an appropriate value of the vertical compartment thickness. Justification for this approach is the fact that measured values for diffusion/dispersion under field conditions are difficult to assess. The transport term is approximated by:

$$- \frac{\partial J_s}{\partial z} = - \frac{\partial}{\partial z} \left(q c - \theta D_{ad} \frac{\partial c}{\partial z} \right) \approx \frac{q_{i-1/2}}{\Delta z} c_{i-1} - \frac{q_{i+1/2}}{\Delta z} c_i \quad (25)$$

where $q_{i-1/2}$ and $q_{i+1/2}$ are the inflowing resp. the outflowing waterfluxes and c_{i-1} is the concentration of adjacent upstream soil layer. The implications of these assumptions with respect to the mathematical dispersion and numerical stability are discussed in Paragraph 2.2.4.

Sinks and sources

All decomposition processes such as the transformation of organic compounds and the nitrification of ammonium have been described by first order rate kinetics. The liquid concentration or the solid contents of the substances itself are the rate limiting factors of these processes. An exception has been made for the decomposition of nitrate by denitrification (see Par. 2.4.5). The general formulation reads:

$$R_d = k_1 \theta_i c_i \quad (26)$$

where k_1 is the first order rate coefficient of the decomposition processes. Crop uptake of nutrients is described proportional to the liquid concentration of the soil water phase and the transpiration flux q_r towards plant roots. A multiplication factor has been introduced to account for preferential uptake when the nutrient availability is not sufficient to fulfill the crop requirement by passive uptake with the water flow. The general equation reads:

$$R_u = \sigma \frac{q_r}{\Delta z} c_i \quad (27)$$

where σ is the selectivity factor to account for specific deficit or surplus situations. The assessment of this parameters is given for nitrogen in Paragraph 2.4.3. and for phosphorus in Paragraph 2.5.3.

Sources are described as zero-order terms. In the carbon cycle, formation of dissolved organic carbon from the solubilization of fresh organic matter and the formation of the humus/biomass pool is described by zero-order kinetics. These processes have also been described in the nitrogen and phosphorus cycle. The formation of ammonium and mineral phosphate is considered as a zero-order process when one considers the ammonium and the mineral phosphate balance respectively. Looking in detail to the nitrate balance, the formation of nitrate through nitrification has been described as a zero-order term.

Numerical expressions for the CTE

The conservation equation can be developed as follows when the expressions for the average differential sorption coefficient and the first order rate sorption are substituted:

$$\{ \theta(t_0) + \varphi t + \rho_d \bar{K}_d \} \frac{dc_i}{dt} = \frac{q_{i-\frac{1}{2}} c_{i-1}}{\Delta z} - \frac{q_{i+\frac{1}{2}}}{\Delta z} c_i - \frac{\sigma q_{tr}}{\Delta z} c_i - k_1 \theta c_i + R_p - \varphi c_i \quad (28)$$

When precipitated chemicals are absent at low concentration levels the conservation equation given in Eq. 28 can be rewritten as follows:

$$\frac{dc_i}{dt} + \frac{A}{\theta(t_0) + \varphi t + \rho_d \bar{K}_d} c_i = \frac{B}{\theta(t_0) + \varphi t + \rho_d \bar{K}_d} \quad (29)$$

where:

$$A = \frac{q_{i+\frac{1}{2}}}{\Delta z} + \frac{\sigma q_{tr}}{\Delta z} + k_1 \bar{\theta} + \varphi \quad (30)$$

$$B = \frac{q_{i+\frac{1}{2}} c_{i-1}}{\Delta z} + R_p \quad (31)$$

The moisture fraction θ in the decomposition rate term of Eq. 28 is approximated by the average moisture content $\bar{\theta}$. The general solution to this differential equation reads:

$$c_i(t) = \xi_1(t) c_i(t_0) + \xi_2(t) B \quad (32)$$

The time averaged concentration \bar{c} can be determined by integration of Eq. 32 between $t = t_0$ and $t = t$, and dividing by the length of the time step:

$$\bar{c}_i = \zeta_1(t) c_i(t_0) + \zeta_2(t) B \quad (33)$$

The functions $\xi_1(t)$, $\xi_2(t)$, $\zeta_1(t)$ and $\zeta_2(t)$ are defined in Annex 2.

2.2.4 Numerical analysis

Numerical dispersion

The dispersion term of Eq. 25 comprises the physical (apparent) dispersion which occurs as a result of a number of natural processes. In some model approaches these natural processes are defined as the sum of molecular diffusion and dispersional mixing. The numerical approach in the ANIMO-model assumes that dispersion is the dominating process and diffusion is ignored.

The natural dispersion term resulting from physical processes in Eq. 25 is replaced by a dispersion term which accounts for the mathematical dispersion. Neglecting sink and source terms and focusing on the concentration in the liquid phase results in the following equation:

$$\frac{\partial c}{\partial t} = -\frac{q}{\theta} \frac{\partial c}{\partial z} + D_n \frac{\partial^2 c}{\partial z^2} \quad (34)$$

where D_n is the numerical dispersion coefficient. When D_n equals D_{da} , the equation gives a good approximation of the convective and dispersive processes as has been described by Eq. 25. The convection / dispersion equation is solved by means of a pseudo-analytical method given by Groenendijk *in prep*. The computation scheme yields the following sources of numerical dispersion:

- as a result of spatial discretization;
- as a result of temporal discretization and the assumption of time averaged constant concentration values within a time interval.

Groenendijk *in prep*. shows that numerical dispersion resulting from the computation algorithm can be quantified under restricted circumstances. An expression for the numerical dispersion coefficient D_n is derived, allowing manipulation of model variables such as time interval and layer thickness to achieve agreement between physical and numerical dispersion.

In this analysis, steady state soil moisture flow conditions are assumed and the soil profile is schematized to layers with equal thickness. The spatial term ∂z is discretised to finite increments with thickness Δz . This results in a schematization of the convective transport into a flow through a series of perfectly mixed soil layers. In first instance, the dispersion term of Eq. 25 is ignored since computation algorithm introduces a numerical dispersion, which is utilized to describe physical dispersion.

Both concentrations in the liquid phase of layer i and of adjacent upstream layer $i-1$ are functions of time. This time function $c_{i-1}(t)$ is replaced by the time averaged concentration in the inflowing soil water from an upstream layer to facilitate the solution of the differential equation. This results in the differential equation for layer i :

$$\frac{dc_i}{dt} = \frac{q}{\theta \Delta z} \bar{c}_{i-1} - \frac{q}{\theta \Delta z} c_i(t) \quad (35)$$

where Δz is the layer thickness and the subscripts i and $i-1$ denote the layer numbers. The averaged concentration is determined by calculating the integral and dividing by the length of the time interval considered:

$$\bar{c}_{i-1} = \frac{1}{\Delta t} \int_{t_0}^{t_0+\Delta t} c_{i-1}(t) dt \quad (36)$$

The introduction of the time averaged constant value obeys to the mass conservation law. Subject to the initial condition $c_i = c_i(t_0)$ at $t = t_0$, the solution to this differential equation reads:

$$c_i = c_i(t_0) e^{-\frac{q}{\theta \Delta z} \Delta t} + \bar{c}_{i-1} (1 - e^{-\frac{q}{\theta \Delta z} \Delta t}) \quad (37)$$

At small values of Δt , the resulting concentration c_i will be determined nearly complete by the initial value of the concentration. At large values of Δt , the resulting concentration will approach the value of the forcing function c_{i-1} . This solution can be considered as a combination of an explicit and an implicit numerical solution to a finite difference computation scheme. The measure of dependency of the initial value and the value of the forcing function is determined by the exponential function $\exp(-q\Delta t/\theta\Delta z)$.

The residence time of the soil moisture in the layer considered can be defined as:

$$t_{res} = \frac{\theta \Delta z}{q} \quad (38)$$

The term $\Delta t(q/(\theta\Delta z))$ is a dimensionless constant and expresses the number of pore water refreshments within a time increment. The product of the pore water velocity and the layer thickness $q\Delta/\theta$ can be replaced by:

$$\frac{q}{\theta} \Delta z = \frac{(\Delta z)^2}{t_{res}} \quad (39)$$

After some laborious algebraic manipulations, the resulting expression of numerical dispersion coefficient reads:

$$D_n = \frac{(\Delta z)^2}{t_{res}} \left(\frac{\frac{\Delta t}{t_{res}}}{1 - e^{-\frac{\Delta t}{t_{res}}}} - \frac{1}{2} \left(1 + \frac{\Delta t}{t_{res}} \right) \right) \quad (40)$$

For comparison, the relation between numerical dispersion and number of pore water refreshments have been given for the cascade model TRADE (Roest and Rijtema, 1983) and the 'Mixing Cell' model based on a finite difference approximation of the convection/dispersion equation (Van Ommen, 1985). The numerical dispersion coefficient in both mentioned models:

$$\text{Cascade model : } D_n = \frac{q}{\theta} \frac{\Delta z}{2} = \frac{1}{2} \frac{(\Delta z)^2}{t_{res}} \quad (41)$$

$$\text{Mixing Cell model : } D_n = \frac{q}{\theta} \left(\frac{\Delta z}{2} - \frac{q \Delta t}{\theta} \right) = \frac{1}{2} \frac{(\Delta z)^2}{t_{res}} \left(1 - \frac{\Delta t}{t_{res}} \right) \quad (42)$$

The numerical dispersion coefficient can be multiplied by $t_{res}/(\Delta z)^2$ to obtain a dimensionless entity. This variable is given as a function of the number of pore water refreshments in Figure 11.

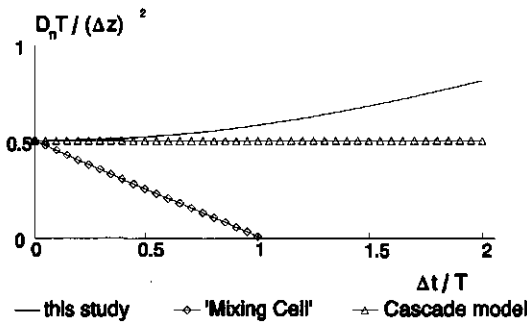


Fig. 11 Dimensionless numerical dispersion as a function of the number of pore water refreshments

The following conclusions may be drawn from this figure:

- Numerical dispersion can be used to simulate physical dispersion by manipulating the layer thickness when Δt and t_{res} have been chosen.
- The numerical dispersion derived in this study approximates the numerical dispersion in the Cascade model at small time increments. The characteristic length which is used to quantify dispersion equals $\Delta z/2$ at $\Delta t/t_{res} \rightarrow 0$.
- The numerical dispersion in this study is always larger than in the Cascade model, when equal thicknesses have been chosen in both models.
- Plug flow ($D_m \partial^2 c / \partial z^2 = 0$) can not be simulated by the model presented in this study. Neither can plug flow be simulated by the Cascade model, but in the Mixing Cell model zero dispersion can be simulated by choosing the time step equal to the residence time.

Stability of the mathematical solution

One of the most well-known procedures for stability estimation of finite difference approaches is the Von Neumann-method. The method assumes the propagation of error E_i to be described by the computation rules for calculation the concentration c_i . The error E_i in the concentration can be replaced by the expression:

$$E_i = \Theta^\gamma e^{i\beta\delta\Delta z} \quad (43)$$

where:

- Θ : the amplification factor
 β : frequency of the error
 γ : number of the time step since the beginning of the simulation
 δ : layer number.

The imaginary number i is defined as $i^2 = -1$. Substitution of this expression in the discretized form of the conservation and transport equation (Eq. 35) and further elaboration yields the following expression for Θ :

$$\Theta = e^{-\frac{q\Delta t}{\theta\Delta z}} \quad (44)$$

The mathematical solution is stable when the following condition has been satisfied:

$$|\Theta| \leq 1 \quad (45)$$

When the ratio $(q\Delta t)/(\theta\Delta z)$ is greater than zero, the amplification factor Θ is always less than one. It can be concluded that as long as the computation order proceeds in the flow direction the mathematical solution presented in this study is always stable. This condition is always met in the ANIMO model.

2.3 Organic cycle

Organic matter pools

Leaching of dissolved organic matter results from additions and dissolution processes in the carbon cycle (Fig. 12). Four organic substances are distinguished:

- Fresh organic matter: This material consists mainly of root and other crop residues after harvesting and of the organic parts of manure. These are materials that come available at clearly defined points in time. Fresh organic matter is divided into fractions (1-*nf*) characterised by a first order decomposition rate and a C-, N- and P-content.
- Root exudates: These are organic products excreted by living roots and dead root cells discarded by plants. These products are added to the soil continuously as long as living roots are present.
- Dissolved organic matter: This soluble material is produced, because part of the fresh organic matter passes the stage of solubilization.
- Humus, soil organic matter or living biomass. This material consists of dead organic soil material and of the living biomass. This material is formed from root exudates, dissolved organic matter and from part of the fresh organic material.

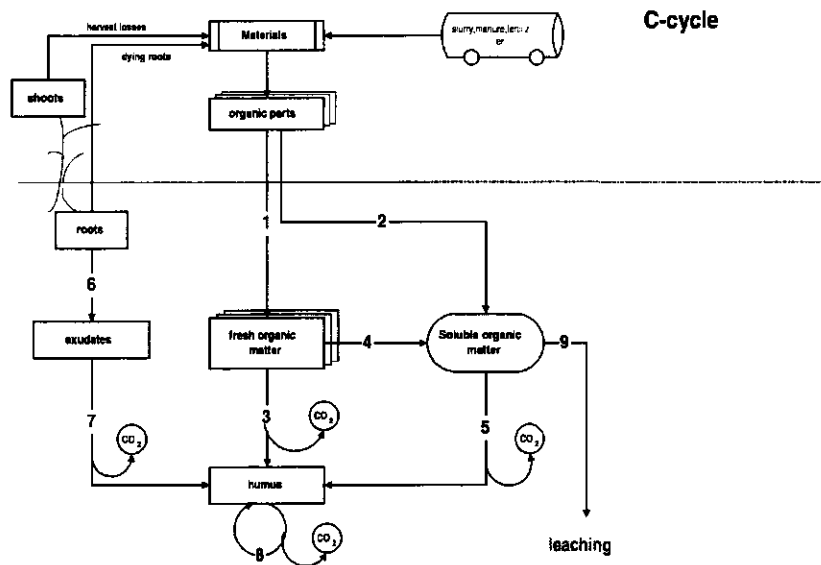


Fig. 12 Relational diagram of the organic matter cycle described in the ANIMO-model

Decomposition of fresh organic materials results in dissimilation of organic carbon, solubilization and transformation to the humus/biomass pool. Decomposition of dissolved organic compounds results in dissimilation and transformation to the humus/biomass pool. The humus/biomass pool decomposes to a residual fraction, accompanied by partial dissimilation of these residues. This residual material has been lumped with the humus/biomass pool, so only nett dissimilation of this pool has been taken into consideration.

Characterization of fresh organic materials

The fresh organic materials can be applied to the soil system and can optionally be mixed with the present organic materials in one or more top layers. These materials can vary strongly in quality. Each kind of material is considered to exist of one or more fractions with each fraction with its own decomposition rate and nitrogen and phosphorus contents. The model requires a definition of the organic and mineral (anorganic) fractions of the introduced materials. The decomposition of each fraction is assumed to follow first order rate kinetics. In the ANIMO model, a fixed number of possible materials consisting of a fixed number classes have to be defined by the model user. This allows the mathematical simulation of empirical decomposition curves as given by Kolenbrander (1969) or Janssen (1986). When appropriate parameter sets are chosen for combination of class-fractions and first order rate constants of a certain organic material, the ANIMO concept is able to reproduce equivalent relations to these empirical approaches. In the ANIMO model, decomposition of fresh organic materials is described by:

$$\begin{aligned}
\frac{dM_1(t)}{dt} &= f_{1,1} OM_1(t_0) e^{-k_1(t-t_0)} + f_{1,2} OM_2(t_0) e^{-k_2(t-t_0)} + \dots \\
\frac{dM_2(t)}{dt} &= f_{2,1} OM_1(t_0) e^{-k_1(t-t_0)} + f_{2,2} OM_2(t_0) e^{-k_2(t-t_0)} + \dots \\
\frac{dM_i(t)}{dt} &= f_{i,1} OM_1(t_0) e^{-k_1(t-t_0)} + f_{i,2} OM_2(t_0) e^{-k_2(t-t_0)} + \dots + f_{i,n} OM_n(t_0) e^{-k_n(t-t_0)} + \dots
\end{aligned}
\tag{46}$$

where:

- $M_i(t)$: organic part of the i^{th} type material (kg m^{-3})
 $OM_{fn}(t)$: quantity organic material attributed to the fn^{th} class (kg m^{-3})
 $f_{i,fn}$: fraction of the fn^{th} class as a part of the i^{th} material (-)
 k_{fn} : first order decomposition rate constant of the fn^{th} class material (d^{-1})

When one wants to derive a parameter set for a certain material on the basis of an empirical relation, it should be kept in mind that most of these relations describe the overall decay. The capabilities of the ANIMO-concept to reproduce the Janssen-relation is illustrated in Figure 13.

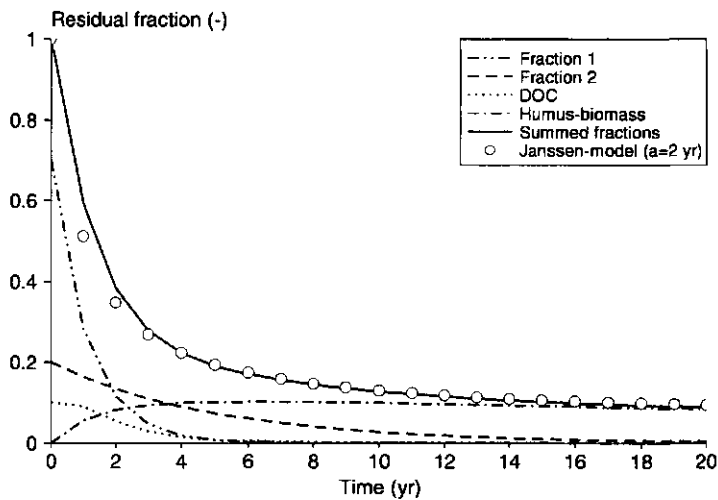


Fig. 13 Simulation of the Janssen decay relation by an appropriate choice of parameters in the ANIMO model

When a certain quantity of organic material has been introduced into the soil system, only the quantities per class have to be simulated, because the schematization of organic materials into certain defined classes follows a linear approach.

2.3.1 Additions to the soil system

Fresh organic matter

Fresh organic materials and dissolved organic matter are applied as instantaneous pulse-type doses. The organic part of the applied substance is divided over fresh organic matter and dissolved organic matter.

The amount of fresh organic matter at the start of the time step is calculated by summarizing the initial quantity and the applied dose (Fig. 12, relation 1):

$$OM_{fn}(t+\tau) = OM_{fn}(t) + (f_{i,fn} - f_{i,fn}^L) \frac{f_i^O M_i}{\Delta z} \quad (47)$$

where:

- $OM_{fn}(t+\tau)$: volumic mass of organic matter class fn after addition (kg m^{-3})
- $OM_{fn}(t)$: volumic mass of organic matter class fn before addition (kg m^{-3})
- $f_{i,fn}$: fraction of the fn^{th} class as a part of material applied (-)
- $f_{i,fn}^L$: liquid fraction of the fn^{th} class as a part of material applied (-)
- f_i^O : organic fraction of the applied material (-)
- M_i : areic mass of applied material (kg m^{-2})
- τ : infinite small time increment (d)

Residual root materials of arable crops are applied to the soil layers of the root zone at the end of the growing season. During the growing season, the growth and maintenance of the root system produces dead root cells and hair roots. These materials are defined as root exudates which are described by a separate pool. The ANIMO model comprises a sub-model for dry matter production and nutrient uptake of grassland. In this sub-model grassroots die continuously throughout the year. These dead grass roots are added to the soil system as one of the defined fresh organic materials during each simulation time step. These dead grass roots are distributed in the rootzone linearly decreasing with depth.

Dissolved organic matter

The impact of fertilization or other additions on liquid concentration of dissolved organic matter is calculated according to (Fig. 12, relation 2):

$$c_{OM}(t+\tau) = c_{OM}(t) + \sum_{fn=1}^{nf} f_{i,fn}^L f_i^O \frac{M_i}{\theta \Delta z} \quad (48)$$

where:

- $c_{OM}(t+\tau)$: concentration dissolved organic matter after addition (kg m^{-3})
- $c_{OM}(t)$: concentration dissolved organic matter before fertilization (kg m^{-3})
- nf : number of organic matter classes (-)

Root residues

The process roots dying for grassland is described by a dynamic submodel (see Par. 2.4.3). Root material died during the previous timestep is added to the root zone at the beginning of the current timestep. Dead roots are considered as a composition of

two classes of fresh organic material. The first class has a high nutrient content and the second is characterized by low nutrient fractions. The dead roots are divided over these two materials subject to the condition that the nutrient content of the mixture is in accordance with the nutrient fraction calculated by the dynamic submodel. Since the death rate has been modelled proportional to the root mass, information is available to distribute the materials with depth. Grazing losses and harvest losses of grass shoots are treated in a similar way, but are added to the top layer only.

Dry matter production of arable crops is defined as input to the model. No specific nutrient balances of roots or shoots have been formulated. By-products of root growth are described as root exudates (see Par. 2.3.2) with fixed nitrogen and phosphorus contents. At harvest, the root material is added to the root zone as a fresh organic material. The nutrient contents are calculated from the realized dry matter production and the cumulative nutrient uptake. The addition of dead roots and dead over-ground parts are treated in a similar way as grass roots. They are considered as a composition of two classes organic material and the division over these materials is calculated from the defined nutrient fractions and the actual nitrogen fractions of the remaining plant parts.

2.3.2 Transformations

Organic substances can be transformed from one species into another with production as a source and decomposition as a sink term in the general mass conservation and transport equation. These terms will be given for the four organic substances: fresh organic matter, dissolved organic matter, humus/biomass and exudates.

Fresh organic matter

The introduction of fresh organic matter occurs by additions of manure, root materials, grazing and harvest losses and any other organic materials defined in the input files. Decomposition of fresh organic matter into humus (Fig. 12, relation 3) is described by first order kinetics:

$$R_{d,OM-HU} = - \frac{dOM_{fn}}{dt} = f_h k_{fn} \rho_d OM_{fn} \quad (49)$$

where:

- f_h : fraction of fresh organic matter which is not subject to solubilization (-)
- k_{fn} : first order rate constant of organic class fn (d^{-1})
- ρ_d : dry bulk density ($kg\ m^{-3}$)

Transformation into dissolved organic matter (Fig. 12, relation 4) is described:

$$R_{d,OM-DOC} = - \frac{dOM_{fn}}{dt} = (1-f_h) k_{fn} \rho_d OM_{fn} \quad (50)$$

where:

- $(1-f_h)$: fraction fresh organic matter which is subject to solubilization (-)

Dissolved organic matter

Formation of dissolved organic matter (Fig. 12, relation 4) results from the decomposition of the different fresh organic matter classes and is formulated as:

$$R_{p,DOC} = \frac{d\theta c_{OM}}{dt} = (1-f_h) \frac{1}{\Delta t} \int_{t_0}^{t_0+\Delta t} \sum_{fn=1}^{nf} k_{fn} OM_{fn} dt \quad (51)$$

Decomposition of dissolved organic matter (Fig. 12, relation 5) is described as a first order process:

$$R_{d,DOC} = - \frac{d\theta c_{OM}}{dt} = k_s \theta c_{OM} \quad (52)$$

where:

k_s : first order rate constant for decomposition of dissolved organic matter (d^{-1})
 c_{OM} : concentration of dissolved organic matter ($kg\ m^{-3}$)

Exudates

Production of exudates (Fig. 12, relation 6) is considered for arable crops only. The ANIMO model contains a sub-model for grassland which simulates dry matter production of shoots and roots as well as the death rate of roots. For arable crops, the exudate production has been formulated proportionally to the root mass increase. The root growth characteristic has to be defined as model input and from these data, the model calculates the increase of root mass during the simulation timestep. Within the simulation timestep, the root growth is assumed constant. On the basis of scarce literature data Berghuijs-van Dijk *et al.*, (1985) derived an exudate production of 41% of the gross dry matter production of roots. Hence, it follows:

$$R_{p,EX} = \frac{dEX}{dt} = 0.41 \frac{R_{t_0+\Delta t} - R_{t_0}}{\Delta t} \quad (53)$$

Decomposition of exudates into humus (Fig. 12, relation 7) is described as a first order process:

$$R_{d,EX} = - \frac{dEX}{dt} = k_{ex} EX \quad (54)$$

where k_{ex} (d^{-1}) is the first order rate constant for decomposition of exudates.

Humus/biomass

Production of humus/biomass results from the decomposition of fresh organic matter, dissolved organic matter, exudates and an internal turnover of humus. The assimilation process is accompanied by a dissimilation which requires most of the organic material for energy supply of the living biomass. The assimilation ratio a is taken constant for all organic matter pools. Up to ANIMO version 3.5, no distinction has been made between the assimilation ratios of the different fresh organic classes, exudates, dissolved organic matter and humus/biomass.

Production of humus/biomass as a result of the decomposition of fresh organic matter (Fig. 12, relation 3) is given by the following equation:

$$R_{p,OM-HU} = \frac{dHU}{dt} = f_h a \sum_{fn=1}^{nf} k_{fn} OM_{fn} dt \quad (55)$$

Production of humus/biomass as a result of the decomposition of dissolved organic matter (Fig. 12, relation 5):

$$R_{p,DOC-HU} = \frac{dHU}{dt} = a \frac{1}{\Delta t} \int_{t_0}^{t_0+\Delta t} k_S \theta c_{OM} dt \quad (56)$$

Production of humus/biomass as a results from the decomposition of exudates (Fig. 12, relation 7):

$$R_{p,EX-HU} = \frac{dHU}{dt} = a k_{ex} EX \quad (57)$$

In the ANIMO model, no separate production of humus/biomass as a result of humus/biomass turnover has been formulated explicitly, because the residual humus/biomass material has been lumped with the total humus/biomass pool and the rate constant has been formulated for the nett decomposition. The gross decomposition rate and the formation rate of humus biomass can be written as:

$$\left(\frac{dHU}{dt} \right)_{decomp} = - \frac{1}{1-a} k_{hu} HU \quad (58)$$

$$\left(\frac{dHU}{dt} \right)_{form} = \frac{a}{1-a} k_{hu} HU$$

The nett decomposition rate:

$$R_{d,HU} = -k_{hu} HU \quad (59)$$

2.3.3 Transport of organic substances

Inflow and outflow of dissolved organic matter in a model compartment is described by the conservation and transport equation. The mathematical solution of this equation includes vertical mass transport in upward or downward direction (Fig. 12, relation 9).

Lateral mass transport towards surface water systems is formulated as a sink term:

$$R_{x,DOC} = - \frac{d(\theta c)}{dt} = k_d c_{OM} \quad (60)$$

where k_d is the drainage rate ($\text{m}^3 \text{m}^{-3} \text{d}^{-1}$). The drainage rate is given by the results of the water balance simulations. If the lateral water flux is negative (infiltration) the sink term turns into a source term.

2.4 Nitrogen cycle

Leaching of the dissolved organic nitrogen substances, nitrate and ammonium causes contamination of groundwater and surface water systems. Since the nitrogen behaviour in soil is closely related to the organic matter transformations, organic nitrogen processes are described analogous to the carbon cycle (Fig. 12).

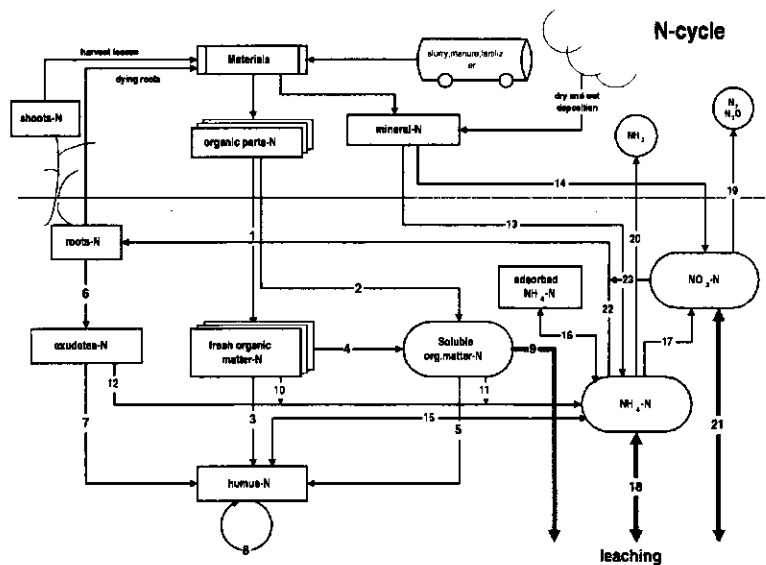


Fig. 14 Relational diagram of the nitrogen cycle described in the ANIMO-model

2.4.1 Ammonium sorption

Ammonium may be adsorbed to the soil complex, consisting of the negative surfaces of clay particles and humic compounds. The sorption process (Fig. 14, relation 16) results in an equilibrium between ammonium in liquid and sorbed phase, an equilibrium which is described by a linear sorption isotherm:

$$X_{e,NH_4} = K_{e,NH_4} c_{NH_4} \quad (61)$$

where:

X_{e,NH_4} : sorbed ammonium content (kg kg⁻¹)

K_{d,NH_4} : adsorption or partitioning coefficient (m³ kg⁻¹)

Hoeks *et al.*, (1979) showed the influence of the clay content on the adsorption affinity of ammonium. Exploring the theory of cation exchange in multi-component systems, a relation can be derived between the linear adsorption coefficient and the Cation Exchange Capacity (CEC). The Gapon equation for NH₄⁺ - Ca²⁺ exchange:

$$\frac{\Gamma_{NH_4}}{\Gamma_{Ca}} = K_G \frac{(NH_4^+)}{\sqrt{(Ca^{2+})}} \quad (62)$$

where:

Γ_{NH_4} ; Γ_{Ca} : ammonium; calcium complex occupation (meq per 100 g)

(NH_4^+) ; (Ca^{2+}) : molar concentrations of ammonium and calcium (mol l⁻¹)

K_G : Gapon exchange coefficient.

Assuming constant levels of Γ_{Ca} and (Ca^{2+}) , the Gapon equation describes the linear sorption of ammonium, where the linear sorption coefficient K_{e,NH_4} is related to the Gapon coefficient according to:

$$K_{e,NH_4} = 10^{-5} K_G \frac{\Gamma_{Ca}}{\sqrt{(Ca^{2+})}} \quad (63)$$

Values of the Gapon coefficient are reported by e.g. Bruggenwert and Kamphorst (1982) and Appelo (1988). From their data, a value of 0.5 (range: 0.3-0.7) was found as a good approximation. In most soils having favourable pH-values for agricultural production, calcium occupies the greatest part of the exchange complex (50 à 90%). The ammonium concentrations only changes this occupation to a slight extent.

$$K_{e,NH_4} = 10^{-5} K_G \frac{f_{Ca} CEC}{\sqrt{(Ca^{2+})}} \quad (64)$$

Where f_{Ca} is the calcium fraction of the total adsorbed cationic composition. The fraction shows a range from 0.5 to 0.9 and is highly dependent on pH. Inserting a CEC-value of 5 meq per 100 g, a calcium occupation fraction of 0.7 and a calcium concentration of 3 mmol l⁻¹ yields a K_{e,NH_4} -value of 3·10⁻⁴ m³ kg⁻¹. When only data on CEC-values are available, the relation $K_{e,NH_4} \approx 6 \cdot 10^{-5} \cdot CEC$ can be used as a first estimation.

2.4.2 Fertilization, volatilization and tillage

Fresh organic matter-nitrogen

Fertilization has been described as a pulse-wise addition of materials with a defined composition. The quantity of organic nitrogen after the introduction of a certain organic material (e.g. manure application) is calculated by summarizing the quantity before the addition and the applied dose (Fig. 14, relation 1):

$$ON_{fn}(t+\tau) = ON_{fn}(t) + f_{N,fn} (f_{i,fn}^O - f_{i,fn}^L) \frac{f_i^O M_i}{\Delta z} \quad (65)$$

where:

$ON_{fn}(t+\tau)$: volumic mass of organic nitrogen after application (kg m^{-3})
 $ON_{fn}(t)$: volumic mass of organic nitrogen before application (kg m^{-3})
 $f_{N,fn}$: nitrogen content of organic matter class fn (-)

Dissolved organic nitrogen

The concentration of dissolved organic nitrogen is calculated according to (Fig. 14, relation 2):

$$c_{ON}(t+\tau) = c_{ON}(t) + \sum_{fn=1}^{nf} f_{N,fn} f_{i,fn}^L \frac{f_i^O M_i}{\theta \Delta z} \quad (66)$$

where:

$c_{ON}(t+\tau)$: dissolved organic nitrogen concentration after addition (kg m^{-3})
 $c_{ON}(t)$: dissolved organic nitrogen concentration before addition (kg m^{-3})

Mineral nitrogen

Similar to the addition of dissolved organic nitrogen, the mineral compounds can be added to the soil system pulse-wise. The nitrate content after an addition reads (Fig. 14, relation 13):

$$\theta c_{NO_3}(t+\tau) = \theta c_{NO_3}(t) + \frac{f_{NO_3,i} M_i}{\Delta z} \quad (67)$$

where:

$c_{NO_3}(t+\tau)$: nitrate concentration after addition ($\text{kg m}^{-3} \text{ N}$)
 $c_{NO_3}(t)$: nitrate concentration before addition ($\text{kg m}^{-3} \text{ N}$)
 $f_{NO_3,i}$: nitrate-N content of the applied material i (kg kg^{-1})

Ammonium volatilization is assumed to occur momentarily at the time of a slurry addition and is defined by a fraction of the ammonium input by animal manure. This fraction must be specified for each addition by the user in the model input. The ammonium content after an addition reads (Fig. 14, relation 13):

$$(\theta + \rho_d K_d) c_{NH_4}(t+\tau) = (\theta + \rho_d K_d) c_{NH_4}(t) + (1-f_{v,i}) \frac{f_{NH_4,i} M_i}{\Delta z} \quad (68)$$

$c_{NH_4}(t+\tau)$: ammonium concentration after addition ($\text{kg m}^{-3} \text{ N}$)
 $c_{NH_4}(t)$: ammonium concentration before addition ($\text{kg m}^{-3} \text{ N}$)
 $f_{NH_4,i}$: ammonium-N content of the applied material i (kg kg^{-1})
 $f_{v,i}$: ammonium volatilization fraction of material i (-)

2.4.3 Crop uptake

Nitrogen uptake by grassland

Nutrient uptake by plant roots R_u is described following a two-compartment model: a soil compartment and a plant compartment. This concept accounts for the transport of nutrients from the root system to the shoots. The nitrate concentration in the shoots liquid fraction can be considered as the internal concentration of the plant. Plant uptake is calculated by balancing the demand of the crop and the supply by the soil.

Nutrient availability of grassland soils

The calculation method of supply potential is based on the assumption that total uptake is determined by the sum of convective flow and diffusive flow.

$$R_{u,N} = R_{u,c} + R_{u,d} \quad (69)$$

where the subscripts c and d denote the convective resp. diffusive transport. The uptake due to convective wateruptake of resp. nitrate and ammonium by roots is computed by:

$$R_{u,c} = \frac{q_{tr}}{\Delta z} \bar{c}_{NO_3} \quad (70)$$

$$R_{u,c} = \left(1 + \frac{\rho_d}{\theta} K_{e,NH_4}\right) \frac{q_{tr}}{\Delta z} \bar{c}_{NH_4} \quad (71)$$

where:

q_{tr} : transpiration flux in a layer (m d^{-1})
 Δz : thickness of the layer (m)
 K_d : linear adsorption coefficient of ammonium ($\text{m}^3 \text{ kg}^{-1}$)
 \bar{c}_{NO_3} and \bar{c}_{NH_4} : average soil moisture concentration of nitrate and ammonium ($\int \int c(z,t) dt dz / \Delta z \Delta t$) (kg m^{-3})

The diffusive nitrate uptake is determined by:

$$\begin{aligned} \bar{c}_{NO3} > \frac{f_{N,r,min}}{f_{N,s,min}} c_{pl} & : R_{u,d} = \theta k_{gr,dif} (\bar{c}_{NO3} - \frac{f_{N,r,min}}{f_{N,s,min}} c_{pl}) \\ \bar{c}_{NO3} < \frac{f_{N,r,min}}{f_{N,s,min}} c_{pl} & : R_{u,d} = 0 \end{aligned} \quad (72)$$

where the diffusion rate is proportional to a first order rate constant $k_{gr,dif}$ (d^{-1}) and the difference between the nitrate concentration in soil moisture and in plant roots. The internal concentration in plant roots has been assumed proportional to the concentration in plant shoots and the ratio between the nitrogen fractions in plant roots and plant shoots.

In numerical computation schemes, the soil system is schematized to homogeneous layers with thickness Δz_i . The nitrate uptake in layer i is then determined by (Fig. 14, relation 23):

$$R_{u,i} = \frac{q_{tr,i}}{\Delta z_i} \bar{c}_{NO3,i} + \theta_i k_{gr,dif} (\bar{c}_{NO3,i} - \frac{f_{N,r,min}}{f_{N,s,min}} c_{pl}) \quad (73)$$

The ammonium uptake reads (Fig. 14, relation 22):

$$R_{u,i} = (1 + \frac{\rho_d}{\theta} K_{e,NH4}) \frac{q_{tr,i}}{\Delta z_i} \bar{c}_{NH4,i} \quad (74)$$

The uptake process has been incorporated in the conservation and transport equation by defining the uptake parameters $\sigma_{NO3,i}$ and $\sigma_{NH4,i}$ per soil layer i and redefining the zero-production term $k_{0,NO3}$. When the nitrogen accumulation has not lead to nitrogen contents above a defined threshold level, the uptake parameters are defined by:

$$\sigma_{NO3,i} = 1 + \theta_i k_{gr,dif} \frac{\Delta z_i}{q_{tr,i}} \quad \text{and} \quad k_{0,NO3,i}^* = k_{0,NO3,i} + \theta_i k_{gr,dif} \frac{f_{N,r,min}}{f_{N,s,min}} c_{pl} \quad (75)$$

$$\sigma_{NH4,i} = (1 + \frac{\rho_d}{\theta} K_{e,NH4}) \quad (76)$$

For situations where the nitrogen availability exceeds the requirement of the crop, the ammonium uptake parameter will be cut off as will be explained in the following sub-paragraphs. The internal concentration c_{pl} of nitrate ($kg\ m^{-3}$) is calculated from a relation between the concentration and the N-fraction in the shoots, based on experimental data in Ruurlo. The internal plant concentration within the plant is assumed to be proportional to the nitrate fraction of the shoots:

$$c_{pl} = \frac{f_{ds}}{1-f_{ds}} 1000 f_{pl,NO3} \quad (77)$$

The nitrate fraction in the shoots is related to the total nitrogen fraction. In an

analysis of experimental field data of Ruurlo, both the $\text{NO}_3\text{-N}$ concentrations (kg m^{-3}) and the total nitrogen fractions have been calculated as a annual average values, based on 7 cuttings per field plot (Fig. 15).

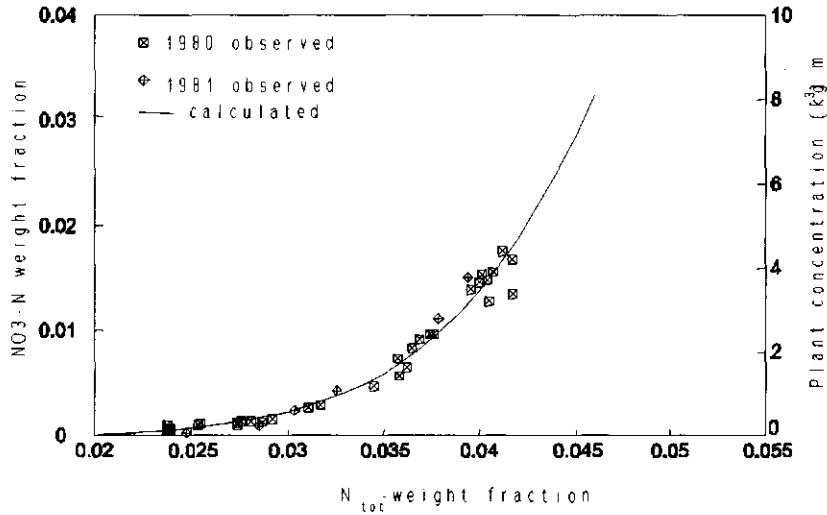


Fig. 15 Relation between nitrate-N weight fraction and total nitrogen weight fraction in grass shoots

The nitrate weight fraction f_{pl,NO_3} is related to the total nitrogen fraction $f_{pl,N_{tot}}$ according to a fitted relation:

$$\begin{aligned}
 f_{pl,N_{tot}} \leq 0.023 & & f_{pl,NO_3} &= 0 \\
 0.023 < f_{pl,N_{tot}} \leq 0.04 & & f_{pl,NO_3} &= 45 (f_{pl,N_{tot}} - 0.023)^2 \\
 f_{pl,N_{tot}} < 0.04 & & f_{pl,NO_3} &= \frac{0.06561}{1 + e^{(-140f_{pl,N_{tot}} + 7)}}
 \end{aligned} \tag{78}$$

The total nitrogen fraction $f_{pl,N_{tot}}$ of the shoots is calculated according to:

$$f_{pl,N_{tot}} = \frac{U(t)}{Q_s(t)} \tag{79}$$

where:

$U(t)$: accumulated nitrogen uptake since the last cutting (kg m^{-2})
 $Q_s(t)$: nett dry matter production of the shoots (kg m^{-2})

The assessment of this fraction necessitates the simulation of the dry matter production and the nitrogen budget of the plant system.

Nutrient requirement of grassland

The demand of the crop is computed by a regionalized dry matter production model, assuming unconstrained nitrogen conditions. The actual daily production rate of the shoots is given by the expression:

$$\frac{dQ_s(t)}{dt} = f_{NP} \chi f_{sh} \frac{Et_{re}}{Et_{pot}} P_{st}(t) \left(1 - e^{-\kappa \frac{Q_s(t)}{Q_{s,ref}}}\right) - W \quad (80)$$

$Q_s(t)$:	amount of dry matter in shoots (kg m^{-2})
κ :	coefficient related to light absorption coefficient (-)
$Q_{s,ref}$:	reference value Q_s related to κ (kg m^{-2})
$P_{st}(t)$:	gross photosynthesis under standard conditions ($\text{kg m}^{-2} \text{CH}_2\text{O}$)
Et_{re} :	real transpiration (m d^{-1})
Et_{pot} :	potential transpiration (m d^{-1})
κ :	coefficient related to light absorption coefficient (-)
χ :	efficiency factor (-)
f_{sh} :	shoot fraction (-)
W :	sink function expressing the uptake by grazing ($\text{kg m}^{-2} \text{d}^{-1}$)

For Dutch weather conditions, this equation holds within the period 10th april - 20th nov. Nett shoot production is assumed zero between 20th nov and 10th april. The standard gross dry matter production $P_{st}(t)$ is calculated from a sinusoidal wave function which is based on empirical data of De Wit (1965):

$$P_{st}(t) = 0.0161 + 0.0159 f_{cl} + (0.0118 + 0.0092 f_{cl}) \sin\left(2\pi \frac{t + 284}{365}\right) \quad (81)$$

where f_{cl} is the cloudiness factor. The sink function for grazing W is expressed by:

$$W = \frac{1}{10\,000} \frac{14}{1 - f_{gr,loss}} N_{lse} \quad (82)$$

where N_{lse} is the average number of live stock units per hectare during the growing season and $f_{gr,loss}$ is the fraction of grazing losses. In most of the regional model applications, N_{lse} has been taken as a regional seasonal average value. The daily herbage intake per cow is set at $14 \text{ kg d}^{-1} \cdot \text{cow}^{-1}$ and the factor $1/10000$ accounts for the number of live stock units per m^2 . During spring, when the shoot production is insufficient to allow grazing, W is set to zero. The starting date for grazing is determined by the model when a treshold level of $Q_s = 0.25 \text{ kg m}^{-2}$ is exceeded. When this criterium has not been reached before 10th of May, grazing will start at this date. The sward will be cut when a treshold level of 0.4 kg m^{-2} has been exceeded. A part of this yield is considered as a loss and remains at the field ($f_{ha,loss}$). At the end of the growing season (20th Nov.), the standing sward is cut and applied to the first soil layer. In this regionalized approach, the swards always increase between two cuttings, due to the low regional and seasonal mean value of live stock units.

The gross increase in dry matter due to transport of assimilates to the root system is proportional to the gross production of shoot dry matter:

$$\frac{dQ_r(t)}{dt} = \frac{1-f_{sh}}{f_{sh}} \left(\frac{dQ_s(t)}{dt} + W \right) \quad (83)$$

A first order process is assumed for the dying of roots. The death rate is assumed proportional to the actual quantity of roots. The nett increase of dry matter amount in roots:

$$\frac{dQ_r(t)}{dt} = \frac{1-f_{sh}}{f_{sh}} \left(\frac{dQ_s(t)}{dt} + W \right) - k_{gr,death} Q_r(t) \quad (84)$$

where $k_{gr,death}$ is a first order decay constant. Died roots and grazing losses are applied to the soil continuously. Harvest losses are added to the upper soil layer when a harvest event occurs.

Limited crop production of grassland

The nitrogen uptake under unconstrained conditions equals the mineral nitrogen availability:

$$U(t_0 + \Delta t) = U(t_0) + \Phi_{NO_3} + \Phi_{NH_4} \quad (85)$$

where the mineral nitrogen availability is approximated by:

$$\begin{aligned} \Phi_{NO_3} &= \int_{t_0}^{t_0 + \Delta t} \sum_{i=1}^{N_r} (q_{ev,i} + k_{gr,d} \theta_i \Delta z_i) c_{NO_3,i}(t) dt - c_{pl} \frac{f_{N,r,min}}{f_{N,s,min}} \sum_{i=1}^{N_r} k_{gr,d} \theta_i \Delta z_i \Delta t \\ \Phi_{NH_4} &= \int_{t_0}^{t_0 + \Delta t} \sum_{i=1}^{N_r} \left(\left(1 + \frac{\rho_d}{\theta} K_{e,NH_4} \right) q_{ev,i} + k_{gr,dif} \left(1 + \frac{\rho_d}{\theta} K_{e,NH_4} \right) \theta_i \Delta z_i \right) c_{NH_4,i}(t) dt \end{aligned} \quad (86)$$

The nitrogen requirement for plant growth is defined as the gross dry matter production multiplied by the actual nitrogen content of shoots and roots:

$$\begin{aligned} \Omega_N &= \max \left(1, \frac{U(t)}{f_{N,s,min} Q_s(t) + f_{N,r,min} Q_r(t)} \right) f_{N,s,min} \int_{t_0}^{t_0 + \Delta t} \frac{dQ_s(t)}{dt} + \\ &W + \frac{f_{N,r,min}}{f_{N,s,min}} \left(\frac{dQ_r(t)}{dt} + k_{d,gr} Q_r(t) \right) dt \end{aligned} \quad (87)$$

When the nitrogen demand can not be fulfilled by the potential soil supply, the reduction of crop growth is assumed proportional to the shortage. Under optimal conditions, the factor for nutrient limitation f_{NP} is set to one, but when the ratio between $U(t)$ and the minimum accumulation level in shoots and roots ($f_{N,s,min} Q_s(t) + f_{N,r,min} Q_r(t)$) tends to value less than unity, the value one for this ratio is maintained

and crop production will be reduced by taking f_{NP} a value less than one according to:

$$f_{NP} = \frac{U(t) - f_{N,s,min} Q_s(t_0) - f_{N,r,min} Q_r(t_0)}{f_{N,s,min} \Delta Q_{s,gr} + f_{N,r,min} \Delta Q_{r,gr}} \quad (88)$$

where $\Delta Q_{s,gr}$ and $\Delta Q_{r,gr}$ are the gross quantities of produced shoot and root material f_{NP} within the time increment under unconstrained conditions. The numerator is an expression for the uptake during the timestep plus the accumulated surplus from previous timesteps. The denominator is an expression for the required nitrogen supply for growth of shoots and roots.

Reaction of grass uptake to nitrogen excess and nitrogen deficit

The description given in this subparagraph applies to recent developments of the model later than version 3.5. The new formulations were implemented on the occasion of the Water Reconnaissance study in 1995/1996 (Boers *et al.*, 1997).

In situations where the mineral nitrogen availability exceeds the crop requirement, the uptake parameter σ_{NH_4} for ammonium will be adjusted on the basis of a defined maximum requirement. Due to electro-neutrality considerations, a preference for nitrate uptake is assumed. The maximum uptake requirement $\Omega_{N,max}$ and the mean uptake requirement $\Omega_{N,mean}$ have been defined as:

$$\Omega_{N,max} = Q_s(t) f_{N,s,max} + Q_r(t) f_{N,r,max} - U(t_0) \quad (89)$$

$$\Omega_{N,mean} = Q_s(t) \frac{f_{N,s,max} + f_{N,s,min}}{2} + Q_r(t) \frac{f_{N,r,max} + f_{N,r,min}}{2} - U(t_0) \quad (90)$$

Based on these defined uptake requirements and the availability of nitrogen, the selectivity factor for ammonium uptake is determined. If the nitrate availability exceeds the maximum requirement, no ammonium will be taken up:

$$\Phi_{NO_3} > \Omega_{N,max} \quad = \quad \sigma_{NH_4} = 0 \quad (91)$$

If the nitrate availability is less than the maximum requirement, but the sum of nitrate availability and ammonium uptake by convective transpiration waterflow is greater than the maximum requirement, the uptake parameter is calculated as follows:

$$\Phi_{NO_3} < \Omega_{N,max} < \Phi_{NO_3} + \int_{t_0}^{t_0+\Delta t N_r} \sum_{i=1} q_{tr,i} \left(1 + \frac{\rho_d}{\theta} K_{e,NH_4}\right) c_{NH_4,i}(t) dt \quad \rightarrow$$

$$\sigma_{NH_4} = \frac{\Omega_{N,max} - \Phi_{NO_3}}{\int_{t_0}^{t_0+\Delta t N_r} \sum_{i=1} q_{tr,i} \left(1 + \frac{\rho_d}{\theta} K_{e,NH_4}\right) c_{NH_4,i}(t) dt} \quad (92)$$

When the sum of nitrate availability and ammonium uptake by convective transpiration waterflow is less than the maximum nitrogen requirement, but greater than the mean nitrogen requirement:

$$\Omega_{N,mean} < \Phi_{NO_3} + \int_{t_0}^{t_0+\Delta t N_r} \sum_{i=1} q_{tr,i} \left(1 + \frac{\rho_d}{\theta} K_{e,NH_4}\right) c_{NH_4,i}(t) dt < \Omega_{N,max} \Rightarrow \sigma_{NH_4}=1 \quad (93)$$

When the mean requirement is less than mineral nitrogen availability, but greater than the sum of nitrate availability and ammonium uptake by convective transpiration waterflow, the preferential parameter for ammonium uptake reads:

$$\Phi_{NO_3} + \int_{t_0}^{t_0+\Delta t N_r} \sum_{i=1} q_{tr,i} \left(1 + \frac{\rho_d}{\theta} K_{e,NH_4}\right) c_{NH_4,i}(t) dt < \Omega_{N,mean} < \Phi_{NO_3} + \Phi_{NH_4} \Rightarrow$$

$$\sigma_{NH_4} = \left(1 + \frac{\rho_d}{\theta} K_{e,NH_4}\right) \left(1 + \theta_i k_{gr,dif} \frac{\Delta z_i}{q_{ev,i}}\right) \frac{\Omega_{N,mean} - \Phi_{NO_3}}{\Phi_{NH_4}} \quad (94)$$

In all other situations the preferential parameter σ_{NH_4} takes the maximum value as defined in Eq. 77. The nitrate uptake parameters as defined in Eq. 76 are not adjusted, because the feed-back of nitrate-status of plant liquid to the uptake parameters has already been taken into consideration.

Tabel 3 denotes the set of parameters which has been used for Dutch climatic conditions all the time since the development of this sub-model in 1987.

Table 3 Parametrization of grassland related parameters in the ANIMO model

Parameter	Value	Unit
$Q_{s,ref}$	0.35	(kg m ⁻²)
κ	2.3	(-)
f_{ct}	0.321	(-)
f_{sh}	0.725	(-)
χ	0.62	(-)
$k_{gr,death}$	0.0055	(d ⁻¹)
$f_{gr,loss}$	0.2	(-)
$f_{ha,loss}$	0.2	(-)
threshold level Q_s for harvesting	0.4	(kg m ⁻²)
remaining quantity of shoots after harvesting (non-grazed pastures)	0.075	(kg m ⁻²)
remaining quantity of shoots after harvesting (grazed pastures)	0.165	(kg m ⁻²)
$k_{gr,dif}$	0.03	(d ⁻¹)
$f_{xs,min}$	0.019	(-)
$f_{N,r,min}$	0.0076	(-)
$f_{N,s,max}$	0.05	(-)
$f_{N,r,max}$	0.02	(-)
f_{ds}	0.2	(-)

Nitrogen uptake by arable crops

The nutrient uptake by arable crops has been described by a simple model. The growth period has been divided into two periods. During each period the concentration in the transpiration flux resulting in optimum growth is defined as:

$$c_{opt,1} = \frac{U^*_1}{t_c \sum_p q_{tr}} \quad c_{opt,2} = \frac{U^*_2}{t_h \sum_c q_{tr}} \quad (95)$$

where:

- $c_{opt,1}; c_{opt,2}$: optimal concentrations in the transpiration flux (kg m⁻³)
- $U^*_1; U^*_2$: reference cumulative uptake within the time span (kg m⁻²)
- $\sum q_{tr}$: expected cumulative transpiration within the time span (m)
- t_p : planting time (-)
- t_c : transition between both growing periods (-)
- t_h : harvesting date (-)

The expected optimal cumulative uptake and cumulative transpiration flow are defined by the user in the model input files. For years with higher or lower transpiration rates, the total crop uptake will increase or decrease proportionally. Under optimal circumstances, the plant uptake parameters σ_{NO_3} and σ_{NH_4} are defined as:

$$\sigma_{NO_3} = \frac{c_{opt,1}}{c_{NO_3}(t_0)} \quad \text{or} \quad \sigma_{NO_3} = \frac{c_{opt,2}}{c_{NO_3}(t_0)} \quad (96)$$

and:

$$\sigma_{NH4} = \frac{c_{opt,1}}{c_{NH4}(t_0)} \quad \text{OR} \quad \sigma_{NH4} = \frac{c_{opt,2}}{c_{NH4}(t_0)} \quad (97)$$

Under non-optimal conditions (excessive supply or uptake deficit), the parameters are adjusted according to the hypothesis that actual crop uptake depends on both the soil availability and on crop requirement. The mineral nitrogen requirement during a simulation time interval is defined in three categories.

1. Demand due to deficit in N-uptake during previous time steps:

$$\Omega_{N,def} = \sum_{t=t_p}^{t_0} \sum_{i=1}^{N_r} c_{opt} q_{tr,i} \Delta t - \sum_{t=t_p}^{t_0} \sum_{i=1}^{N_r} (c_{NO3,i} + (1 + \frac{\rho_d}{\theta} K_{e,NH4}) c_{NH4,i}) q_{tr,i} \Delta t \quad (98)$$

2. Demand due to dry matter increase of the crop during the time interval:

$$\Omega_{N,gr} = c_{opt} \Delta t \sum_{i=1}^{N_r} q_{tr,i} \quad (99)$$

3. Luxurious consumption, which occurs under excessive supply conditions in the soil:

$$\Omega_{N,lux} = \left(\sum_{t=t_p}^{t_0} \sum_{i=1}^{N_r} c_{opt} q_{tr,i} \Delta t + c_{opt} \Delta t \sum_{i=1}^{N_r} q_{tr,i} \right) \frac{\sum_{i=1}^{N_r} \theta_i \Delta z_i (c_{NO3,i}(t) + (1 + \frac{\rho_d}{\theta} K_{e,NH4}) c_{NH4,i}(t))}{1000 f_{r_N} \sum_{i=1}^{N_r} \theta_i \Delta z_i} \frac{1 - f_{ds}}{f_{ds}} \quad (100)$$

where f_{r_N} is the nitrogen fraction in dry matter. A numeric value of 0.25 was found by calibration for the factor $(1 - f_{ds}) / (f_{ds} 1000 f_{r_N})$. Soil availability of mineral nitrogen is also determining the uptake of nitrate and ammonium. A preference for nitrate is assumed, based on the condition of electro-neutrality, and availability of nitrate and ammonium is considered separately. For arable land, the nitrate and ammonium availability are defined by:

$$\begin{aligned} \Phi_{NO3} &= \int_{t_0}^{t_0 + \Delta t} \sum_{i=1}^{N_r} q_{ev,i} c_{NO3,i}(t) dt \\ \Phi_{NH4} &= \int_{t_0}^{t_0 + \Delta t} \sum_{i=1}^{N_r} \left((1 + \frac{\rho_d}{\theta} K_{e,NH4}) q_{ev,i} c_{NH4,i}(t) \right) dt \end{aligned} \quad (101)$$

Combining both soil availability and crop demand, the following definitions for the

nitrate and ammonium selectivity factors can be given:

$$\begin{aligned} \Omega_{N,def} + \Omega_{N,gr} + \Omega_{N,lux} < \Phi_{NO3} & \rightarrow \\ \sigma_{NO3} = \frac{\Omega_{N,def} + \Omega_{N,gr} + \Omega_{N,lux}}{\Phi_{NO3}} \quad \wedge \quad \sigma_{NH4} = 0 & \end{aligned} \quad (102)$$

$$\begin{aligned} \Omega_{N,def} + \Omega_{N,gr} < \Phi_{NO3} < \Omega_{N,def} + \Omega_{N,gr} + \Omega_{N,lux} & \rightarrow \\ \sigma_{NO3} = \frac{\Omega_{N,def} + \Omega_{N,gr}}{\Phi_{NO3}} \quad \wedge \quad \sigma_{NH4} = 0 & \end{aligned} \quad (103)$$

$$\begin{aligned} \sigma_{N,max} \Phi_{NO3} < \Omega_{N,def} + \Omega_{N,gr} < \sigma_{N,max} \Phi_{NO3} + \Phi_{NH4} & \rightarrow \\ \sigma_{NO3} = \sigma_{N,max} \quad \wedge \quad \sigma_{NH4} = \frac{\Omega_{N,def} + \Omega_{N,gr} - \sigma_{N,max} \Phi_{NO3}}{\Phi_{NH4}} & \end{aligned} \quad (104)$$

$$\sigma_{N,max} (\Phi_{NO3} + \Phi_{NH4}) < \Omega_{N,def} + \Omega_{N,gr} \rightarrow \sigma_{NO3} = \sigma_{N,max} \quad \wedge \quad \sigma_{NH4} = \sigma_{N,max} \quad (105)$$

The uptake selectivity factor is bounded to a maximum value $\sigma_{N,max}$ in cases where the requirement exceeds a maximum level of the soil availability. In the national Water Systems Reconnaissance study in 1995/1996, $\sigma_{N,max}$ was taken 5.0.

Crop damage due to unfavourable mineral nitrogen status of the soil is assumed when the actual realized cumulative uptake is less than a certain fraction of the cumulative uptake for optimum growth. The permissible nitrogen deficit is bounded to a maximum value by adjusting the expected optimal cumulative uptake:

$$\begin{aligned} \Omega_{N,def,max} = f_{def,max} \sum_{t=t_p}^{t_0+\Delta t} \sum_{i=1}^{N_r} c_{opt} q_{tr,i} \Delta t & \\ - \sum_{t=t_p}^{t_0+\Delta t} \sum_{i=1}^{N_r} (c_{NO3,i} + (1 + \frac{\rho_d}{\theta} K_{e,NH4}) c_{NH4,i}) q_{tr,i} \Delta t & \end{aligned} \quad (106)$$

where $\Omega_{N,def,max}$ (kg m^{-2}) is the maximum uptake deficit and $f_{def,max}$ (-) is the fraction of cumulative uptake below which nutrient shortage results in unrecoverable crop damage. The reduction of the potential uptake level is illustrated in Figure 16.

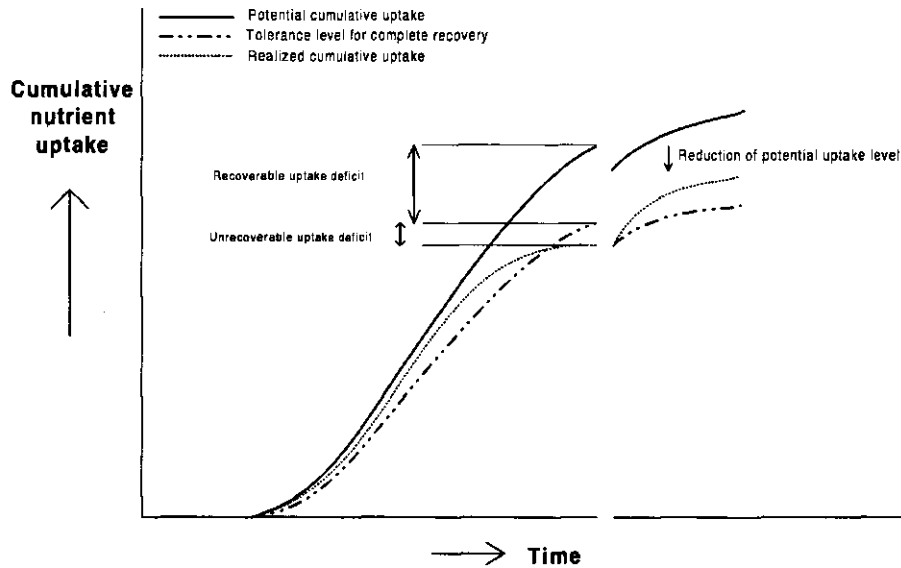


Fig. 16 Reduction of the potential uptake level when the uptake deficit exceeds a defined tolerance level

In the national Water Systems Reconnaissance study in 1995/1996, $f_{def,max}$ was taken 0.9. The optimal expected N-uptake is adjusted according to:

$$\left(\sum_{t=t_p}^{t_0+\Delta t} \sum_{i=1}^{N_r} c_{opt} q_{tr,i} \Delta t \right)_{adj} = \sum_{t=t_p}^{t_0+\Delta t} \sum_{i=1}^{N_r} c_{opt} q_{tr,i} \Delta t - \Omega_{N,def,max} \quad (107)$$

This unrecoverable crop damage ratio is also applied to the optimal expected phosphate uptake curve.

2.4.4 Mineralization and immobilization

As a result of organic matter dissimilation, part of the organic nitrogen is transformed into the mineral status. Another part of the organic nitrogen remains in the organic status in dead humic components. On the other hand, part of the mineral nitrogen can be immobilized through the biomass-synthesis in the living biomass. Depending on the assimilation ratio and the ratio between nitrogen content in parent fresh organic material and the nitrogen weight fraction of the humus/biomass pool, the transformation yields or requires mineral N. The nett mineralization (Fig. 14, relation 10, 11, 12 and 15) has been formulated as a zero-order term in the CTE of ammonium, defined by:

$$R_{p,NH_4} = \frac{1}{\Delta t} \int_{t_0}^{t_0+\Delta t} \left(\sum_{fn=1}^{nf} (f_{N,fn} - af_{N,hu}) f_{hu} k_{fn} OM_{fn}(t) + (f_N^L - af_{N,hu}) k_s (\theta c_{OM}) + (f_{N,ex} - af_{N,hu}) k_{ex} EX(t) + f_{N,hu} k_{hu} HU(t) \right) dt \quad (108)$$

where:

$f_{N,hu}$: nitrogen weight fraction of humus/biomass (-)

When the right hand side of the equation takes a negative value, ammonium is immobilized. No immobilization of nitrate has been assumed. When the initial quantity of ammonium at the beginning of the timestep is not sufficient to cover the total immobilization requirement, the assimilation ratio is decreased and less humus/biomass will be formed. In case of nitrogen shortage, the transformation occurs less efficient.

2.4.5 Nitrification and denitrification

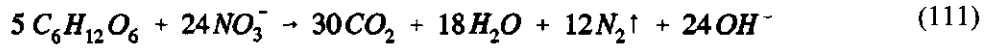
Under (partial) aerobic conditions in the soil system, ammonium is oxidized to nitrate (Fig. 14, relation 17). The production rate of nitrate is assumed proportional to the liquid concentration of ammonium. In the conservation and transport equation of ammonium, this process has been described by a first order rate kinetics:

$$R_{d,NH_4} = k_{nit} \theta c_{NH_4} \quad (109)$$

where k_{nit} is the first order rate constant. Under complete aeration and other favourable soil conditions, this constant equals the reference value as must be specified by the model user. When the moisture condition in soil leads to (partial) anaerobiosis, this constant is adapted by a multiplicative correction factor f_{ae} . At complete aeration f_{ae} takes the value one, at complete anaerobiosis f_{ae} equals zero. The numeric value of this factor is computed in a sub-model which describes the aeration process on the basis of oxygen diffusion in air filled soil pores and in saturated soil aggregates (Par. 2.6.1). In the conservation and transport equation of nitrate, the production rate R_p equals the average decomposition rate of ammonium which is given by the expression:

$$R_{p,NO_3} = \frac{1}{\Delta t} \int_{t_0}^{t_0+\Delta t} k_{nit} \theta c_{NH_4}(t) dt \quad (110)$$

Decomposition of organic materials under anaerobic conditions can proceed if sufficient nitrate-oxygen is available to meet the oxygen demand. At high nitrate concentrations, the oxygen requirement of organic decomposition processes is the rate limiting factor. At low nitrate contents, the NO_3 concentration can be the rate limiting factor for anaerobic decomposition. In the ANIMO model, it is assumed that denitrification is governed by:



The oxidation of one mol carbon requires 24/30 mol NO_3^- and the weight ratio between nitrogen and carbon reads 14/12. If the carbon content of organic material is taken as 58% on dry weight basis, it follows that the nitrate demand for denitrification can be expressed by a zero-order consumption term:

$$R_{p,den} = -0.58 \frac{24}{30} \frac{14}{12} f_{hetero} \frac{1}{\Delta t} \int_{t_0}^{t_0+\Delta t} \left(\sum_{fn=1}^{nf} (1-a) f_{hu} k_{fn} OM_{fn}(t) + (1-a)k_s(\theta c_{OM}) + (1-a)k_{ex}EX(t) + k_{hu}HU(t) \right) dt \quad (112)$$

The factor f_{hetero} has been introduced to account for the reduced organic matter transformation rates when only nitrate oxygen is available. In many field validations and regional applications, a value 0.5 has been assumed for f_{hetero} . In case the nitrate concentration limits the decomposition of organic materials under anaerobic conditions, the following first order rate expression has been defined:

$$R_{d,den} = k_{den} \theta c_{NO_3}(t) \quad (113)$$

where k_{den} is the first order rate constant to be defined as model input (d^{-1}). Determining which process rate limiting is done by computing both alternatives. The process leading to the highest nitrate concentration at the end of the time interval is subsequently selected by the model.

2.4.6 Transport of nitrogen substances

Inflow and outflow of dissolved organic nitrogen (Fig. 14, relation 9, 18 and 21) is modelled in close relation to the leaching of dissolved organic matter substances. The sink term for lateral mass transport towards surface water systems:

$$R_{x,ON} = k_d c_{ON} \quad (114)$$

$$R_{x,NH_4} = k_d c_{NH_4} \quad (115)$$

$$R_{x,NO_3} = k_d c_{NO_3} \quad (116)$$

2.5 Phosphorus cycle

Leaching of the soluble phosphorus substances organic-P and ortho-P is formulated as a part of the phosphorus cycle (Fig. 17).

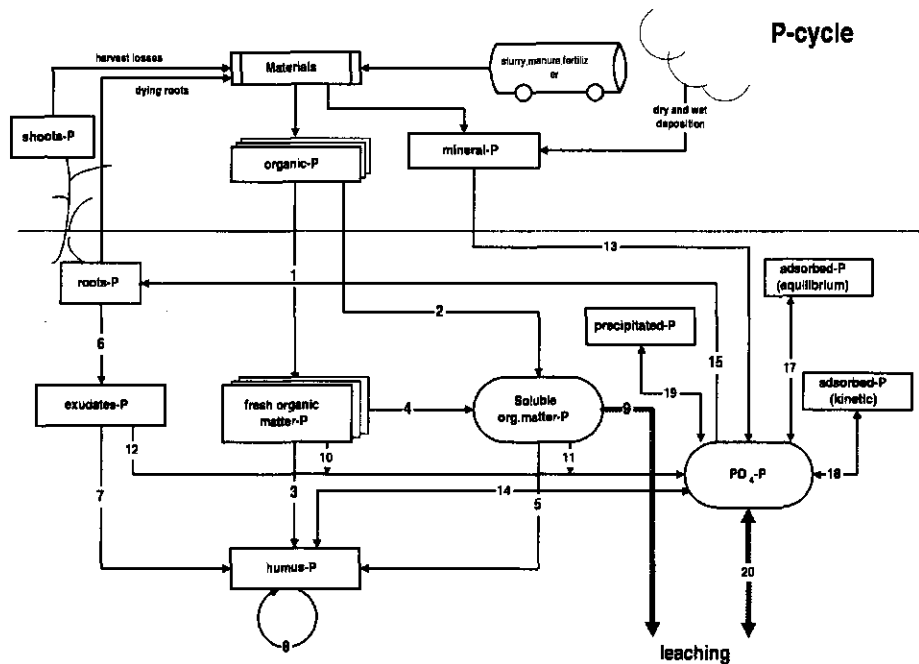


Fig. 17 Relational diagram of the phosphorus cycle described in the ANIMO-model

2.5.1 Phosphate sorption and precipitation

The *Langmuir* isotherm is derived from the assumption of a homogeneous monolayer of adsorbate on the adsorbent. The Langmuir equation is used to describe instantaneous sorption of phosphates to soil constituents (Enfield *et al.*, 1981; Van Noordwijk *et al.*, 1990).

$$X_{e,PO_4} = X_{e,max,PO_4} \frac{K_L c_{PO_4}}{1 + K_L c_{PO_4}} \quad (117)$$

The amount of chemical sorbed to the soil matrix never exceeds the maximum sorption capacity X_{e,max,PO_4} . The formulations given above can be incorporated into the conservation equation by elaborating the differential quotient $\partial X_{e,PO_4} / \partial t$:

$$\rho_d \frac{\partial X_{e,PO_4}}{\partial t} = \rho_d \left(\frac{dX_{e,PO_4}}{dc_{PO_4}} \right) \frac{\partial c_{PO_4}}{\partial t} = \rho_d K_a(c_{PO_4}) \frac{\partial c_{PO_4}}{\partial t} \quad (118)$$

where $K_a(c_{PO_4})$ is the differential sorption coefficient. The differential adsorption coefficient is approximated by the average value $\bar{K}_a(c_{PO_4})$. This value is assessed by calculating the slope of the chord of the adsorption isotherm:

$$\bar{K}_a(c_{PO_4}) = \frac{1}{c_{PO_4}(t) - c_{PO_4}(t_0)} \int_{t_0}^t \left(\frac{dX_{e,PO_4}}{dc_{PO_4}} \right) dc_{PO_4} = \frac{X_{e,PO_4}(t) - X_{e,PO_4}(t_0)}{c_{PO_4}(t) - c_{PO_4}(t_0)} \quad (119)$$

Although $K_a(c_{PO_4})$ is a function of the concentration, its average value is considered to be constant during the timestep. Schoumans (1995) established the following set of parameters of the Langmuir-isotherm which describes the fast phosphate sorption for a wide range of sandy soils: $K_L = 1129 \text{ (m}_w^3 \text{ kg}^{-1} \text{ P)}$ and $X_{e,max,PO_4} = 5.167 \cdot 10^{-6} \rho_d [Al+Fe] \text{ (kg m}_s^{-3} \text{ P)}$ where $[Al+Fe]$ is the aluminium + iron content of the soil in mmol kg^{-1} .

If equilibrium is not achieved rapidly enough compared to advective transport the sorption process must be addressed by kinetic models (Pignatello, 1989; Selim and Amacher, 1988). In such cases, sorption appears to be limited by a type of chemical reaction rate or physical mass transfer resistance. Desorption of phosphates, even when far-reaching measures are implemented, may cause an exceedance of water quality standards for long periods. Although considerable efforts have been dedicated to model phosphate behaviour in soils (Van der Zee, 1988; Van der Zee and Van Riemsdijk, 1991), their theory defining the exposure integral as a variable characterizing long-term sorption/precipitation has not yet delivered operational tools for prediction of leaching after fertilization reductions. The exposure integral results from the so called 'unreacted shrinking core model' which is based on phosphate transfer in soil aggregates by diffusion and the formation of solid phosphate minerals at the inner boundary of the reaction-zone. The normalized exposure integral I is defined as:

$$I = \frac{1}{c_r t_r} \int_{t_0}^t (c - c_e) dt \quad (120)$$

where $c_r t_r$ is a reference value referring to experimental conditions. Empirical relations are used to relate the exposure integral to experimental field data. Until now the exposure integral appears not appropriate to describe the reverse reactions. Therefore, descriptive formulations have been chosen which have also been utilized to address time dependent sorption behaviour of pesticides (Boesten, 1986). The diffusive transition zone is described by one lumped first order rate equation and the chemical fixation by a Freundlich sorption isotherm. The Freundlich equation represents a composition of Langmuir-curves. An individual Langmuir-curve describes the fixation of a chemical substance to a sorptive medium of limited capacity. Therefore, the Freundlich relation appears more suitable for a heterogeneous soil medium, composed of a finite number of homogeneous soil aggregates. The general formulation of a first

order rate sorption (chemical nonequilibrium) model is:

$$\begin{aligned} f_s(c_{PO4}) > X_{n,PO4} & \quad \rho_d \frac{\partial X_{n,PO4}}{\partial t} = \rho_d k_{ads} (f_s(c_{PO4}) - X_{n,PO4}) \\ f_s(c_{PO4}) < X_{n,PO4} & \quad \rho_d \frac{\partial X_{n,PO4}}{\partial t} = \rho_d k_{des} (f_s(c_{PO4}) - X_{n,PO4}) \end{aligned} \quad (121)$$

where k_{ads} and k_{des} (d^{-1}) are rate constants and $f_s(c_{PO4})$ is the solid phase solute concentration determined by equilibrium adsorption isotherms. The difference between the equilibrium concentration which is reached in the steady state situation and the actual solid phase concentration is considered as the driving force for mass transfer. In the case of kinetic phosphate sorption, the rate equation is defined as follows:

$$\rho_d \frac{\partial X_{n,PO4}}{\partial t} = \rho_d (k_{ads} k_{des}) (K_F c_{PO4}^{N_{PO4}} - X_{n,PO4}) \quad (122)$$

When appropriate parameters are chosen, the formulations given in the preceding section can be utilized to simulate the phosphate diffusion/precipitation model presented by Van der Zee and Bolt (1991) and Van der Zee and Van Riemsdijk (1991). Mansell *et al.*, (1977) applied a rate dependent model to describe non-equilibrium behaviour of phosphate sorption in sandy soils.

The ANIMO-model describes the rate dependent phosphate sorption to soil constituents by considering three separate sorption sites:

$$\rho_d \frac{\partial X_{n,PO4}}{\partial t} = \rho_d \sum_{i=1}^3 \frac{\partial X_{n,PO4,i}}{\partial t} = \rho_d \sum_{i=1}^3 (k_{ads,i} k_{des,i}) (K_{F,i} c_{PO4}^{N_{PO4,i}} - X_{n,PO4,i}) \quad (123)$$

In a validation study for a wide range of Dutch sandy soil, Schoumans (1995) assessed the following parameters for Eq. 125:

Table 4 Parameters describing the rate dependent phosphate sorption for a wide range of Dutch sandy soils (after Schoumans, 1995)

Sorption Parameter class i	$k_{ads,i}$ (d^{-1})	$K_{F,i}$ ($kg\ m_s^{-3}$) ($kg\ m_w^{-3}$) ^{-N}	$N_{PO4,i}$ (-)
1	1.1755	$11.87 \cdot 10^{-6} \rho_d^a [Al+Fe]^b$	0.5357
2	0.0334	$4.667 \cdot 10^{-6} \rho_d [Al+Fe]$	0.1995
3	0.0014382	$9.711 \cdot 10^{-6} \rho_d [Al+Fe]$	0.2604

^a dry bulk density in $kg\ m^{-3}$

^b aluminium and iron content in $mmol\ kg^{-1}$

Data on the first order rate coefficient of the desorption relation $k_{des,i}$ are still missing. Numerical elaboration of the rate dependent sorption equation requires an expression for the differential quotient. This expression can be obtained by taking the value of the time averaged concentration instead of the concentration $c_{PO4}(t)$ at time $t = t$. Integration of the differential equation between limits t_0 and $t_0 + \Delta t$ and dividing by

the time increment Δt yields:

$$\frac{1}{\Delta t} \int_{t_0}^{t_0+\Delta t} \frac{dX_{n,PO_4}}{dt} dt = \frac{X_{n,PO_4}(t_0+\Delta t) - X_{n,PO_4}(t_0)}{\Delta t} \quad (124)$$

where $X_{n,PO_4}(t_0)$ is the amount of chemical bounded to non-equilibrium sorption sites at the beginning of the time interval. In order to calculate the amount of chemical assigned to X_{n,PO_4} at the end of the time interval, the function which describes the exchange between solution and time dependent sorption phase $f_s(c)$ is linearized. The function $f_s(c)$ is approximated by $f_s(\bar{c})$ where \bar{c} is the average concentration during the time-interval.

$$\frac{\partial X_{n,PO_4}}{\partial t} = (k_{ads}k_{des}) (f_s(\bar{c}_{PO_4}) - X_{n,PO_4}) \quad (125)$$

Although the average concentration is unknown at the start of the computations, \bar{c}_{PO_4} can be considered as a constant. The following solution can be derived subject to the condition $X_{n,PO_4} = X_{n,PO_4}(t_0)$ at the beginning of the time interval.

$$X_{n,PO_4}(t_0+\Delta t) = f_s(\bar{c}_{PO_4}) + (X_{n,PO_4}(t_0) - f_s(\bar{c}_{PO_4})) e^{-(k_{ads}k_{des}) \Delta t} \quad (126)$$

In order to obtain an expression for Eq. 123, Eq. 126 can be rewritten as:

$$\frac{X_{n,PO_4}(t_0+\Delta t) - X_{n,PO_4}(t_0)}{\Delta t} = (f_s(\bar{c}_{PO_4}) - X_{n,PO_4}(t_0)) \frac{(1 - e^{-(k_{ads}k_{des}) \Delta t})}{\Delta t} \quad (127)$$

For concentration ranges below the equilibrium level of phosphate precipitation processes, the following conservation-transport equation holds:

$$\frac{d\theta(t)c_{PO_4}(t)}{dt} + \rho_d \bar{K}_a(c_{PO_4}) \frac{dc_{PO_4}(t)}{dt} = \frac{q_{i-\frac{1}{2}} c_{i-1}}{\Delta z} - \frac{q_{i+\frac{1}{2}}}{\Delta z} c_{PO_4}(t) - \frac{\sigma_p q_{tr}}{\Delta z} c_{PO_4}(t) - \quad (128)$$

$$k_1 \theta(t) c_{PO_4}(t) + R_p + \rho_d \sum_{i=1}^3 (X_{n,PO_4,i}(t_0) - K_{F,i} \bar{c}_{PO_4}^{N_{PO_4,i}}) \frac{(1 - e^{-(k_{ads,i}k_{des,i}) \Delta t})}{\Delta t}$$

Phosphate precipitation takes place when the concentration of the bulk solution exceeds a defined equilibrium concentration c_{eq} . The precipitation reaction is modelled as an instantaneous reaction (Fig. 17, relation 19). The reaction occurs immediately and complete when the solute concentration exceeds the equilibrium concentration c_{eq} . The precipitated minerals dissolve immediately when the concentration of the water phase drops below the buffer concentration. When the store of precipitated minerals has been exhausted, the term $\partial X_{p,PO_4} / \partial t$ equals zero. In most of the application of the ANIMO model for Dutch sandy soils, the parametrization of the model has been restricted to the instantaneous precipitation formulation. For establishing the equilibrium concentration, the following relation between pH and c_{eq} has been utilized: While applying the model in combination with the instantaneous precipitation reaction,

$$c_{eq} = 0.135 \cdot 3^{5-pH} \approx 10^{-0.447 pH + 1.516} \quad (129)$$

While applying the model in combination with the instantaneous precipitation reaction, four situations with respect to the concentration course with time within a time increment are relevant to consider:

- | | | | |
|----|---|------------------------|--|
| 1) | $t_0 \leq \text{time} \leq t_0 + \Delta t:$ | $c_{PO4} < c_{eq},$ | $X_{p,PO4} = 0, \partial X_{p,PO4} / \partial t = 0;$ |
| 2) | $t_0 \leq \text{time} < t_1:$ | $c_{PO4} < c_{eq},$ | $X_{p,PO4} = 0, \partial X_{p,PO4} / \partial t = 0;$ |
| | $t_1 \leq \text{time} \leq t_0 + \Delta t:$ | $c_{PO4} = c_{eq},$ | $X_{p,PO4} \geq 0, \partial c_{PO4} / \partial t = 0;$ |
| 3) | $t_0 \leq \text{time} < t_1:$ | $c_{PO4} = c_{eq},$ | $X_{p,PO4} > 0, \partial c_{PO4} / \partial t = 0;$ |
| | $t_1 \leq \text{time} \leq t_0 + \Delta t:$ | $c_{PO4} \leq c_{eq},$ | $X_{p,PO4} \geq 0, \partial X_{p,PO4} / \partial t = 0;$ |
| 4) | $t_0 \leq \text{time} < t_0 + \Delta t:$ | $c_{PO4} = c_{eq},$ | $X_{p,PO4} > 0, \partial c_{PO4} / \partial t = 0.$ |

The four possibilities to consider are explained in Figure 18.

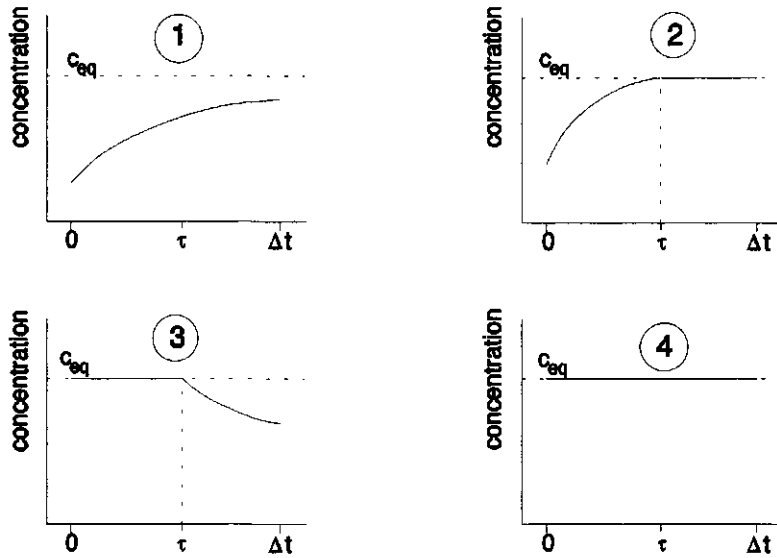


Fig. 18 Four possibilities of the concentration course with time within a timestep Δt establishing an eventual exceedance of the equilibrium concentration c_{eq}

In the 2th and 3th situation the time interval has to be split up into two parts. The length of the first part t_1 is calculated from its specific conditions combined with the conservation equation.

Under the presence of precipitated phosphate, the concentration $c(t)$ as well as the average concentration \bar{c} equals the equilibrium concentration c_{eq} ($\partial c_{PO4} / \partial t = 0$). Then, the conservation equation reads as follows:

$$\rho_d \frac{dX_{p,PO_4}}{dt} = \frac{q_{i-1/2} c_{i-1}}{\Delta z} - \frac{q_{i+1/2}}{\Delta z} c_{PO_4}(t) - \frac{\sigma_p q_{tr}}{\Delta z} c_{PO_4}(t) - k_1 \theta(t) c_{PO_4}(t) + R_p \quad (130)$$

$$+ \rho_d \sum_{i=1}^3 (X_{n,PO_4,i}(t_0) - K_{F,i} \bar{c}_{PO_4}^{N_{PO_4,i}}) \frac{(1 - e^{-(k_{ads,i} + k_{des,i}) \Delta t})}{\Delta t}$$

2.5.2 Fertilization and tillage

Fresh organic matter-phosphorus

Similar to the nitrogen sub-model, fertilization has been described as a pulse-wise addition of materials with a defined composition. The quantity of organic P after the introduction of a certain material is calculated by summarizing the quantity before the addition and the applied dose (Fig. 17, relation 1):

$$OP_{fn}(t+\tau) = OP_{fn}(t) + f_{P,fn} (f_{i,fn} - f_{i,fn}^L) \frac{f_i^O M_i}{\Delta z} \quad (131)$$

where:

- $OP_{fn}(t+\tau)$: volumic mass of organic phosphorus after application (kg m^{-3})
- $OP_{fn}(t)$: volumic mass of organic phosphorus fn before application (kg m^{-3})
- $f_{P,fn}$: phosphorus content of organic matter class fn (-)

Soluble phosphorus compounds

The concentration of dissolved organic P is calculated by (Fig. 17, relation 2):

$$c_{OP}(t+\tau) = c_{OP}(t) + \sum_{fn=1}^{nf} f_{P,fn} f_{i,fn}^L \frac{f_i^O M_i}{\theta \Delta z} \quad (132)$$

where:

- $c_{OP}(t+\tau)$: dissolved organic phosphorous concentration after addition (kg m^{-3})
- $c_{OP}(t)$: dissolved organic phosphorous concentration before addition (kg m^{-3})

Similar to additions of other dissolved substances, the mineral compounds can be added to the soil system pulse-wise. The mineral phosphorus concentrations after an addition read (Fig. 17, relation 13):

$$\theta c_{PO_4}(t+\tau) + \rho_d X_{e,PO_4,\max} \frac{K_L c_{PO_4}(t+\tau)}{1 + K_L c_{PO_4}(t+\tau)} = \quad (133)$$

$$\theta c_{PO_4}(t) + \rho_d X_{e,PO_4,\max} \frac{K_L c_{PO_4}(t)}{1 + K_L c_{PO_4}(t)} + \frac{f_{PO_4} M_i}{\Delta z}$$

where:

$c_{PO_4}(t+\tau)$: phosphate concentration after addition (kg m^{-3} P)
 $c_{PO_4}(t)$: phosphate concentration before addition (kg m^{-3} P)
 f_{PO_4} : phosphate content of the applied substance M (kg kg^{-1})

If the liquid concentration tends to exceed the buffer concentration, $c_{PO_4}(t+\tau)$ takes the value of the equilibrium concentration and the remaining part of the addition is added to the precipitation pool:

$$\theta c_{eq} + \rho_d X_{e,PO_4,max} \frac{K_L c_{eq}}{1 + K_L c_{eq}} + X_{p,PO_4}(t+\tau) = \theta c_{PO_4}(t) + \rho_d X_{e,PO_4,max} \frac{K_L c_{PO_4}(t)}{1 + K_L c_{PO_4}(t)} + \frac{f_{PO_4} M_i}{\Delta z} \quad (134)$$

2.5.3 Crop uptake

Phosphate uptake by grassland

Uptake of mineral phosphate by plant roots has been described in strong relation to nitrogen uptake. However, for phosphorus no accumulation for future growth has been assumed.

$$R_{u,P} = \sigma_P \frac{q_r}{\Delta z} c_{PO_4}(t) \quad (135)$$

The selectivity factor σ_P is defined on the basis of soil availability and crop requirement. Soil availability of phosphate is calculated as the sum of the amounts present in the liquid phase, the fast sorption pool X_e (equilibrium) and the precipitation pool X_p . The phosphorus uptake under unconstrained conditions equals the mineral P availability:

$$U(t_0 + \Delta t) = U(t_0) + \Phi_{PO_4} \quad (136)$$

where the mineral phosphorus availability is approximated by:

$$\Phi_{PO_4} = \int_{t_0}^{t_0 + \Delta t} \sum_{i=1}^{N_r} \left(1 + \frac{\rho_d}{\theta_i} K_{d,i}^{ap} \right) q_{r,i} c_{PO_4,i}(t) dt \quad (137)$$

with K_d^{ap} as the apparent linear sorption coefficient defined by:

$$K_{d,i}^{ap} = \frac{X_{e,i} + X_{p,i}}{c_{PO_4,i}} \quad (138)$$

The phosphate requirement for plant growth is defined as the gross dry matter production multiplied by the actual phosphorus content of shoots and roots:

$$\Omega_P = \max\left(1, \frac{U(t)}{f_{P,s,\min} Q_s(t) + f_{P,r,\min} Q_r(t)}\right) f_{P,s,\min} \int_{t_0}^{t_0+\Delta t} \left(\frac{dQ_s(t)}{dt} + W + \frac{f_{P,r,\min}}{f_{P,s,\min}} \left(\frac{dQ_r(t)}{dt} + k_{d,gr} Q_r(t) \right) \right) dt \quad (139)$$

The P-fractions relate to the total N-fractions according to an empirical relation given by Rijtema *et al.*, (1999):

$$fr_P = 0.0318 (fr_N)^{0.59} \quad (140)$$

Based on the demand and the availability, the plant uptake parameter σ_P is defined by:

$$\Phi_P > \Omega_P \Rightarrow \sigma_P = \frac{\Omega_P}{\Phi_P} \quad (141)$$

$$\Omega_P > \sigma_{P,\max} \Phi_P \Rightarrow \sigma_P = \sigma_{P,\max} \quad (142)$$

In the Water Systems Reconnaissance study (1995/1996) the maximum value of the plant parameter ($\sigma_{P,\max}$) has been taken one.

Phosphate uptake by arable crops

P-uptake by arable crops has been described similarly to the nitrogen uptake. The model user has to define expected optimal cumulative uptake quantities for two periods of the growing season. Optimal uptake concentrations are derived from these quantities. The uptake parameter σ_P is defined as the ratio between the optimal uptake concentration and the current liquid concentration in the root zone. An unfavourable nutrient status can thus lead to an increased value of this parameter σ_P . The value of σ_P is bounded to a maximum due to limited soil availability.

Three types of crop demand have been identified: luxurious demand, growth and maintenance demand and a demand induced by an uptake deficit:

1. Demand due to deficit in P-uptake during previous time steps:

$$\Omega_{P,def} = \sum_{t=t_p}^{t_0} \sum_{i=1}^{N_r} c_{opt} q_{n,i} \Delta t - \sum_{t=t_p}^{t_0} \sum_{i=1}^{N_r} \left(1 + \frac{\rho_d}{\theta} K_d^{ap}\right) c_{PO4,i} q_{n,i} \Delta t \quad (143)$$

2. Demand due to growth during the time interval:

$$\Omega_{P,gr} = c_{opt} \Delta t \sum_{i=1}^{N_r} q_{tr,i} \quad (144)$$

3. Luxurious consumption, which is assumed to take place under excessive supply conditions in the soil:

$$\Omega_{P,lux} = \left(\sum_{t=t_p}^{t_0} \sum_{i=1}^{N_r} c_{opt} q_{tr,i} \Delta t + c_{opt} \Delta t \sum_{i=1}^{N_r} q_{tr,i} \right) \cdot \frac{\sum_{i=1}^{N_r} \theta_i \Delta z_i \left(1 + \frac{\rho_d}{\theta} K_d^{ap} c_{PO_4,i}(t) \right)}{1000 fr_p \sum_{i=1}^{N_r} \theta_i \Delta z_i} \frac{1 - f_{ds}}{f_{ds}} \quad (145)$$

where fr_p is the phosphorus fraction in dry matter of productive parts and K_d^{ap} is the apparent linear sorption coefficient as has been given in Eq. 138. Based on the crop requirement and the soil availability, the following selectivity coefficients are calculated:

$$\Phi_P > \Omega_{P,def} + \Omega_{P,gr} + \Omega_{P,lux} \Rightarrow \sigma_P = \frac{\Omega_{P,def} + \Omega_{P,gr} + \Omega_{P,lux}}{\Phi_P} \quad (146)$$

$$\Omega_{P,def} + \Omega_{P,gr} < \Phi_P < \Omega_{P,def} + \Omega_{P,gr} + \Omega_{P,lux} \Rightarrow \sigma_P = 1 \quad (147)$$

$$\frac{(\Omega_{P,def} + \Omega_{P,gr})}{\sigma_{P,max}} < \Phi_P < \Omega_{P,def} + \Omega_{P,gr} \Rightarrow \sigma_P = \frac{\Omega_{P,def} + \Omega_{P,gr}}{\Phi_P} \quad (148)$$

In all other situations, the selectivity factor takes the maximum value $\sigma_{P,max}$.

Crop damage due to limited P-availability is estimated similar to the crop response to a shortage of mineral nitrogen in the root zone. If a certain threshold phosphorus deficit is exceeded, the expected optimal cumulative uptake is adjusted:

$$\Omega_{P,def,max} = f_{def,max} \sum_{t=t_p}^{t_0+\Delta t} \sum_{i=1}^{N_r} c_{opt} q_{tr,i} \Delta t - \sum_{t=t_p}^{t_0+\Delta t} \sum_{i=1}^{N_r} \left(1 + \frac{\rho_d}{\theta} K_d^{ap} \right) c_{PO_4,i} q_{tr,i} \Delta t \quad (149)$$

where $\Omega_{P,def,max}$ (kg m^{-2}) is the maximum uptake deficit. The optimal expected P-uptake is adjusted according to:

$$\left(\sum_{t=t_p}^{t_0+\Delta t} \sum_{i=1}^{N_t} c_{opt} q_{tr,i} \Delta t \right)_{adj} = \sum_{t=t_p}^{t_0+\Delta t} \sum_{i=1}^{N_t} c_{opt} q_{tr,i} \Delta t - \Omega_{P,def,max} \quad (150)$$

This unrecoverable crop damage ratio results also in a reduction of the optimal nitrogen uptake curve.

2.5.4 Mineralization and immobilization

Mineralization of organic phosphorous and immobilization (Fig. 17, relation 10, 11, 12, 14) of mineral phosphorus compounds is formulated analogous to nitrogen mineralization and immobilization. Depending on the assimilation ratio and the ratio between nitrogen content in parent fresh organic material and the phosphorus weight fraction of the humus/biomass pool, the organic transformation processes yield or require mineral P. The nett mineralization has been formulated as a zero-order term in the CTE of mineral phosphate, defined by:

$$R_{P,PO_4} = \frac{1}{\Delta t} \int_{t_0}^{t_0+\Delta t} \left(\sum_{fn=1}^{nf} (f_{P,fn} - a_{f_{P,hu}}) f_{hu} k_{fn} OM_{fn}(t) + (f_P^L - a_{f_{P,hu}}) k_s (\theta c_{OM}) + (f_{P,ex} - a_{f_{P,hu}}) k_{ex} EX(t) + f_{P,hu} k_{hu} HU(t) \right) dt \quad (151)$$

where:

$f_{P,hu}$: phosphorus weight fraction of humus/biomass (-)

When the right hand side of the equation takes a negative value, phosphate is immobilized. In case the initial quantity of readily available phosphate at the beginning of the timestep is not sufficient to cover the total immobilization requirement, the assimilation ratio is decreased and less humus/biomass will be formed.

2.5.5 Transport of phosphorous substances

Inflow and outflow of dissolved organic phosphorus (Fig. 17, relation 9, 20) is modelled through the leaching of dissolved organic matter substances. The sink term for lateral mass transport towards surface water systems reads:

$$R_{x,OP} = k_d c_{OP} \quad (152)$$

$$R_{x,PO_4} = k_d c_{PO_4} \quad (153)$$

2.6 Environmental influences on transformation rates

Transformation rate coefficients decomposition of fresh organic materials, dissolved organic matter, exudates and humus biomass and the nitrification rate coefficient are defined by a reference value k_{ref} . Environmental influences are taken into account by multiplication factors for reduced aeration at wet conditions, drought stress at dry conditions, temperature and pH. For organic transformation processes:

$$k = f_{ae,OM} f_T f_{\theta} f_{pH} k_{ref} \quad (154)$$

For the nitrification process:

$$k = f_{ae} f_T f_{\theta} f_{pH} k_{ref} \quad (155)$$

where:

- k : actual transformation rate (d^{-1})
- k_{ref} : reference value of the rate constant under optimal conditions (d^{-1})
- f_{ae} : factor accounting for of the availability of atmospheric oxygen (-)
- $f_{ae,OM}$: factor for the combined effect of the oxygen availability and the nitrate availability on organic matter transformations (-)
- f_T : factor accounting for temperature (-)
- f_{θ} : factor accounting for dry conditions (-)
- f_{pH} : factor accounting for the influence of pH (-)

2.6.1 Aeration

Partitioning between aerobic and anaerobic phase

Aeration has a major influence on transformation rates of all micro-biological processes in agricultural eco-systems. Since one of the model aims is to evaluate the environmental impacts of water management for a wide range of soil types and a wide range of hydrological conditions, a detailed sub-model describing oxygen diffusion in the soil gas phase and in soil aggregates has been implemented. The aeration fraction f_{ae} depends on a number of factors:

- Oxygen demand, as a result of organic transformations and nitrification. Oxidation of other reduced components (e.g. sulphur) have been ignored;
- Soil physical constitution;
- Hydrological conditions (partitioning between soil moisture and soil air).

The aeration factor f_{ae} has been formulated as an multiplicative factor. At $f_{ae} = 1$, organic transformation and nitrification processes are optimal (Fig. 19). For sub-optimal conditions ($f_{ae} < 1$), the diffusive capacity of the unsaturated zone is insufficient to fulfill the oxygen requirement. In situations where partial anaerobiosis occurs, the oxygen demand for the organic transformations is met by atmospheric oxygen as well as by nitrate-oxygen. The nitrification rate will be sub-optimal. Under these conditions, the available nitrate will be reduced partial or complete (denitrification). Under unfavourable wet conditions the upper layers consume all

oxygen which can enter the soil profile by diffusion and the atmospheric oxygen will not penetrate into the lower part of the unsaturated zone.

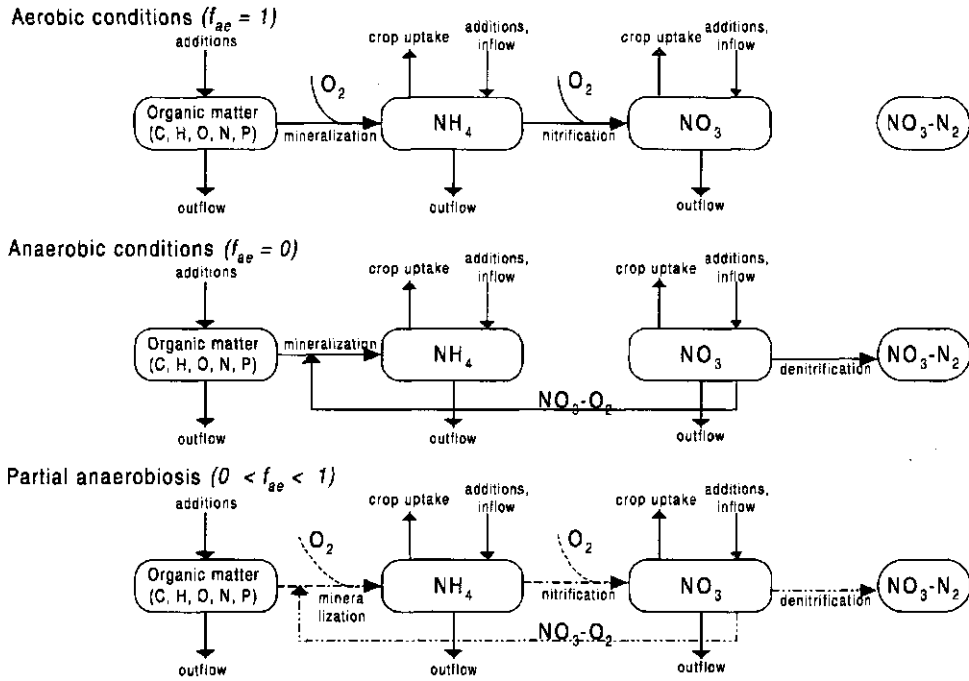


Fig. 19 Atmospheric oxygen and nitrate oxygen related processes in the ANIMO model

The partitioning between the aerobic soil fraction and the anaerobic soil fraction is determined by the equilibrium between oxygen demand for organic conversion processes plus nitrification and the oxygen supply capacity of the soil air and soil water system. Both the vertical diffusion in air filled pores and the lateral oxygen diffusion in the soil moisture phase are taken into consideration. Figure 20 shows the separation of both diffusive transports schematically.

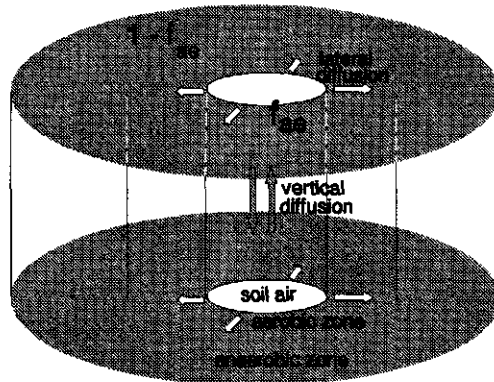


Fig. 20 Schematic representation of diffusive oxygen transport in the aeration module

Diffusion in soil gas phase

The vertical diffuse transport of oxygen in the airfilled pores in the soil system is described by:

$$\frac{\partial \theta_g c_g}{\partial t} = \frac{\partial}{\partial z} \left(D_g \frac{\partial c_g}{\partial z} \right) - f_{ae} 2.564 \cdot 10^{-3} (T+273.15) \Omega_{ox} \quad (156)$$

where Ω_{ox} is the demand for atmospheric oxygen. The factor $2.564 \cdot 10^{-3} (T+273.15)$ results from the Law of Boyle Gay-Lussac. The diffusion coefficient D_g is described as a function of soil moisture:

$$\frac{D_g}{D_o} = p_1 (\theta_{sat} - \theta)^{p_2} \quad (157)$$

Several expressions can be found to relate the diffusion coefficient in the soil gas phase to the diffusion coefficient in air. In literature different relations between the diffusion coefficient and the volumetric gas content can be found, but the formulation given in Eq. 160 has been chosen for reasons of data acquisition. Bakker *et al.*, (1987) provide a review on different formulations and experimental data.

Table 5 Parametrization of the relation between the oxygen diffusion coefficient and volumetric gas content according to Bakker et al., (1987)

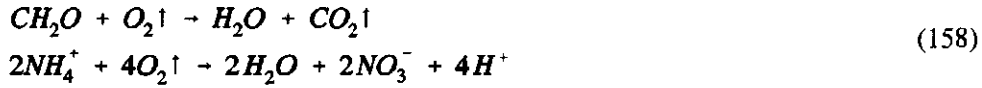
Soil type	p_1	p_2
Poor loamy and humusless sands	1.5	3.0
Structureless loamy sands	7.5	4.0
Weakly aggregated topsoils of loamy sands, light clays and humous sands, subsoils of light clays	2.5	3.0
Aggregated light clays	2.0	2.5
Dense clay soils	0.3	1.5

In most regional model applications, the diffusive properties of soils have been schematized to three classes: good, moderate and bad capabilities for oxygen diffusion.

Table 6 Assumed parametrization of the relation between the oxygen diffusion coefficient and the volumetric gas content in some regional studies

Diffusive property	p_1	p_2	Soil units according 'Staring Reeks'
Good	0.3	1.5	B07, B09, B10, B11, B12, B16, B18
Moderate	2.0	2.5	B03, B04, B08, B13, B14, B15, B17
Bad	2.5	3.0	B01, B02, B05, B06

Organic decomposition as well as nitrification require oxygen. Stoichiometric factors are based on the assumption that these transformations are governed by:



The oxygen demand which results from nitrification and aerobic decomposition of organic materials is expressed by Ω_{ox} :

$$\begin{aligned}
\Omega_{ox} = \frac{32}{12} 0.58 \left(\sum_{fn=1}^{nf} (1-a) f_{hu} k_{fn} OM(t) + (1-a) k_{ex} EX(t) + \right. \\
\left. (1-a) k_s (\theta c_{OM}(t)) + k_{hu} HU(t) \right) + \frac{128}{28} k_{nit} \theta c_{NH_4}(t)
\end{aligned}
\tag{159}$$

The oxygen requirement of respiratory processes of living roots has been neglected. When the defined oxygen requirement can be fully satisfied by supply from the atmosphere, the factor f_{ae} takes the value one. However, when the diffusive process in the water filled aggregate pores is not fast enough to create complete aerobic circumstances, part of the soil layer will be anaerobic. The oxygen consumption of such a layer will be smaller than Ω_{ox} . Under these circumstances nitrification does not occur and it is assumed that the activity of the organic biomass is less and that the transformations occur at lower rates.

$$\begin{aligned}
\Omega_{ox} = \frac{32}{12} 0.58 f_{hetero} \left(\sum_{fn=1}^{nf} (1-a) f_{hu} k_{fn} OM(t) + (1-a) k_{ex} EX(t) + \right. \\
\left. (1-a) k_s (\theta c_{OM}(t)) + k_{hu} HU(t) \right)
\end{aligned}
\tag{160}$$

where f_{hetero} is a factor accounting for the lower transformation rates at unfavourable circumstances within the anaerobic part of a soil layer.

The introduction of the reduction factor f_{ae} enables the calculation of an oxygen profile on the basis of actual oxygen consumption rates. Under field conditions, the oxygen transport in the soil gas phase will be in equilibrium within a few hours. The diffusion coefficient of oxygen in air will take the value $1.64 \text{ m}^2 \text{ d}^{-1}$ at 10°C . Taking p_1 and p_2 as 2.0 and 2.5 and assuming a volumetric gas content of 10% yields $10^{-2} \text{ m}^2 \text{ d}^{-1}$ as the value of D_g . When the layer thickness equals 0.1, the factor $D_g/(\Delta z)^2$ will amount 1 d^{-1} . For longer time increments (e.g. 10 days), equilibrium will be achieved within a fraction of the time step and the diffusion process can be approximated by steady-state diffusion profiles. Such a diffusion equation reads:

$$\frac{d}{dz} \left(D_g \frac{dc_g}{dz} \right) = f_{ae} 2.564 \cdot 10^{-3} (T+273.15) \Omega_{ox}
\tag{161}$$

The factor f_{ae} is a function of the oxygen concentration in the gas phase, the potential oxygen consumption rate and soil moisture conditions related to the soil type.

The soil system is divided into a number of layers, each with its own thickness. The

diffusion coefficient D_g and the oxygen consumption rate b are considered to be constant per soil layer and per timestep. Since the factor f_{ae} is dependent on the oxygen concentration, an iterative computation scheme is required to determine its value. In the first iteration round, the factor is set to 1 and oxygen concentrations are calculated using the vertical diffusion model. Then new values of f_{ae} are calculated per layer using the radial diffusion model. This model uses the calculated oxygen concentrations and the potential oxygen consumption rate as input. After determining f_{ae} -values, a new computation round starts. The iteration procedure will be terminated when the cumulative difference between old and new values is less than a certain criterium.

When solving the differential equation for vertical diffusive transport, two boundary conditions can be identified. At the ground surface, the soil air concentration equals the concentration in the free atmosphere. At the groundwaterlevel, a zero-diffusion flux is assumed. If the diffusive capacity is not sufficient to satisfy the oxygen demand, anaerobic conditions in the unsaturated layers above the groundwater table can occur. In this case, the effective diffusion depth can be calculated from the condition that both the diffusion flux and the concentration take the value zero.

Partial anaerobiosis fraction

The partial anaerobiosis fraction f_{ae} is calculated utilizing a sub-model which describes the radial diffusion in soil water around a pore. The general equation for cylindrical diffusion:

$$\frac{\partial \theta_{sat} c_w}{\partial t} = \frac{1}{r} \frac{\partial}{\partial r} \left(r \frac{\theta_{sat} D_w}{\lambda_r} \frac{\partial c_w}{\partial r} \right) - \Omega_{ox} \quad (162)$$

in which:

- c_w : aqueous oxygen concentration (kg m_w^{-3})
- θ_{sat} : moisture fraction at saturation ($\text{m}_w^3 \text{m}_s^{-3}$)
- D_w : oxygen diffusion coefficient in water ($\text{m}^2 \text{d}^{-1}$)
- λ_r : tortuosity factor for diffusion in saturated soil particles ($\text{m}_w \text{m}_s^{-1}$)
- r : distance from the centre of air filled pores (m)

A default value 0.3 has been assumed for the tortuosity factor λ_r . Under normal field conditions, $\theta_{sat} D_w / \lambda_r$ takes the value $7.5 \cdot 10^{-6} - 8.0 \cdot 10^{-6} \text{ m}^2 \text{ d}^{-1}$. The average radius of an aerated around an airfilled pore amounts less than 10^{-4} m , so the factor $\theta_{sat} D_w / (\lambda_r r^2)$ will be greater than 10. The oxygen profile around an air filled pore will be at equilibrium within one hour. This allows a steady state approximation of Eq. 73:

$$\frac{1}{r} \frac{\partial}{\partial r} \left(r \frac{\theta_s D_w}{\lambda_r} \frac{\partial c_w}{\partial r} \right) = \Omega_{ox} \quad (163)$$

This equation is subject to the following boundary conditions (Fig. 21):

- The aqueous concentration is in equilibrium with the concentration in air filled pores at the air-water interface ($r = r_{por} \rightarrow c_w = c_{we}$).

- At the outside of the aerobic zone, both the flux and the concentration equal zero ($r = r_{aer} \rightarrow dc_w/dr=0$).

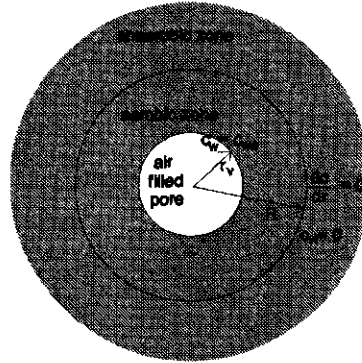


Fig. 21 Schematization of an aerobic and an anaerobic zone around and air filled pore

The solution which satisfies the zero flux condition at $r = r_{aer}$ and the concentration condition at $r = r_{por}$, combined with the zero concentration condition at $r = r_{aer}$ yields an expression from which the variable r_{aer} is determined:

$$4 \frac{\theta_s D_w}{\lambda_r \Omega_{ox} r_{por}^2} \frac{c_{we}}{c_{we}} = \left(\frac{r_{aer}}{r_{por}} \right)^2 \ln \left(\frac{r_{aer}}{r_{por}} \right)^2 - \left(\frac{r_{aer}}{r_{por}} \right)^2 + 1 \quad (164)$$

The equilibrium concentration at the air-water interface can be calculated from the oxygen concentration in gas:

$$r = r_{por} \Rightarrow c_{we} = \frac{\alpha_B}{2.564 \cdot 10^{-3} (T + 273.15)} c_g \quad (165)$$

where α_B is Bunsen's coefficient of solubility ($m^3 m^{-3}$) and the denominator is a factor to convert from volumic concentration to mass concentration, as can be derived from the rule of Boyle Gay-Lussac. Both the diffusion coefficient of oxygen in water and the Bunsen's coefficient depend on temperature. Tabel 7 represents data reported by Gliński and Stepniewski (1985).

Table 7 Diffusion coefficient in water, Bunsen's coefficient of oxygen and surface tension of water as a function of temperature

Temperature (°C)	Diffusion coefficient (m ² d ⁻¹)	Bunsen's coefficient (m ³ m ⁻³)	Surface tension (J m ⁻²)
0	8.554·10 ⁻⁵	0.0489	7.56·10 ⁻²
4			7.50·10 ⁻²
5	1.097·10 ⁻⁴	0.0436	
10	1.331·10 ⁻⁴	0.0394	7.42·10 ⁻²
15	1.572·10 ⁻⁴	0.0360	7.27·10 ⁻²
20	1.814·10 ⁻⁴	0.0333	7.11·10 ⁻²
25	2.056·10 ⁻⁴	0.0309	6.95·10 ⁻²
30	2.307·10 ⁻⁴	0.0290	6.79·10 ⁻²

The average radius of air filled pores r_{por} follows from the relation between suction and height of capillary rise in thin tubes at static equilibrium. In general:

$$r = \frac{2\eta}{\Delta p} \quad (166)$$

in which:

η : surface tension of water (N m⁻¹)

Δp : pressure difference between air phase and water phase in a soil pore (Pa)

If ψ is the suction in cm's water pressure in the soil layer, the corresponding smallest air-filled pore radius r (m) can be calculated as:

$$r = \frac{0.0015}{\psi} \quad (167)$$

When the air entry point of the soil is at suction ψ_a (cm), the corresponding radius of the biggest pore equals r_a (m). The average radius r_{por} of the airfilled pores is assumed to equal the geometrical mean of r_a and r_v :

$$r_{por} = \frac{0.0015}{\sqrt{\psi_a \psi}} \quad (168)$$

From Eq. 166, the aerated radius r_{aer} can be solved. For a soil system containing one pore, the aerated area around the pore A_{ae} per surface unit can be calculated as follows:

$$A_{ae} = \pi (r_{aer}^2 - r_{por}^2) \quad (169)$$

If the volume per unit depth of a pore in soil layer is estimated as $\lambda_v \cdot \pi \cdot r_{por}^2$ and the soil moisture difference between the suctions ψ_a and ψ is $\Delta\theta$, the number of airfilled pores can be approximated as:

$$N_{por} = \frac{\Delta \theta}{\lambda_v \pi r_{por}^2} \quad (170)$$

where λ_v is a factor accounting for the tortuosity of the air-filled pores. If all air-filled pores would be regularly distributed, without any interference, the aerated soil fraction would be:

$$f_{ae} = N_{por} A_{ae} = \frac{\Delta \theta}{\lambda_v} \frac{r_{aer}^2 - r_{por}^2}{r_{por}^2} \quad (171)$$

In practise, the distribution of the pores is random. Assuming a geometric distribution of air-filled pores, the aerated soil surface per square unit can be expressed as the sum of a geometric sequence with first term A_{ae} and ratio $(1 - A_{ae})$. In other words, when the chance that a new air-filled pore interferes with an already aerated soil part is defined as being proportional to the aerated part, the total aerated soil fraction will be:

$$f_{ae} = A_{ae} + (1 - A_{ae})A_{ae} + (1 - A_{ae})^2 A_{ae} + \dots + (1 - A_{ae})^{N_{por}} A_{ae} = 1 - (1 - A_{ae})^{N_{por}} \quad (172)$$

In anaerobic part of the soil, the oxygen demand for organic matter transformations is met by the utilization of nitrate oxygen (Par. 2.4.5). It has been assumed that organic matter transformations proceeds slower when only nitrate oxygen is available. Therefore, a factor f_{hetero} has been introduced to account for the reduced process rates (see Eq. 112). The multiplication factor for the combined availability of atmospheric oxygen and nitrate oxygen on respiratory activities has been formulated as:

$$f_{ae,OM} = f_{ae} + (1 - f_{ae}) \min \left(1, \frac{-\frac{1}{\Delta t} \int_{t_0}^{t_0 + \Delta t} R_{d,den} dt}{R_{p,den}} \right) \quad (173)$$

The minimum function in the right hand side of the equation expresses the selection of the rate limiting process. When $-\int R_{d,den} dt / (\Delta t R_{p,den})$ takes a value less than one, the nitrate availability seems to be rate limiting.

2.6.2 Temperature

The correction factor for temperature (f_T) is described by an Arrhenius equation:

$$f_T = \exp \left[-\frac{\mu}{R_{gas}} \left(\frac{1}{T+273} - \frac{1}{T_{ref}+273} \right) \right] \quad (174)$$

where:

μ : molar activation energy (J mol⁻¹)

R_{gas} : gas constant (J mol⁻¹ K⁻¹)

T_{ref} : reference temperature at which the conversion rates have been determined (°C)

T : actual soil temperature (°C)

In all model simulation up to version 3.5, the molar activation energy was taken as 74826 (J mol⁻¹). The gas constant equals 8.314 (J mol⁻¹ K⁻¹). A reference temperature (T_{ref}) of 11 °C is applied in the model, being the average annual temperature for the Dutch climate. Substitution of these values leads to an alternative formulation:

$$f_T = 1.118^{(T-T_{ref})} \quad (175)$$

The soil temperature at a certain depth (z) from the soil surface and at a certain day of the year can be given as input to the model or can be simulated using a sinus wave submodel with a damping effect for depths below the soil surface:

$$T = T_a + A_o \exp\left(-\frac{z}{D_m}\right) \cos\left(\omega t + \phi - \frac{z}{D_m}\right) \quad (176)$$

where:

T : temperature at depth z and time t (°C)

T_a : average yearly temperature (°C)

A_o : amplitude of the temperature wave (°C)

D_m : damping depth (m)

z : depth below the soil surface (m)

t : time as daynumber (d)

ω : frequency of the temperature wave (rad d⁻¹)

ϕ : phase shift (rad)

Due to the limited heat diffusivity of the soil, the amplitude of the heat wave decreases with soil depth. This phenomenon is accounted for by the introduction of the damping depth D_m , which is the depth where the amplitude of the temperature fluctuation has decreased to $A_o/e \approx 0.37 A_o$. The damping depth depends on the thermal properties of the soil and on the angular frequency of the temperature wave:

$$D_m = \sqrt{\frac{2 D_h}{\omega}} \quad \text{with:} \quad D_h = \frac{\lambda_h}{C_h} \quad (177)$$

where:

D_h : heat diffusivity (m² d⁻¹)

C_h : differential heat capacity (J m⁻³ °C⁻¹)

λ_h : heat conductivity (J m⁻¹ d⁻¹ °C⁻¹)

2.6.3 pH

For the effect of pH on reaction rates only one function for the organic transformation processes and the nitrification process has been formulated. The multiplication factor for the influence of pH f_{pH} is given as:

$$f_{pH} = \frac{1}{1 + e^{-2.5(pH-5)}} \quad (178)$$

Time independent pH-values are defined by the user for each soil horizon. It has been assumed that under optimal agricultural practises, the pH-value will not change and the seasonal fluctuation has been ignored.

The relation is based on soilwater quality data, so pH-values have to be considered as pH-H₂O values. In most model applications, only pH-KCl values are available from soil information systems. A linear relation has been fitted between pH-KCl and pH-H₂O values which yielded the following set of regression coefficients.

Table 8 Transfer functions for assessment of pH-values from soil chemical properties

Soil type	Relation	Soil units according to 'Staring reeks'
Sandy soils	pH=0.7262pH-KCl+2.1160	B7, B8, B9, B10, B11, B12, B13, B14
Peat soils	pH=0.8510pH-KCl+1.3842	B1, B2, B3, B4, B5, B6
Sandy loam soils	pH=0.7819pH-KCl+1.9772	B15, B16
Dense clay soils	pH=0.7623pH-KCl+2.2517	B17, B18, B19, B20, B21

2.6.4 Soil moisture content

The reduction in the transformation rate coefficients under wet conditions is generally caused by dilution effects and lack of atmospheric oxygen in the soil system. Both effects have been treated by the CTE and influence of aeration. Drought stress of micro-organisms has been described by the multiplication factor f_{θ} . The pF-value has been used to describe the drought respons of micro-organisms, based on the analogy of the root activity respons to dry conditions. Below wilting point, the function of micro-organisms are disturbed. Based on experimental data from Ruurlo and model calibration it has been assumed that within the rootzone between the values pF 3.2 and pF 4.2 the multiplication factor f_{θ} decreases linearly from 1.0 to 0.2. The influence of the moisture content is described by:

$$\begin{aligned} pF < 3.2 & \Rightarrow f_{\theta} = 1 \\ 3.2 < pF < 4.2 & \Rightarrow f_{\theta} = 1 - 0.8(pF - 3.2) \\ pF > 4.2 & \Rightarrow f_{\theta} = 0.2 \end{aligned} \quad (179)$$

Below the rootzone, no adaptation for dry conditions is considered.

2.7 Initial conditions

2.7.1 Soil organic matter

The model requires initial values of soil organic matter contents for each distinguished class of fresh material, the humus/biomass pool, the exudate pool and the dissolved organic matter pool. In general, the exudate and the dissolved organic matter pool are defined as rapidly decomposing substances. Input errors with respect to the initial contents of these pools will not affect the final results of the model simulation to a large extent. The initial estimates of fresh materials and the humus/biomass pool however, can have a great influence on the mineralization.

Field validations

In most validation studies, the distinction between initially present fresh organic matter and humus biomass has been based on a rule of thumb resulting from the model calibrations of Berghuijs-van Dijk *et al.*, (1985). They derived a fractional division of 90% assigned to humus/biomass and 10% attributed to fresh organic matter within the rootzone. The model calibration was conducted using experimental data from a lysimeter experiment with high doses of pig slurry (Steenvoorden, 1983). This ratio has been adopted in nearly all the model applications. The assignment of 10% fresh material to the distinguished classes has been done on arbitrary basis. In most of the simulations the assignment of organic fractions in the subsoil was based on the assumption of an increasing stability with depth. The upper soil layer contains more readily decomposable material and the deeper soil layer shows a decreased average decomposition rate.

Regional applications

In regional applications of the model, an initialization procedure has been developed to describe the initial situation with respect to fractional distribution of organic materials and mineral phosphate attributed to the fast and slow sorption pool as a function of land use and model parameters. For the year the historical run starts (e.g. 1941), organic matter contents resulting from a soil chemical schematization of the region are defined for each simulation plot. The fractional division between the different classes has been done for field validation studies. Then, simulations were carried out with an assumed historical fertilization practise. The results of these historical simulation runs allow verification to measured field data and provide insight in the overall performance of the model.

2.7.2 Root residues and produced dry matter

The schematization of organic materials allows the definition of a material representing root residues. To facilitate a flexible model use, a simulation can start at any day of the growing season. The initial produced quantities of shoots and roots dry matter ($Q_s(t_0)$ and $Q_r(t_0)$) as well as the initial quantities of N-uptake $U_N(t_0)$ and P-uptake $U_P(t_0)$ should be specified by the user in the model input.

2.7.3 Nitrogen

Organic nitrogen contents are defined by their weight fractions in the distinguished organic pools. The C/N ratio is a common figure in soil data systems and can easily be obtained from the analysis of soil samples. The model user can verify his choice for either the initial contents of organic pools or his assignment of nitrogen weight fractions to the organic materials by comparing the resulting C/N ratio to field data. The C/N ratio follows from:

$$C/N = \frac{0.58 \left(\sum_{fn=1}^{nf} OM_{fn}(t_0) + EX(t_0) + \theta c_{OM}(t_0) + HU(t_0) \right)}{\sum_{fn=1}^{nf} f_{N,fn} OM_{fn}(t_0) + f_{N,ex} EX(t_0) + \theta c_{ON}(t_0) + f_{N,hu} HU(t_0)} \quad (180)$$

The input of mineral nitrogen compounds are given as initial liquid concentrations of nitrate and ammonium. Due to the high reaction rates of these compounds, input errors with respect to the initial concentrations of NO_3^- and NH_4^+ do only affect the final results of the model simulation to a small extent.

2.7.4 Phosphorus

Input of initial organic phosphorus contents follows a procedure similarly to the organic nitrogen content. The model user must attribute phosphorus weight fractions to the organic materials. The result should be verified by comparing the resulting C/P ratio to field data. The C/P ratio follows from:

$$C/P = \frac{0.58 \left(\sum_{fn=1}^{nf} OM_{fn}(t_0) + EX(t_0) + \theta c_{OM}(t_0) + HU(t_0) \right)}{\sum_{fn=1}^{nf} f_{P,fn} OM_{fn}(t_0) + f_{P,ex} EX(t_0) + \theta c_{OP}(t_0) + f_{P,hu} HU(t_0)} \quad (181)$$

For mineral phosphorous, the model user should use one of three options for the description of the initial phosphorus contents. The first option should be selected if the contents of all individual phosphorus pools (liquid concentration, fast sorption, time dependent slow sorption) are known from lab-experiments or model simulations. The second option should be chosen if total P-contents P_{tot} ($kg\ kg^{-1}$) and the liquid concentrations are known. The third option should be used when only total P-contents are known.

In the initialization procedure, the total phosphate stock is distributed over the pools. With option 2, the liquid concentration is known and the fast sorption pool can be estimated from the liquid concentration:

$$X_{e,PO_4}(t_0) = X_{e,PO_4,max} \frac{K_L c_{PO_4}(t_0)}{1 + K_L c_{PO_4}(t_0)} \quad (182)$$

The sum of the slow sorption fractions is calculated as the remaining part. For the estimation of the quantities assigned to slow sorption fractions, a hypothetical equilibrium concentration c^*_{eq} occurring during the last years is assumed. This hypothetical equilibrium concentration can be calculated from:

$$\rho_d \sum_{i=1}^3 K_{F,i} (c^*_{eq})^{N_{PO_4,i}} = \rho_d P_{tot} - \theta c_{PO_4}(t_0) - \rho_d X_{e,PO_4,max} \frac{K_L c_{PO_4}(t_0)}{1 + K_L c_{PO_4}(t_0)} \quad (183)$$

The value of c^*_{eq} is obtained by a Newton-Raphson iteration procedure. The resulting value is used to calculate the initial quantities $X_{n,PO_4,i}(t_0)$ in the slow sorption pool according to:

$$X_{n,PO_4,i}(t_0) = K_{F,i} (c^*_{eq})^{N_{PO_4,i}} \quad (184)$$

In the third option with only total P-contents known, the slow sorption is assumed to be at equilibrium. Both sorption pools can be written as a function of the liquid concentration. The sum of all pools should equals P_{tot} :

$$\theta c_{PO_4}(t_0) + \rho_d X_{e,PO_4,max} \frac{K_L c_{PO_4}(t_0)}{1 + c_{PO_4}(t_0)} + \rho_d \sum_{i=1}^3 K_{F,i} c_{PO_4}(t_0)^{N_{PO_4,i}} = \rho_d P_{tot} \quad (185)$$

The value of $c_{PO_4}(t_0)$ is obtained iteratively by a Newton-Raphson procedure. After assessing this value, the quantities in the fast sorption pool and the time dependent slow sorption pool are determined straight forward.

2.8 Boundary conditions

Boundary conditions are input to the model and have to be specified for all soluble substances for the boundaries at the top, lateral and bottom of the simulated soil system. The boundary concentrations are applied to all soluble substances described by the ANIMO model: dissolved organic compounds, ammonium, nitrate and mineral phosphate.

The boundary condition at the top is given as a concentration of the incoming precipitation water flux, or:

$$J_{s,p} = q_p c_p \quad (186)$$

where:

$J_{s,p}$: solute flux across the top boundary ($\text{kg m}^{-2} \text{d}^{-1}$)

q_p : precipitation water flux ($\text{m}^3 \text{m}^{-2} \text{d}^{-1}$)

c_p : concentration of the precipitation water (kg m^{-3})

In case part of the precipitation water consists of irrigation water, the concentrations in the rain water should be calculated as a mixture of the rainfall concentrations and the concentrations in irrigation water, proportional to the originating volumes.

The boundary condition at the lateral sides of the model system is given as a concentration in the incoming (infiltrating) surface-water flux, or:

$$J_{s,x} = \sum_i^{N_{dr}} q_{d,i} c_{inf} \quad (187)$$

The boundary condition at the bottom is given as concentrations in the incoming seepage water flux, or:

$$J_{s,s} = q_s c_s \quad (188)$$

where:

- $J_{s,x}$: solute flux across the lateral boundary ($\text{kg m}^{-2} \text{d}^{-1}$)
- $J_{s,s}$: solute flux across the bottom boundary ($\text{kg m}^{-2} \text{d}^{-1}$)
- N_{dr} : number of different surface-water systems (-)
- $q_{d,i}$: infiltrating water flux from surface-water system i ($\text{m}^3 \text{m}^{-2} \text{d}^{-1}$)
- q_s : seepage water flux ($\text{m}^3 \text{m}^{-2} \text{d}^{-1}$)
- c_{inf} : concentrations in the infiltrating water from surface-water system i (kg m^{-3}).
- c_s : concentration in the seepage water (kg m^{-3})

3 CONCISE PROGRAMME DESCRIPTION

3.1 General data flow

The model requires a number of input data files and, after execution of a simulation, generates a set of output data files (Fig. 22). Hydrological parameters must be supplied by a hydrological model.

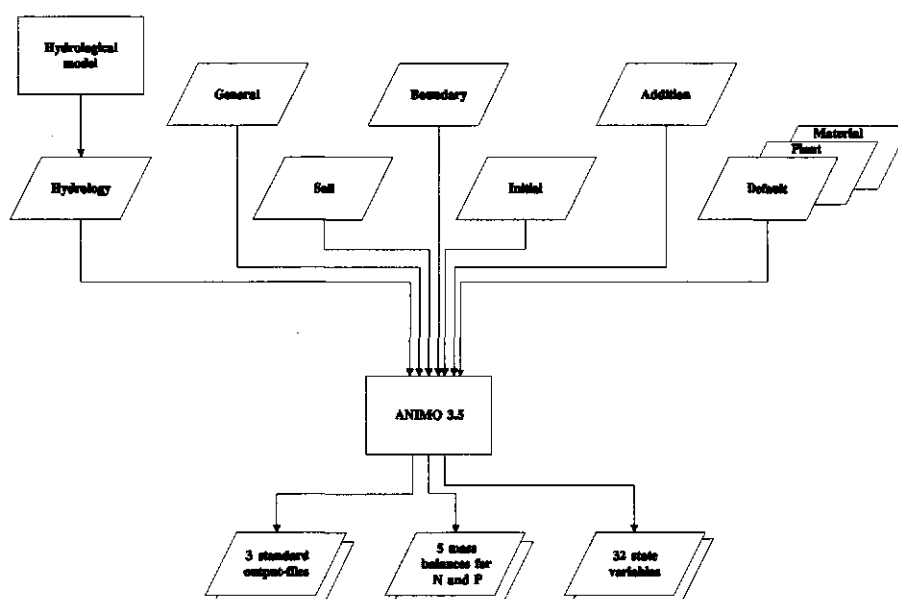


Fig. 22 Flow chart of the input and output data of ANIMO version 3.5

A general data file includes settings of model options for the simulation period, the choice of hydrological model for pre-processing hydrological input data, the simulation of the phosphorous cycle and the type and structure of model output. Soil physical and soil chemical data should be supplied as well as data on boundary and initial conditions and additions (including tillage). Default data are required for materials and plants. Materials are substances with a predefined composition which can be added to the soil system.

3.2 Model structure

In order to provide model users some insight into the model structure, a flow chart of the main module is given in Figure 23. This flow chart will be used to give some insight in the core of the model and explain the model structure. A more description can be found in Kroes and Roelsma (1998).

Initialisation is the first step in the flow chart and in the ANIMO-model. It results in an initial distribution of organic matter and mineral N and P over the model compartments. The simulation then enters a loop with time-intervals, of which the size (e.g. 1 day) is defined by the results of the hydrological model. Results of the hydrological model are read as a terms of a complete water balance for the soil-water-plant system. Next follows simulation of shoot and root development by the ANIMO-model. Soil temperatures are simulated with a sinus wave sub-model. Additions and tillage are executed pulse wise at the beginning of a certain timestep, as defined in the model input. The nitrogen and phosphorus uptake rates are determined as sink terms for the transport and conservation equation (CTE). Reaction rates (sink and source terms) are corrected for the environmental influences of oxygen availability, temperature, dry conditions and pH.

Oxygen is required for the decomposition of organic matter and for nitrification. Therefore, before the process parameters of the conservation and transport equation can be assessed, a good estimate of the oxygen profile has to be made. This is done by a separate module which solves the CTE with optimal values for transformation parameters for all dissolved organic matter and nitrogen substances in order to compute a potential oxygen demand. In the aeration module, the diffusive properties of the soil are taken into account to reach an actual oxygen demand. From the ratio between actual and potential oxygen demand reduction factors for organic matter transformations, nitrification and denitrification follows.

Once the sink term decomposition of dissolved organic matter is known, the CTE can be solved and the mineralization of dissolved organic compounds can be computed. In addition to this process, mineralization is computed in the same module, after which the CTE is solved for ammonium. From its solution the source term nitrification of the nitrate CTE follows; next the CTE for nitrate can be solved. Optionally the phosphate CTE will be solved similarly to ammonium.

At the end of each time-interval, nutrient uptake is integrated and prepared as initial conditions for the next time-interval. Mass balances are verified and results are written to output-files.

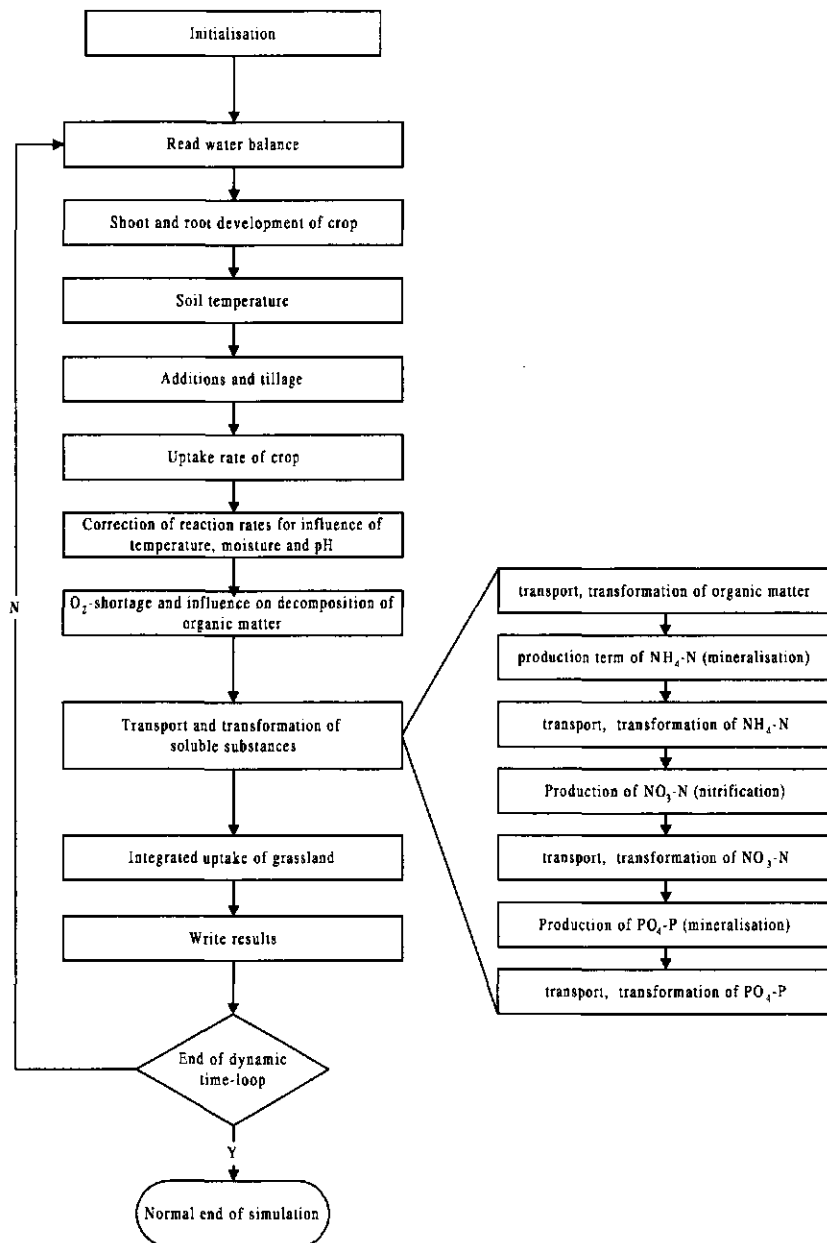


Fig. 23 Flow chart of main module of ANIMO version 3.5

3.3 Inputs and outputs

Application of ANIMO version 3.5 for a single field or subregion requires a minimum set of 10 files (Table 9).

Table 9 Summary of input-files of ANIMO version 3.5

Name of input-file	Content
GENERAL.INP	simulation- and output-options
MATERIAL.INP	standard data on materials (composition, reaction rates)
PLANT.INP	standard crop data (plant growth and uptake parameters)
SOIL.INP	soil chemical and soil physical data
CHEMPAR.INP	soil chemical data for phosphorus
BOUNDARY.INP	boundary conditions
INITIAL.INP	initial conditions
ADDITION.INP	data concerning additions and tillage to the soil system
SWATRE.INP and SWATRE.UNF or: WATBAL.INP and WATBAL.UNF	waterquantity data from a multi layer model (e.g. SWAP) waterquantity data from a two-layer model (e.g. WATBAL)

Hydrological data must be supplied by a hydrological model prior to the simulation with the ANIMO-model. Two options are available, representing linkage with two types of hydrological models:

- A detailed multi-layer model (e.g. SWAP-model; Belmans *et al.*, 1983; Feddes *et al.*, 1978; Van Dam *et al.*, 1997).
- A two-layer model (DEMGEN; Abrahamse *et al.*, 1982; WATBAL; Berghuijs-van Dijk, 1985)

If a multi-layer model is used for preprocessing hydrological data, then a file (SWATRE.UNF) must be created containing all required hydrological data, including data about model-geometry. Additional information is required (file SWATRE.INP) on the kind of crop grown and on the maximum depth of the root zone. If a two-layer hydrological model is used (file WATBAL.UNF), then a more detailed hydrology-related input is required (file WATBAL.INP) to allow ANIMO the data processing from a two-layer system to the multi-layer system.

Linkage of the ANIMO model to a regional groundwaterflow is also an option (Van der Bolt *et al.*, 1996). The hydrological model should generate information on water fluxes of the vadose zone and the upper groundwater zone of each subregion in a series of files with a similar layout as described above. An extensive description of the input-files has been given by Kroes and Roelsma (1998).

Standard output has been organized in three files: TOUT.OUT, INITIAL.OUT, MESSAGE.OUT. All other output-files are optional. The file TOUT.OUT gives output of input and an optional output for each timestep from each subroutine and facilitates the modeller in his examination of the model performance. The file INITIAL.OUT contains the results of all the state variables at the end of the simulation in the same sequence as the input-file INITIAL.INP and can be used to initialize a restart-run. The

file MESSAGE.OUT comprises warning messages on the performance of the simulation error-messages.

Optional output consists of water and material balances from a user defined number of model-layers and a freely choosen simulation interval. In addition to these balances the model can also generate time series of output for each model-layer.

4 VALIDATION AT FIELD SCALE

4.1 Introduction

The ANIMO-model has the ability to make reliable predictions for a wide range of different environmental conditions. This is illustrated by a number of case-studies which include comparisons between measured and simulated values of the soil-water-plant system at field scale. In some case-studies a separated calibration and a validation phase was distinguished, whereas other studies combined both phases. Validations on the scale of submodels or process formulations are not available. In this report, the more practical perspective of model validation has been adopted.

The ANIMO-model was initially developed as a leaching model for nitrogen and therefore the first validations mainly focused on the leaching of nitrate (e.g. Kroes, 1988 and Reiniger *et al.*, 1990). Recent validations include other processes of the nitrogen cycle and a validation of the leaching of mineral P and total P. In this validation procedure, results of field experiments at different locations in The Netherlands have been used. A prerequisite of an appropriate validation is a good description of water and nutrient movement in the soil. Due to the huge amount of data required for this type of dynamic simulation models, complete sets of field data are scarce and the opportunities to conduct a thorough model validation are often limited. Examples will be presented of recent validations using data-sets from different Dutch field experiments (Fig. 24). Jansen (1991a) applied the model using data-sets from different European countries.



Fig. 24 Location of field experiments used to validate the ANIMO-model

Depending on the availability and the suitability of experimental data, the behaviour of one or more substances in the modelled soil-water-plant system was validated (Table 10). At some locations other entities were measured (total-N, ammonium-N, P-uptake, etc) and used to validate the model. Due to their incidental measurements they have been left out of this report, but have been described in the pertinent project reports.

The description in this report is limited to six locations covering a fairly wide range of landuses on different soil types.

Table 10 Validated variables of ANIMO model at different locations in The Netherlands

Experiment		Soil-water-plant system			
nr	Location	Soil	Ground water	Surface water	Plant
1	Heino	mineral-N	nitrate-N		N-uptake
2	Ruurlo	mineral-N	nitrate-N		N-uptake
3	Nagele	mineral-N			N-uptake
4	Lelystad			nitrate-N	
5	Putten	sorbed-P	ortho-P	ortho-P	
6	St. Maartensbrug		total-P	total-P	

Locations 7, 8 and 9 (Fig. 24) refer to other recent validations:

- location 7a and 7b (Vredepeel and Borgerswold): Different management options within integrated arable farming affecting nitrate leaching (Dijkstra and Hack-ten Broeke, 1995) (ANIMO version 3.4);
- location 8 (Cranendonck): high doses of cattle slurry applied in forage maize on sandy soil (Kroes *et al.*, 1996) (ANIMO version 3.5);
- location 9 (Hengelo): Effects of different management options for grazing cattle within dairy farming (Hack-ten Broeke and Dijkstra, 1995) (ANIMO version 3.4).

In all validations data (water fluxes and leached quantities) from long-term field experiments at different fertilization levels were used. The field experiments differ in soil type, land use and fertilizer management (Table 11). The experiments in Heino and Ruurlo were used to validate the model for the leaching of nitrate, crop uptake, and mineral N-storage in soil for grassland and forage maize. The experiment at Nagele was used to validate arable crop uptake of N and soil storage of mineral N. The experiment in Lelystad was used to validate leaching of nitrate to surface waters under grassland. The experiment in Putten validated leaching of mineral phosphorus to field ditches. The experiment in St. Maartensbrug validated the leaching of mineral phosphate and dissolved organic phosphorus in calcareous weakly humous sandy soils to tile drains and open field drains.

Each experiment was modelled by separate simulations for the hydrological and nutrient cycle of the soil-water-plant system. All hydrological simulations were carried out using the SWAP-model (Belmans *et al.*, 1983, Feddes *et al.*, 1978, Van Dam *et al.*, 1997). Results of the hydrological simulations were used as input to the ANIMO-model. Unless explicitly given, all simulations have been carried out with version 3.5 of the ANIMO model.

Table 11 Main characteristics of field experiments used to validate the ANIMO model

Experiment nr	Soil texture location	Land use	Groundwater level (m-surface)	Artificial fertilizer level (kg ha ⁻¹ a ⁻¹)	Animal fertilizer level of (kg ha ⁻¹ a ⁻¹)	Number variants
1	Heino sand	forage maize	0.5 - 1.6	20 - 140 N	180 N	9
2	Ruurlo loamy sand	grassland	0.2 - 1.7	0 - 160 N	0 - 400 N	8
3	Nagele silty loam	winter wheat	0.6 - 1.5	110 - 150 N	-	5
4	Lelystad clay	grassland (grazed)	0.5 - 2.0	0 N	220 N	1
5	Putten sand	grassland (grazed)	0.3 - 1.3	0 P	45 P	2
6	St. Maartensbrug calc. weakly humous sand	flower bulbs	0.6 - 1.0	0 P	0 P	2

¹ some plots combined forage maize with a nitrogen catch crop in winter.

4.2 Forage maize and catch crops on a sandy soil

4.2.1 Introduction

Between 1988 and 1994 research at the experimental farm in Heino was performed to establish the impacts of a nitrogen catch crop after forage maize on nitrate leaching. Field data were reported by Schröder *et al.*, (1992) and Van Dijk *et al.*, (1995). Nitrate concentrations in soil moisture were analyzed and the nitrate leaching mass flux was computed by model simulations of combined water and nitrogen transport. A detailed report of the validation was presented by Kroes *et al.*, (1996). Paragraph 4.2.3 presents results of the comparison between simulated and measured values.

4.2.2 Method

Hydrology was simulated by the SWAP-model using measured groundwaterlevels as a lower boundary condition. Soil physical properties were partly measured and partly derived from standard soil moisture retention curves for the three distinguished soil horizons. The hydrology of the soil-water-plant system was simulated for three different cropping patterns:

- forage maize;
- forage maize with grassland as catch crop;
- forage maize with rye as catch crop;

Hydrological simulations were validated by comparing the simulated and measured pressure heads at a depth of 15 cm. The simulation of the nutrient processes was performed in two phases: a calibration and a validation phase. During the calibration phase only one field plot (forage maize without catch crop, fertilization level of 180 kg ha⁻¹ N) was simulated and input parameters were adapted to obtain a reasonable fit of the simulation results. Only those parameters influencing denitrification and mineralization needed to be adjusted.

During the validation phase the other variants were simulated keeping process parameters identical to the calibration phase, except of course the site specific meteorology and fertilizer input data. Simulation results were evaluated by comparing between measured and simulated values of:

- nitrate concentrations at a depth of 1 m below the soil surface;
- crop uptake by forage maize (nitrogen in harvested parts of crop);
- mineral nitrogen present in the upper 60 cm of the soil.

4.2.3 Results

Some results of the calibration are presented in Figure 25. Simulated mineral N in the layer 0-60 cm below soil surface (Fig. 25a) showed a fairly good comparison between simulated and measured values; largest deviations occur in the summers of the first four years. Simulated nitrate concentrations (Fig. 25b) at 1 m below soil surface are on average 9% below the measured values. Simulated crop uptake of nitrogen is in good agreement with the measured uptake, only in the wet year of 1993 the simulated value is too low. From a statistical evaluation (Kroes *et al.*, 1996) it appeared that the average deviation for mineral-N, nitrate-N and crop uptake is respectively 33%, 65% en 12%.

Results of the validation are presented in Figure 26 as time averaged results of simulated and measured values for the whole period 1988-1994. Mineral-N and nitrate-N are based on comparisons for those time steps where measurements took place; crop uptake is based on a comparison of annual harvested crop yields. Computed average nitrate concentrations (Fig. 26b) shows a good agreement with the measured values. The largest deviations are found for variants with high inorganic fertilization levels, where a maximum overestimation of 28% occurred. Simulated mineral-N (Fig. 26a) and crop uptake (Fig. 26c) tend to slightly underestimate and overestimate measurements at resp. low and high fertilization levels. Other validations for forage maize (Kroes *et al.*, 1996) did not confirm this pattern. It has been concluded that the model performance is satisfactory, but the nutrient uptake by arable crops requires further study and an extended validation.

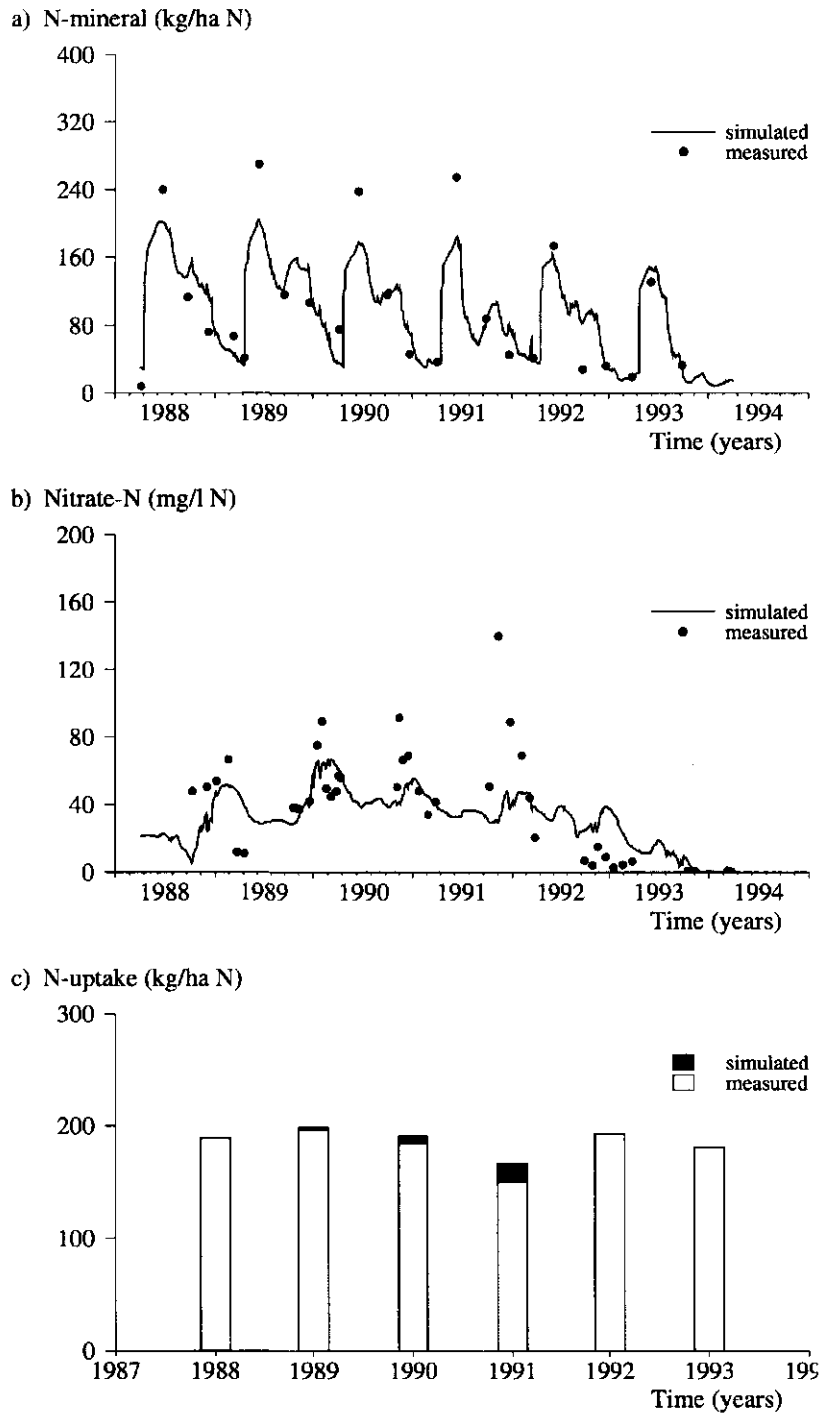


Fig. 25 Calibration on Heino field experiment data: measured and simulated mineral N in 0-60 cm below soil surface (a), concentration of nitrate at 1 m below soil surface (b) and uptake of N by crop (c); forage maize without catch crop and with a fertilizer treatment of 200 kg ha⁻¹ N

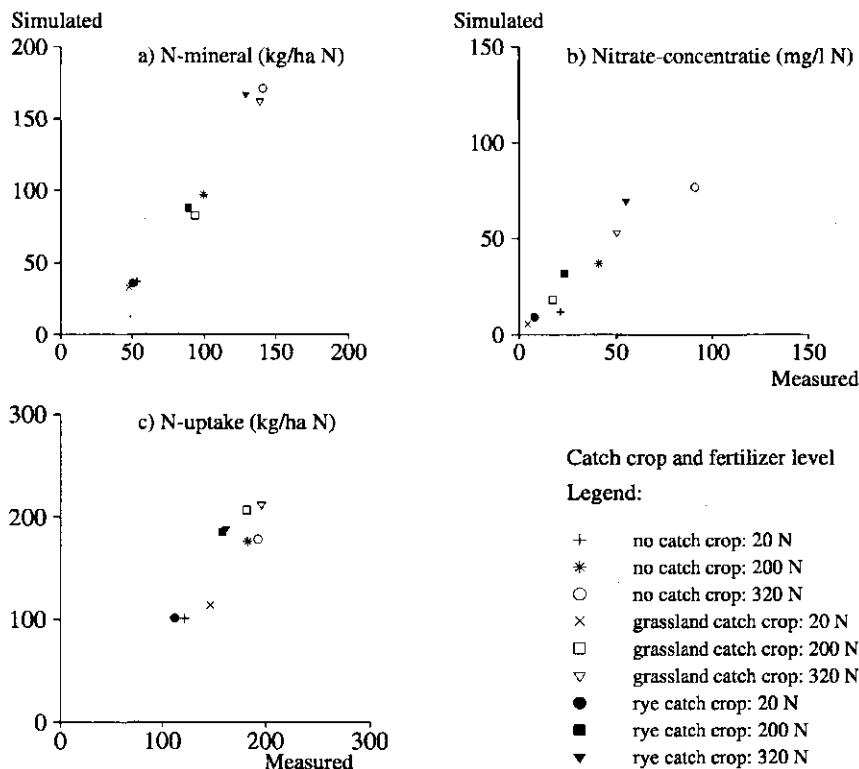


Fig. 26 Validation on Heino field experiment data with different catch crops and different fertilizer treatments: measured and simulated mineral N in 0-60 cm below soil surface (a), nitrate concentration at 1 m below soil surface (b) and N-uptake (c)

4.3 Non-grazed grassland on a sandy soil

4.3.1 Introduction

Between 1980 and 1984 field research at an experimental farm in Ruurlo aimed to quantify the influence of different application techniques on soil fertility, crop yields and nitrate leaching. The data sets have been utilized by Jansen (1991b) to evaluate the performance of the ANIMO model within the framework of a comparison of six nitrate leaching models. The main characteristics of the Ruurlo field plots are:

- soils are classified as loamy sand soils;
- different fertilization levels and application techniques (both injection and surface applications of slurry);
- land use is grassland without grazing;
- high water holding capacity.

Field data were collected during the period 1980-1984, extensively published by Fonck (1982a, 1982b, 1986a, 1986b, 1986c), Wadman and Sluysmans (1992) and Jansen (1991b). Nitrate concentrations in soil water were measured and the nitrate leaching mass flux was computed by means of model simulations of combined water and

nitrogen transport. A more detailed report of the validation was given by Jansen *et al.*, (1991b) and Kroes *et al.*, (1996).

4.3.2 Method

Hydrological simulations were carried out by Jansen (1991a) with the SWAP-model. ANIMO simulation results were verified with measured values of:

- nitrate concentrations at 1 m depth;
- N-uptake as found in all grassland cuttings;
- mineral nitrogen present in the upper 50 cm of the soil.

Nitrogen simulations were calibrated using the data of one fertilization experiment (800 kg ha⁻¹ N; 50% as artificial fertilizer and 50% as animal manure). The animal manure (cattle slurry) was injected into the upper 10 cm of the soil. The data of the other seven experiments were used for model validation. Most important parameter adaptations during the calibration phase were related to decomposition of organic matter in the subsoil.

4.3.3 Results

Results of the calibration phase (Fig. 27) generally exhibit a good agreement between simulated and measured values. The time series of mineral nitrogen (Fig. 27a) shows some deviations during peak periods but the average values fit well. The difference between measured and simulated nitrate concentrations at 1 m depth (Fig. 27b) does not exceed 11%, which is acceptable. The calculated cumulative nitrogen uptake by the grass shoots are in good agreement with the measured data (Fig. 27c). A more detailed comparison of 33 grassland-cuttings (Kroes *et al.*, 1996) has proved that relatively large deviations per cutting for the year 1982 can occur, but the average measured and computed values differ only 9.5% and is therefore quite acceptable.

Results of the model validation are given in Figure 28 showing the comparison of time averaged simulated and measured results with respect to N-mineral, NO₃-concentration and N-uptake. The data relate to the whole experimentation period: 1980-1984. The storage of mineral-N in the toplayer (Fig. 28a) is simulated fairly well; only two variants exhibit a deviation between measured and simulated values greater than 20%.

The overall performance of the model is quite acceptable. Measured and simulated values at these plots are still below the EC drinking water standard (11.3 mg.l⁻¹ NO₃-N). N-yield of the grassland-cuttings is simulated fairly well. The model shows a slight tendency to overestimate crop uptake. A more detailed validation study (Kroes *et al.*, 1996) comprising all individual grassland-cuttings showed that relatively large deviations can occur, but the average values fit fairly well.

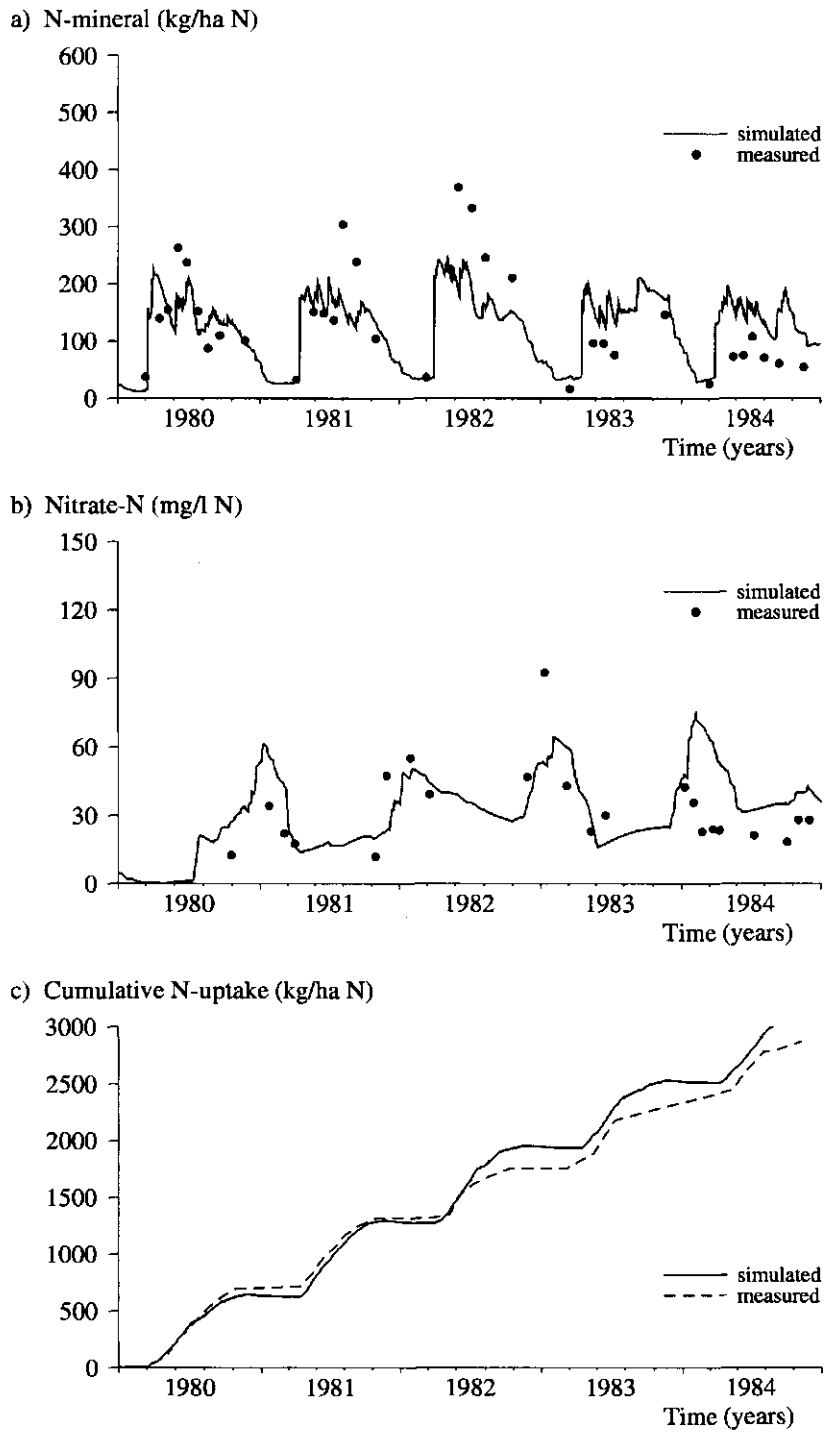


Fig. 27 Calibration Ruurlo: measured and simulated mineral N in 0-50 cm below soil surface (a), concentration of nitrate at 1 m below soil surface (b) and uptake of N by crop (c) during period 1980-1984; variant with subsurface injection of cattle slurry 80 ton/ha and artificial fertilizer of 400 kg ha⁻¹ (total fertilizer level of 800 kg ha⁻¹ N)

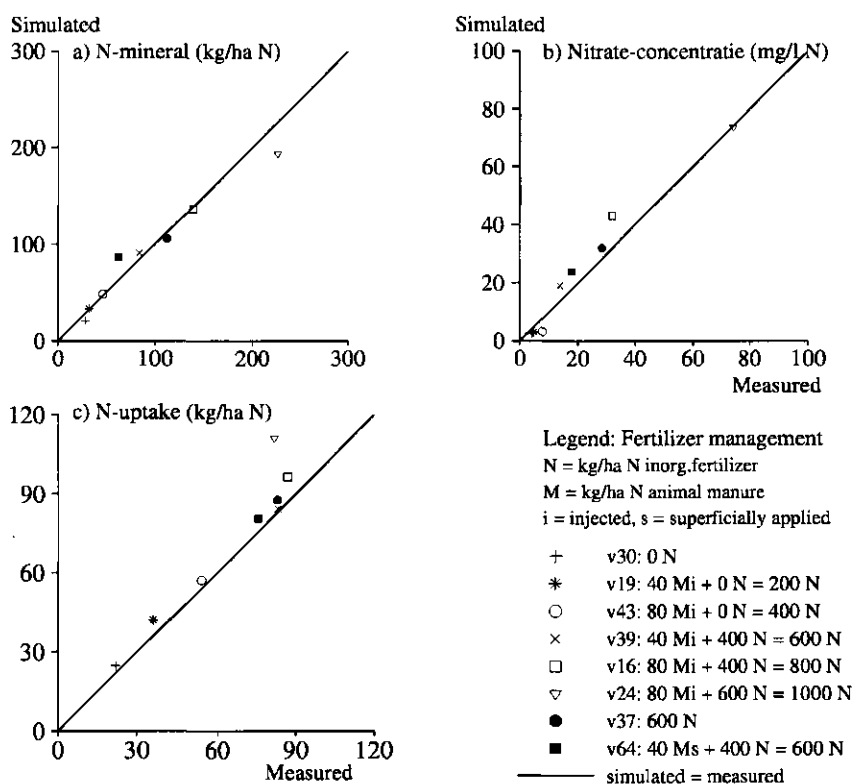


Fig. 28 Validation Ruurlo: measured and simulated mineral N in 0-50 cm below soil surface (a), concentration of nitrate at 1 m below soil surface (b) and uptake of N by crop (c) average values for period 1980-1984; grassland with different fertilizer management

4.4 Winter wheat on silty loam soil

4.4.1 Introduction

Data of extensive field experiments were collected by Groot and Verberne (1991). The objective of these experiments was to obtain reliable data sets on soil nitrogen dynamics, nitrogen uptake, crop growth and crop development in different nitrogen treatments for winter wheat during the growing season. Data from two experiments were used to validate the ANIMO-model on crop uptake by winter wheat and storage of mineral nitrogen (Rijtema and Kroes, 1991). A summary of the validation using data from the field experiment in Nagele (Fig. 24) is presented.

4.4.2 Method

The experimental fields at Nagele can be characterized as:

- soil unit: silty loam;
- groundwater level: 0.6 - 1.5 below surface;
- fertilization level: 110 and 150 kg ha⁻¹ N, applied as artificial fertilizer.

Crop and soil samples were taken at three week intervals before anthesis and at two week interval after anthesis. Groundwater levels were measured during the growing season of the year 1984. Daily weather data were available from the nearest meteorological station. Soil moisture retention curves and hydraulic conductivity data are reported by Groot and Verberne (1991). At each sampling date 0.5 m² crop was harvested in eight replicates for detailed plant analyses.

The SWAP-model was applied to provide the hydrological data required by the ANIMO model. For this purpose measured soil physical data have been used as input. The SWAP-model was applied using measured groundwaterlevels as a lower boundary condition. The nitrogen dynamics was simulated with version 3.0 of the ANIMO-model.

4.4.3 Results

The measured and simulated uptake of nitrogen during growth is presented in Figure 29a for the field with a fertilizer level of 110 kg ha⁻¹ (N1). It appears that measured and simulated nitrogen uptake during growth agree reasonably well. The total mineral nitrogen present in the soil of the N1 field during growth is given for the layer 0-40 cm in Figure 30a and for the layer 0-100 cm in Figure 30b. Figure 31 exhibits the measured and simulated data separately for NH₄-N (Fig. 31a) and NO₃-N (Fig. 31b) for the layer 0-100 cm. Attention is focused on the fertilizer addition of 60 kg ha⁻¹ N applied at daynumber 132 which is not followed by an increase in mineral nitrogen in the measured data. The simulated data, however, show an increase in total mineral nitrogen immediately after the application, followed by a sharp reduction in the days after application. Next to an increased crop uptake after this N-dose also an increased denitrification caused by temporal anaerobiosis due to heavy summer rains reduced the quantity of mineral nitrogen in the soil. The calculated total reduction in mineral nitrogen in the soil follows the measured data reasonably.

Results of measured and simulated nitrogen uptake of two experimental field plots are presented in Figure 29b. The two fields (N2 and N3) received fertilized equal doses of nitrogen (150 kg ha⁻¹). The measured data of both fields have been plotted in Figure 29b to give an impression of the spatial variability of the measured data. The simulated data fit reasonably well with the measured results. Figure 32a and 32b depict the mineral nitrogen storage in the soil profile for the layer 0-40 and 0-100 cm respectively. The duplicate measurements give also an indication of the spatial variability in measured mineral nitrogen data. The simulated data appear to describe the temporal variation in mineral nitrogen in the soil following the fertilizer additions of 60 kg N at daynumber 132 and of 40 kg N at daynumber 172 correctly as compared with the measured data.

The overall performance of the ANIMO-model was judged to be good, but the simulation of reduced concentrations after fertilizer application in June 1984 failed. The most reasonable explanation for this phenomenon was the accelerated growth of living soil biomass, which has not been formulated in the model still.

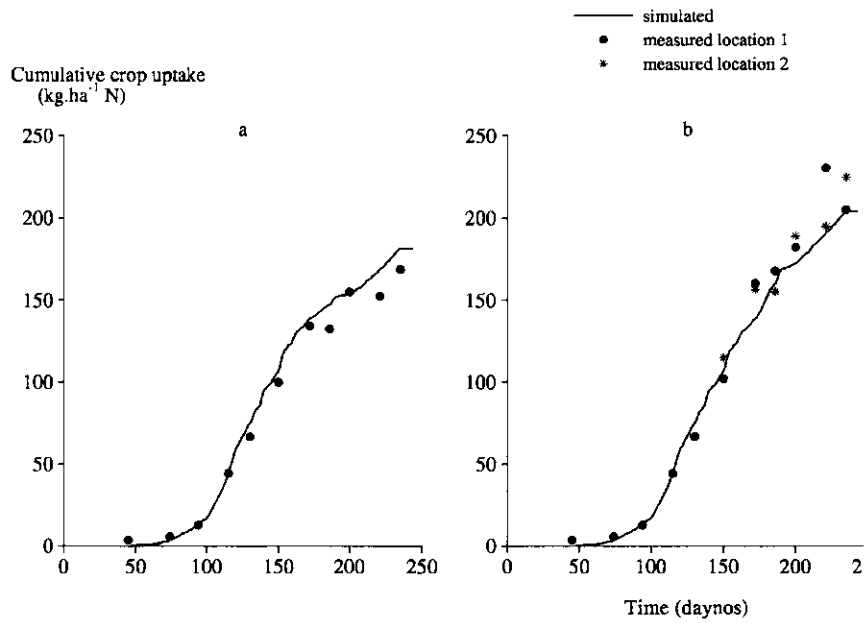


Fig. 29 Measured and simulated N-uptake of winter wheat at Nagele; fertilizer levels of 110 kg ha⁻¹ N (a) and 150 kg ha⁻¹ N (b)

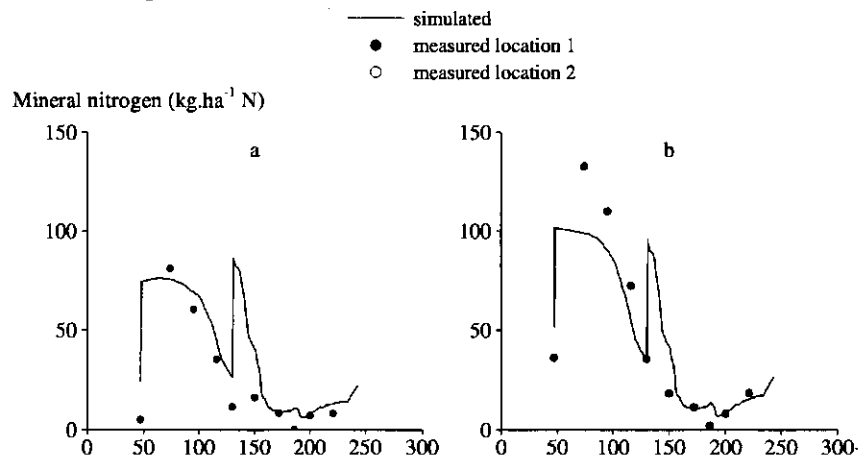


Fig. 30 Measured and simulated soil mineral-N at Nagele, fertilizer level of 110 kg ha⁻¹ N; soil layers 0-40 cm (a) and 0-100 cm (b)

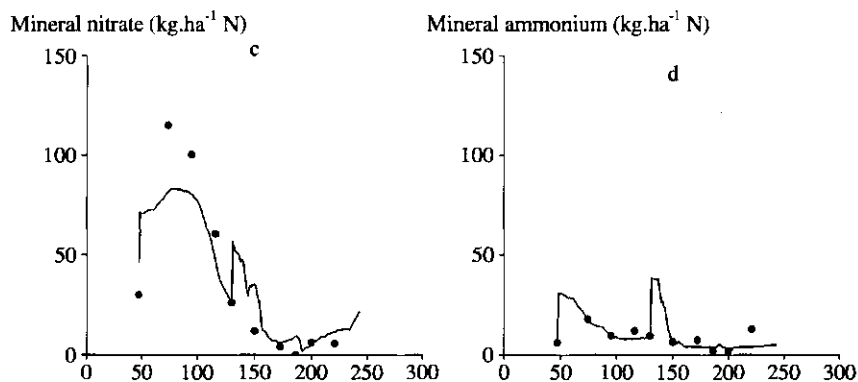


Fig. 31 Measured and simulated soil mineral ammonium (a) and nitrate (b) at Nagele; soil layer 0-100 cm

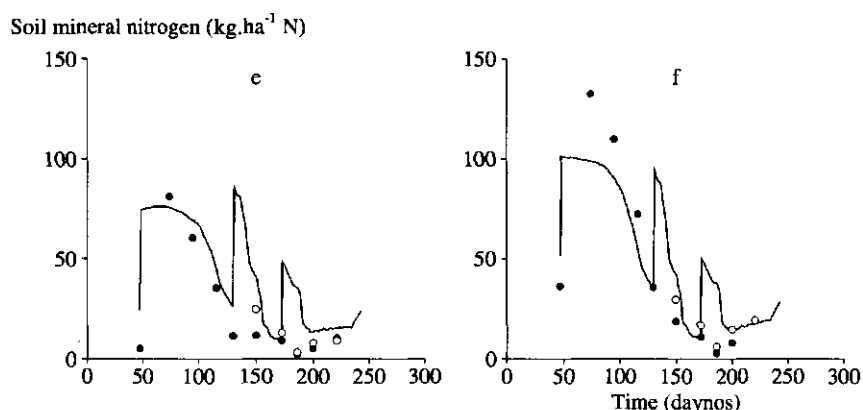


Fig. 32 Measured and simulated soil mineral-N at Nagele, fertilizer level of 150 kg ha⁻¹ N; soil layers 0-40 cm (a) and 0-100 cm (b)

4.5 Grazed grassland on clay soil

4.5.1 Introduction

A research program at the experimental farm Waiboerhoeve (Lelystad) aimed to analyse the influence of white clover on nitrate leaching and soil fertility in grazed grassland. An important feature of the research program was to compare two complete dairy systems: a grassland and grass/clover system. The experiments were conducted with different mixtures of grassland and white clover and during the period 1991-1994 the nitrate leaching was determined by incidental measurements of subsurface drain water discharges and nitrate concentrations (Schils, 1994). To verify the preliminary results and to analyse the nitrate load on surface water by different grass/clover fields,

an additional research programme was conducted to quantify the nitrate leaching during the season 1993/1994 (Kroes *et al.*, 1996). Results of a comparison between simulated and measured nitrate sub-surface discharge from a grass/clover pasture are presented.

4.5.2 Method

The experimental fields at Lelystad can be characterized as:

- soil unit: clay;
- groundwater level: 0.5-2.0 m below soil surface;
- fertilization level :no artificial fertilizer and 220 kg ha⁻¹ N by animal manure.

Quantification of mass-discharges of nitrate by subsurface drains was conducted by sampling of discharge proportional water volumes and analysis on nitrate (Van den Toorn *et al.*, 1994). The hydrological input required by the ANIMO model was generated by the SWAP-model utilizing the soil physical properties derived from standard soil moisture retention curves (Wösten *et al.*, 1994) for the four distinguished soil horizons. A number of calibration runs are carried out with different values of the saturated hydraulic conductivity and lower boundary condition until the measured and simulated data with respect on groundwater levels and drain water discharges fitted well.

Nitrogen dynamics was computed using the ANIMO-model version 3.4.2 Due to an insufficient number of replicants, no data were available for an independent field validation, so only the ability of the ANIMO model to reproduce the dynamic behaviour of nitrate leaching as influenced by climatical conditions could be verified. The empirical parameters p_1 and p_2 describing the vertical oxygen diffusion in the soil gas phase were adapted to obtain a good fit between simulated and measured values.

4.5.2 Results

Verification of nitrogen simulations took place by comparing the computed results with the measured data. A fair agreement between the simulated and the measured results was achieved for both the individual results (Fig. 33a) as well as for the cumulative results (Fig. 33b). The largest deviation occurred in the month of April 1994, where model simulations overestimated the water discharge. This deviation is most probably caused by an overestimation of the saturated hydraulic conductivity which incidentally caused an overestimation in simulated drain water discharge. It has been concluded that the ANIMO model is able to reproduce the dynamic behaviour of the nitrate leaching reasonable. Better results can be achieved by implementing preferential in both the hydrological and the nitrogen model.

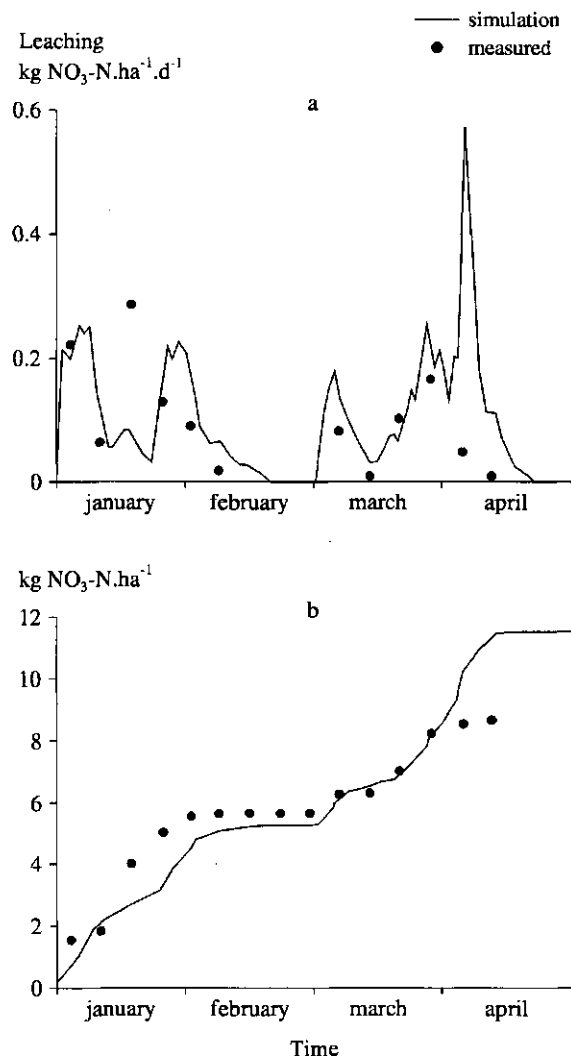


Fig. 33 Validation Lelystad: Measured and simulated nitrate drain discharge of a field cover by a mixture of grass and clover in Lelystad; cumulative (a) and daily (b); period Jan.1994-April 1994

4.6 Phosphorus leaching from grassland on a sandy soil

4.6.1 Introduction

Intensive land use with high fertilizer levels resulted in high leaching of phosphorous compounds to surface water and groundwater systems. During the years 1989-1994 the DLO Winand Staring Centre carried out a research programme to evaluate several options to reduce phosphate leaching. Within this framework Kruyne *et al.*, (1996) validated the phosphate leaching as simulated by the ANIMO model.

4.6.2 Method

The phosphate adsorption formulations were based on and parameterized by data originating from laboratory experiments (Schoumans, 1995) and implemented in the ANIMO-model version 3.5. The new formulation was calibrated on measured data on the penetration depth of the adsorbed phosphorus front and on the phosphate concentration in the liquid phase of the soil. Measured data were obtained at the experimental location in Putten (Schoumans and Kruijne, 1995). This field is characterized by:

soil unit: 'Beekeerd soil';

groundwater level: 0.3 - 1.3 m below soil surface;

P-fertilization: no artificial fertilizer and 45 kg ha⁻¹ P as animal manure.

The validation was carried out by comparing simulated phosphorus mass discharges towards a field ditch with measured data. Quantification of mass-discharges of P took place by analyses of P-concentrations in discharge proportionally collected water samples. A historical period of 45 years was simulated to initialize the ANIMO-model and achieve a good approximation of the initial phosphorous sorption front. The final results of this initialization period were the starting-point for the calibration and validation phase. The hydrology was simulated with the SWAP-model using the second year to calibrate and the third year to validate on measured ground water levels and water discharge to the ditch. Calibration was conducted by adaptation of the bottom boundary conditions, the drainage parameters and the soil physical parameters (Kruyne *et al.*, 1996).

4.6.3 Results

The calibration phase resulted in an acceptable fit of model results to the measured data with respect to the sorbed phase and the liquid phase of the soil. Results of the sorbed phase are presented as measured and simulated fractions of phosphate-sorption in relation to depth in the upper 80 cm of the soil (Fig. 34a). Simulated and measured values are presented as averaged values for the year 1992. Calculation of standard deviation has been based on more than 20 measurements. Results for the liquid phase relate to ortho-phosphate concentrations which have been presented as a function of depth (Fig. 34b).

The model validation was performed by comparison of calculated ortho-phosphate loads towards the ditch with measured values. Measured loads relate to loads as could be determined as P-discharges at the end of a field ditch. The results of this validation (Fig. 35) show a fair agreement between simulated and measured values. Other results have been presented by Kruyne *et al.* (1996).

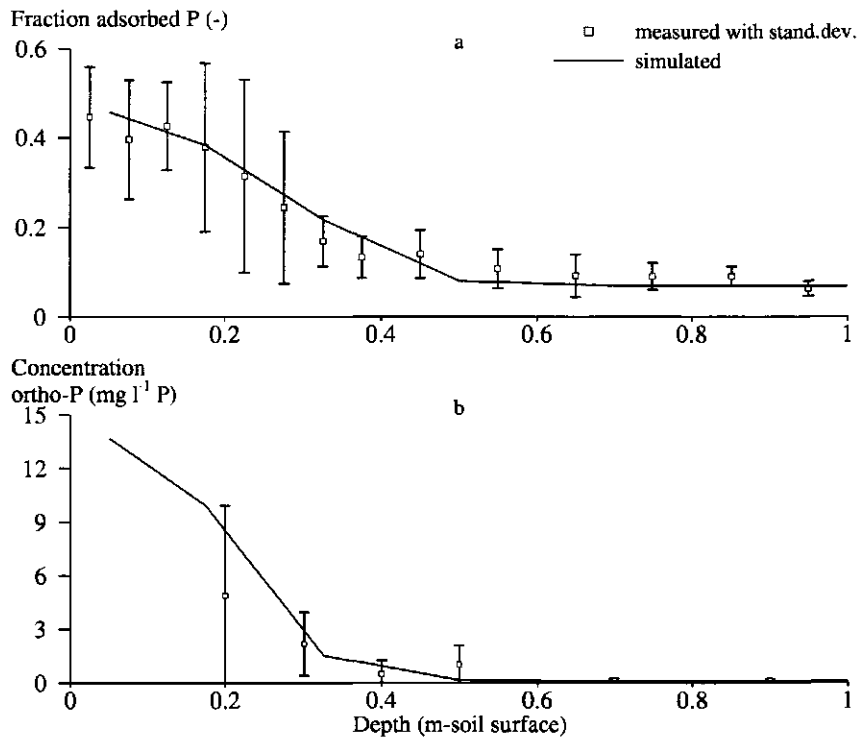


Fig. 34 Calibration Putten: measured and simulated fractions (-) of phosphate-occupation (a) and ortho-phosphate concentrations ($\text{mg l}^{-1} \text{P}$) in the liquid phase (b) in the upper 80 cm of the soil

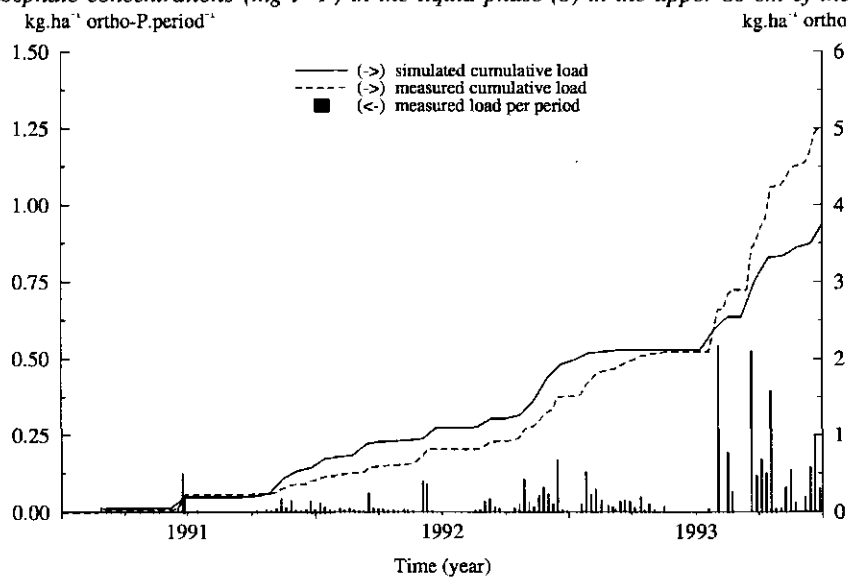


Fig. 35 Validation Putten: simulated (a) and measured loads (b) of ortho-phosphate ($\text{kg ha}^{-1} \text{P}$) discharged by a field ditch

4.7 Flower bulb soils

4.7.1 Introduction

Flower bulb cultivation in The Netherlands can be characterized as an intensive form of agriculture with intensive use of fertilizers and pesticides. An important part of this cultivation is situated at vulnerable weakly humous calcareous sandy soils. Average phosphate surplusses during the eighties have been estimated at 220 kg a⁻¹ P₂O₅ (Steenvoorden *et al.*, 1990). Environmental risks are considerable and research has been conducted to gain quantitative insight to assess these risks. Part of this research programme was a laboratory study of phosphate reactions in calcareous sandy soils (Schoumans and Lepelaar, 1995) resulting in an alternative sorption/precipitation formulation to be implemented in the ANIMO model by an appropriate choice of the input parameters. The formulation was verified on laboratory experiments and validated under field conditions (Dijkstra *et al.*, 1996).

4.7.2 Method

At first, laboratory research employing batch experiments yielded information on the sorption/precipitation mechanisms. The resulting model formulation has been verified in column leaching experiments with two soil samples. Field data on phosphate liquid concentrations in soil, groundwater and drainwater have been used to validate the model under field circumstances.

Two different soil types have been identified as the most important groups to describe the phosphate behaviour in flower bulb cultivated sandy soils: mud-flat sands and coastal dune sands. Laboratory research yielded the parametrization of the Langmuir relation describing the equilibrium sorption (Table 12).

Table 12 Parametrization of Langmuir equation describing the equilibrium sorption of phosphate in calcareous sandy soils

Soil type	K_L (l mg ⁻¹)	X_{e,max,PO_4} (mmol kg ⁻¹ P)	Explained variance (%)
Mud-flat sands	0.101	0.79	88
Coastal dune sands	0.144	0.43	85

Laboratory data supported the assumption that the sorption/diffusive precipitation reaction can be modelled according to a rate dependent Freundlich equation:

$$\frac{dXP}{dt} = k_{ads} (K_F [Ca]^{N_2} [P]^{N_1} - XP)$$

where:

- [Ca] : calcium concentration (mol l⁻¹)
- [P] : phosphate concentration (mol l⁻¹)
- XP : content sorbed / precipitated phosphate (mmol kg⁻¹ P)
- k_{ads} : rate coefficient (d⁻¹)
- K_F : sorption/precipitation coefficient (nmol kg⁻¹P)(mol l⁻¹P)^{-N₁} (mol l⁻¹P)^{-N₂}
- N₁ : P-concentration exponent (-)
- N₂ : Ca-concentration exponent (-)

Seven soil samples have been treated in a series of experiments. The quantity of rate dependent phosphate sorption / precipitation was determined from the total P-fixation minus the calculated quantity assigned to the equilibrium sorption phase. For the assessment of the parameters describing the rate dependent formulation, no distinction could be made between the two soil types. The resulting parametrization reads: K_F = 600908, k_{ads} = 0.02529, N₁ = 1.024 and N₂ = 0.732 and the percentage explained variance was 89,5% (Schoumans and Lepelaar, 1995).

Verification of these parameters was performed by comparing simulated and measured effluent concentrations of a leaching experiment. Two soil samples have been loaded by flushing with a phosphate influent concentration of 50 mg.l⁻¹ P (pH=8). After saturation, the equilibrium sorption phase was removed by leaching with a zero-phosphate concentration. This experiment was simulated by the ANIMO model using the data concerning the experimental circumstances as input data and assuming that the influence of the organic phosphate cycle could be neglected. The rate constant refers to the adsorption reaction, whilst the backward reaction was assumed to be zero.

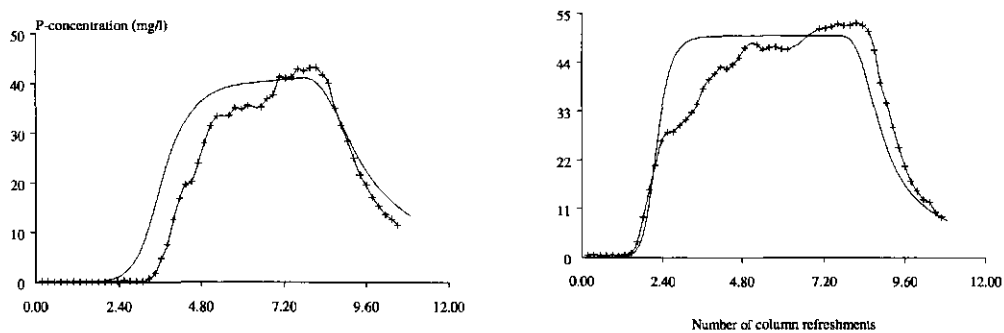


Fig. 36 Breakthrough curves of phosphate leaching experiments conducted with two soil samples originating from 0-25 cm depth (left) and 52-72 cm depth (right)

The results show a fairly good performance of the model. The simulated concentrations agree reasonably well with the measured values. It can be concluded that the proposed process formulation and derived set of parameters is able to describe the average phosphate concentrations in homogeneous calcareous sandy soils.

Field measurements included collection of hydrological data and data concerning nutrient concentrations in soil moisture and drain water. The hydrological conditions of the experimental field are characterized by a groundwater level at 0.6-1.0 m depth, a drain spacing of 5 m and sprinkling during spring and summer season. Once in four

years, a six week inundation period of the soil profile is established to remedy biological soil contamination. No animal manure is dosed for fertilization, but organic compost is applied to prevent wind erosion of soil particles. During winter time, the fields are covered by straw to protect young flower bulbs for freezing.

In this study, the soil management, the material inputs and the nutrient extraction by the flower bulb crops were quantified and the initial condition with respect to the phosphate content of the soil was estimated from soil analyses.

4.7.3 Results

Simulation runs for validation purposes were carried out for a two-year period. Hydrological input data to the ANIMO model were generated by the SWAP model using measured moisture retention curves and measured hydraulic properties. The lower boundary of the model was described by the drainage characteristics as found in the field. The ANIMO model was calibrated on the basis of a qualitative comparison between simulated and measured values. Results of the phosphate concentrations of the soil water phase at different depths in one of the two soil profiles at the St. Maartensbrug site have been depicted in Figure 37. Only minor adaptations of the initial distribution between the quantities present in the equilibrium sorption phase and the rate dependent sorption/precipitation phase were applied.

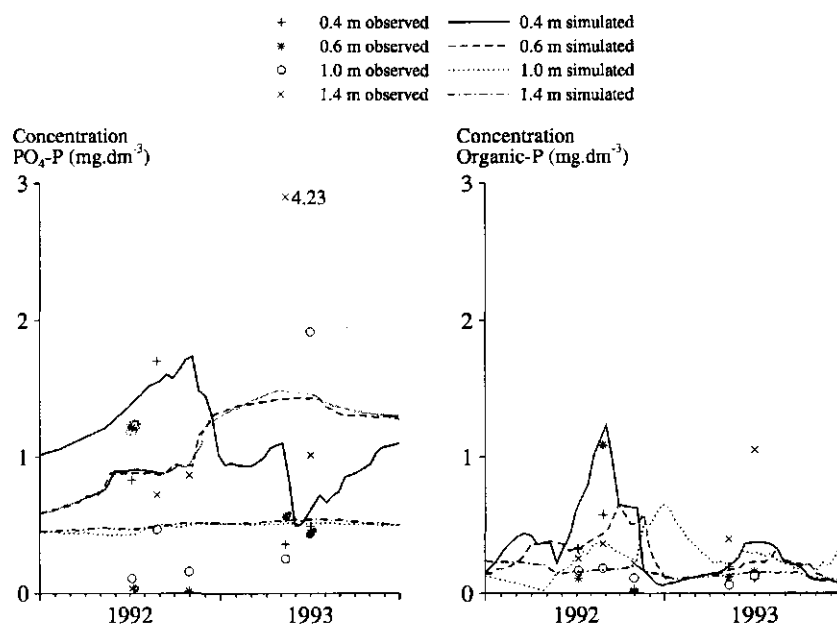


Fig. 37 Measured and simulated ortho-phosphate and dissolved organic phosphate concentrations in soil water at 40 cm, 80 cm, 100 cm and 140 cm depth

The dynamics of the simulated ortho-phosphate concentrations at 40 and 60 cm below soil surface agrees fairly well with the measured values, but dynamics of the the ortho-

P concentrations at 100 and 140 depth could not be reproduced. The organic-P concentrations are described satisfactorily by the model.

The field validation was carried out by an evaluation of the simulated drainwater concentrations (Fig. 38). Both the measured and the simulated concentrations are within the same range while the measured concentrations show a greater variation. The dynamic behaviour of the simulation run is mainly caused by the dynamics of dissolved organic phosphate. This agrees with the dynamics of the ortho-P concentration in the upper groundwater zone. The model was unable to simulate the measured short term dynamics of phosphate concentrations in drainage water. For the purpose of long term predictions, the model performance is judged to be useful.

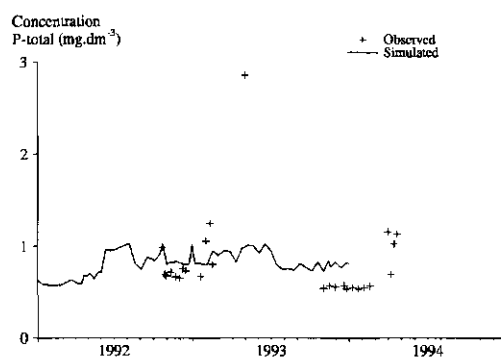


Fig. 38 Measured and simulated total-P concentrations in drainwater of a St. Maartensbrug flower bulb field plot

Validation on the concentrations of another drain situated at a distance of 200 m relative to the experimental drain considered in this paragraph resulted to a worse result. This may be due to the soil heterogeneity within the catchment area of the drain tubes and due to the uncertainty of the initial occupation of the soil complex with phosphate and the initial distribution of sorbed phosphate.

5 REGIONAL MODEL APPLICATIONS

5.1 Introduction

The aim of the ANIMO model is to serve as a tool for evaluation of fertilization strategies and water management measures on nutrient leaching to groundwater and surface water systems at a regional scale. Soon after the first field validations became available in 1987 and 1988, the model was applied at the regional scale (Drent *et al.*, 1988). Regional applications nearly always included comparisons between measured field data and simulated values, but at such a scale only a tentative verification has been possible rather than a thorough validation due to the enormous data requirement. The model was applied for different Dutch conditions with respect to climate, soils, cropping pattern and fertilization strategies on a regional scale which varied from the whole of The Netherlands to specific catchments. Figure 39 refers to the regions where the ANIMO model has been applied. In this chapter, three examples of model applications will be treated:

- National study on leaching of nutrients to groundwater and surface water in the framework of a water management policy analysis in The Netherlands.
- Regional study on leaching of phosphate from P-saturated soils in the Eastern, Central and Southern sand districts of The Netherlands (Fig. 39, left).
- Regional study on the load on groundwater and surface water systems as influenced by fertilization levels differentiated to different land use types from the point of view of town and country planning and water management in the Beerze-Reusel catchment in the Southern part of The Netherlands (Fig. 39, right).

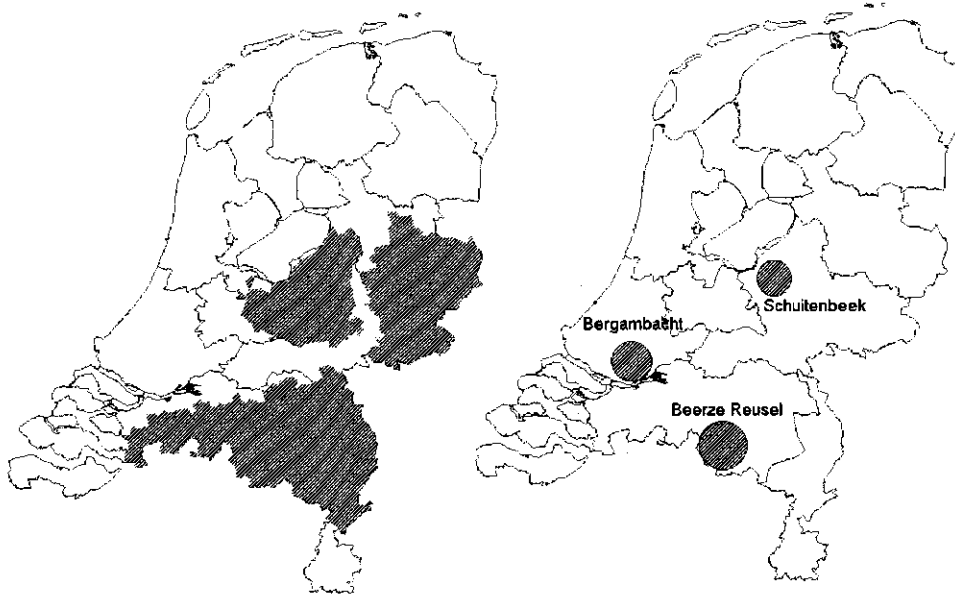


Fig. 39 Four regional applications of the ANIMO-model in The Netherlands: phosphorus leaching from sandy soils (left); nutrient leaching in the regions Bergambacht, Schuitembeek and Beerze-Reusel (right)

Other regional studies pertain to the Southern-Peel region (Drent *et al.*, 1988), the Schuitembeek catchment (Kruijne and Schoumans, 1995) and the peat pasture area in the Bergambacht polder (Hendriks *et al.*, 1994) are not mentioned in this discussion for reasons of conciseness.

5.2 Leaching of nitrogen and phosphorus from rural areas to surface waters in The Netherlands

5.2.1 Introduction

In the framework of the Policy Analysis of Water Management in The Netherlands the ANIMO-model was applied twice: for the Third (NW3; Uunk, 1991) and for the Fourth (NW4; Boers *et al.*, 1997). National Policy Document. In both applications the model was used to analyse the effects of different scenarios of fertilizer management on nitrogen and phosphorus leaching from rural areas into Dutch surface waters. Both studies were initiated and funded by the Institute for Inland Water Management and Waste Water Treatment (RIZA, Lelystad, The Netherlands) and aimed at a reduction of eutrofication of surface waters. The leaching studies were carried out in close cooperation with RIZA, and the DELFT HYDRAULICS. The results from these studies have been used by DELFT HYDRAULICS and RIZA as input information in models

describing the distribution of surface water and the quality of major surface water systems in The Netherlands.

5.2.2 Methodology

A model instrument consisting of a schematization procedure, a static model for fertilizer additions and dynamic models for water transport in soil (DEMGEN) and nutrient leaching to groundwater and surface water (ANIMO) (Fig. 40) was developed and applied. The fertilizer distribution model predicted the impact of policy intentions on the short term and long term field additions. Dynamic models for water and nutrient behaviour in soils were inevitably required because of the combined impact of seasonal variations in meteorology, hydrology and timing of fertilizer applications, which is essential for the leaching of N and P to surface waters.

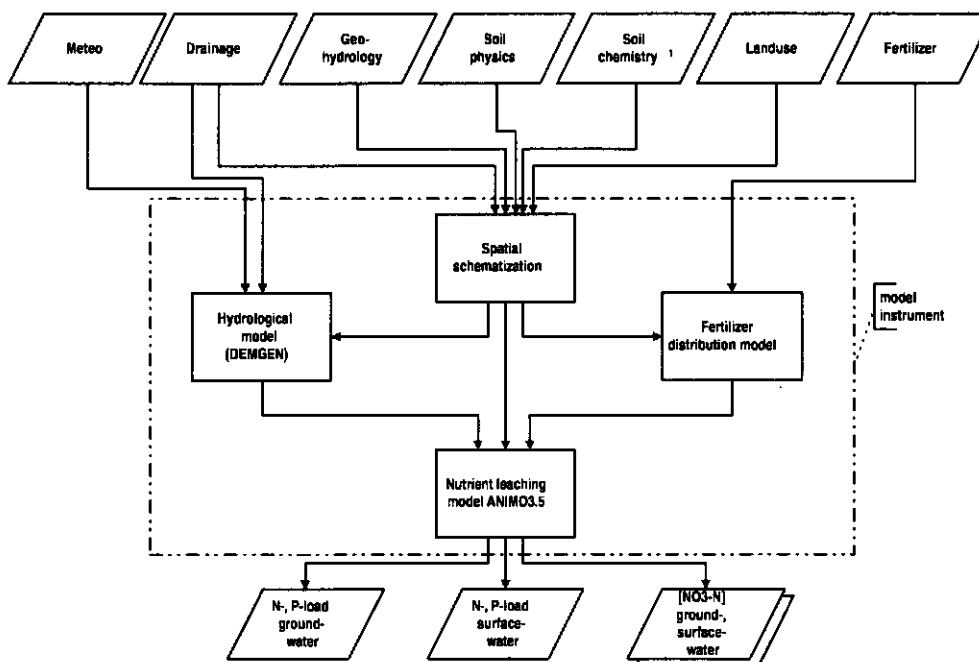


Fig. 40 Model instrument and main data flow

The first step in the application of the model instrument was the determination of a spatial schematization. Basic data related to meteorology, geohydrology and drainage conditions originating from the Institute for Inland Water Management and Waste Water Treatment and data related to soil physics, soil chemistry and land use

originating from the DLO Winand Staring Centre were used to arrive at a set of calculation units (plots). Once the spatial schematization was established, the hydrology of the soil system for each plot was simulated by the DEMGEN model. The fertilizer distribution was assessed by the DELFT HYDRAULICS. Results of both types of computations were transmitted to SC-DLO, who applied the nutrient leaching model to simulate the behaviour of N and P in the soil. These simulations generated N and P mass balances of each plot. The N and P loads towards surface water systems could be derived on the basis of these results.

The ANIMO model requires a good estimate of the initial distribution of N, P and C compounds in solid and liquid phase of the soil system, because poor initial conditions will cause error propagation. However, it is almost impossible to estimate the initial penetration of N and P fronts in the soil and the distribution of compounds over different pools of organic matter (including characteristic C/N and C/P ratios and decay rates). Therefore the decision was made to simulate a historical period from 1940 to the year which served to evaluate historical simulations results to let the nutrient model generate its own initial conditions. Evaluation years were 1985 for NW3 and 1993 for NW4. Results of the evaluation year were used to verify the initial conditions by making a tentative comparison between measured and simulated data and were utilized as initial conditions for future scenarios (until 2045). Results from the hydrological model for the period 1971 to 1985 were used as input for nutrient simulations of history and scenarios. The fertilizer distribution model produced types and level of annual fertilizer applications. Data with respect to the time of application and the kind of fertilizer management were collected by SC-DLO and processed to generate yearly input files. Finally results were analysed using general statistics, in the latest NW4-study within a GIS environment.

5.2.3 Results

This paragraph describes results of the most recent study performed in the framework of the Fourth National Policy Document on Water Management in The Netherlands (NW4). Validation of initial simulations to assess the environmental pollution and the store of minerals in soils in the evaluation year was conducted by comparing simulated and measured concentrations in groundwater and surface water systems. Special attention was paid to the validation of the discharge to surface water systems. Therefore three regions with different soil units were selected: a clay, a peat, and a sandy region. The nutrient leaching model does not include the hydraulic, chemical and biological processes taking place in surface water systems. During the winter period, low temperatures will prevail and process rates will be low. Relatively high discharges in winter cause low residence times and will minimize the influence of processes in the surface water. Consequently, a comparison of winter discharges to the surface water system with measured concentrations in the surface water system can be made more safely than a comparison of summer discharges. An example of a validation result of the nitrogen concentration in the sandy region 'Schuitembeek' located in the central part of The Netherlands is given in Figure 41.

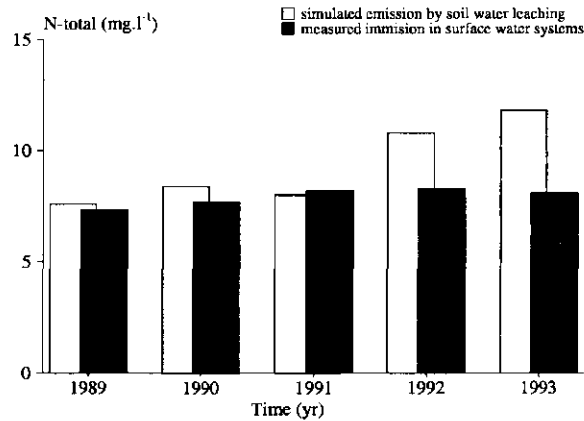


Fig. 41 N concentrations (mg l^{-1} N) in water leaching during the winter period from the soil towards surface waters (simulated) and concentrations in surface waters (measured) in the region 'Schuitembeek'

Five fertilizer scenarios were simulated. Only three will be briefly discussed here: two extreme scenarios and one scenario representing, as good as possible, the present policy as formulated by the Dutch Government in 1995 (scenario '*policy*'). One extreme scenario represents a continuation of the fertilizer use in 1993 (scenario '*present*'), the other extreme scenario represents a prohibition of fertilizer use (scenario '*zero*'). The scenario '*policy*' is aimed at reaching a balance between fertilizer levels, crop uptake and an acceptable loss of nutrients. In the fertilizer distribution model these acceptable losses were converted into fertilizer levels by adding estimates for crop uptake.

Computed nitrate concentrations in groundwater as a result of the scenario '*present*' and the scenario '*policy*' are given in Figure 42 for 1985 and in Figure 43 for 2015. The European nitrate directive for drinking water will be exceeded in 30% and 10% of the rural area when the fertilization scenario '*present*' respectively scenario '*policy*' will be implemented.

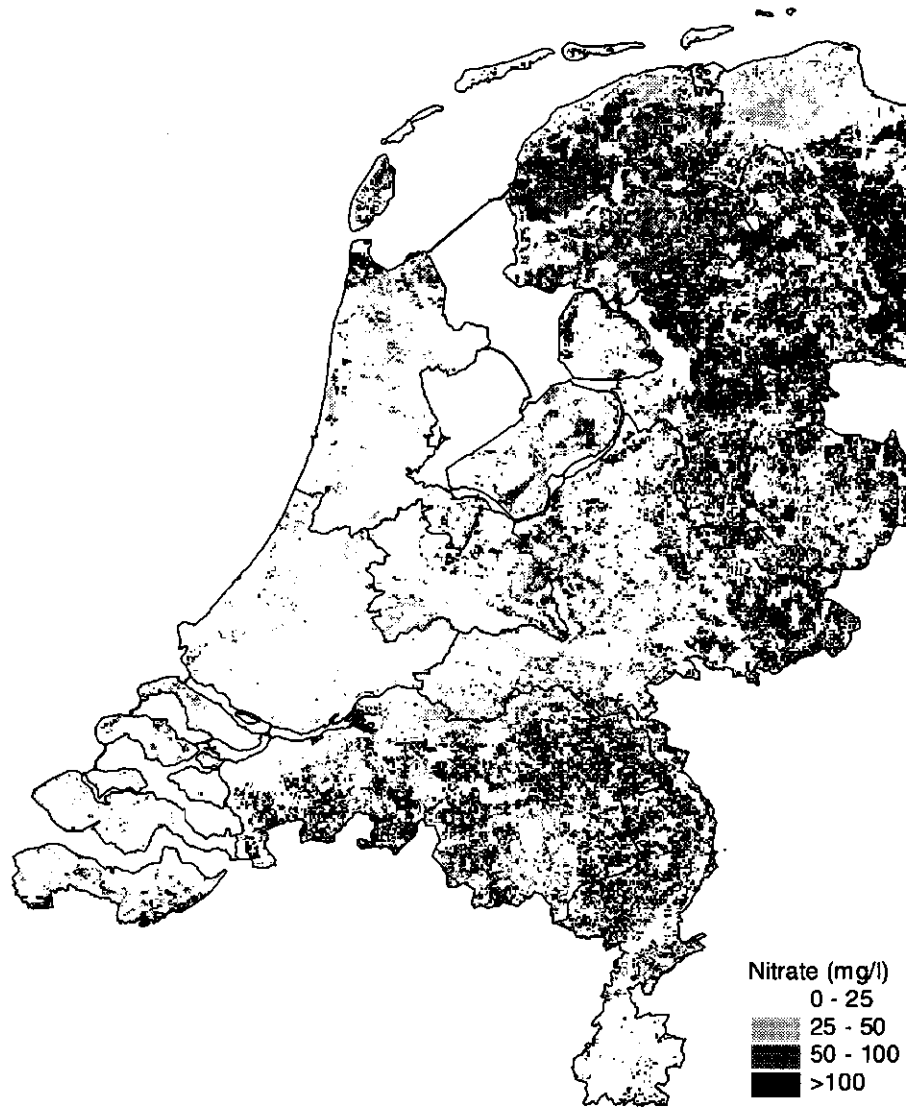


Fig. 42 Nitrate concentrations in groundwater in 1985 as a result of historical land use

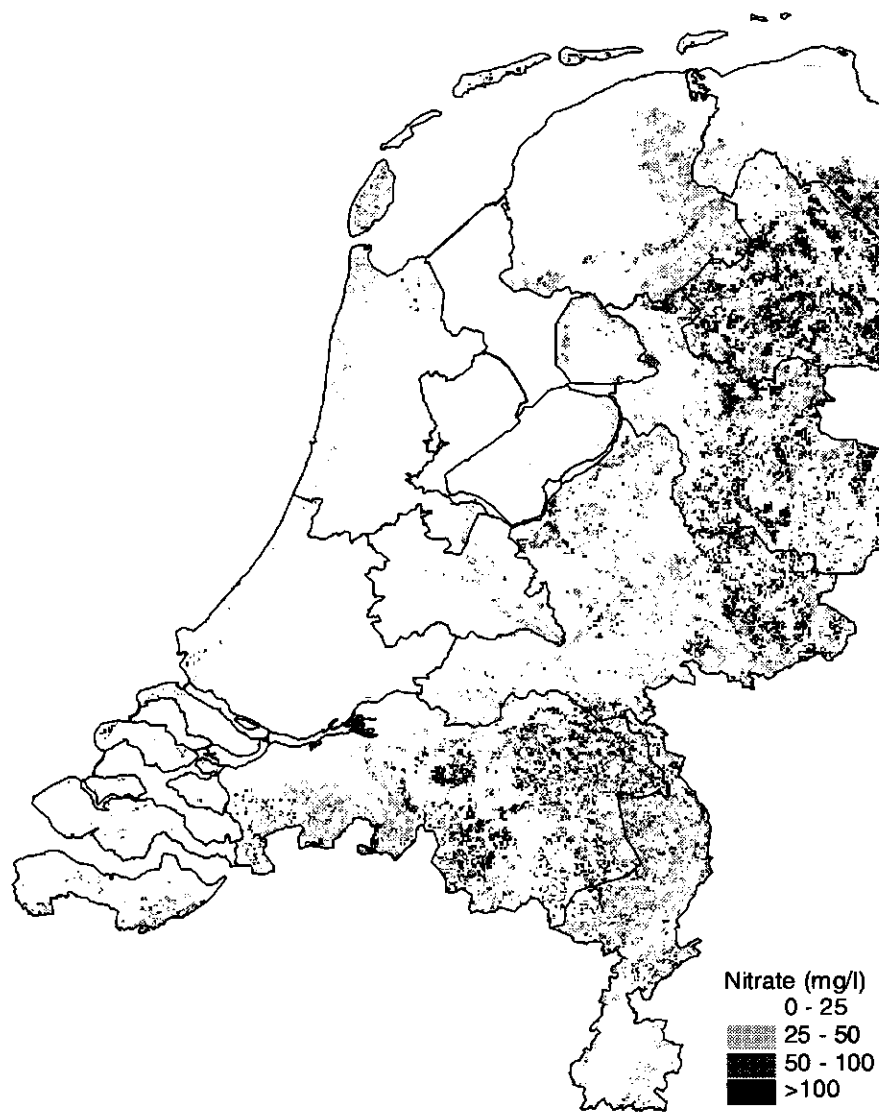


Fig. 43 Nitrate concentrations in groundwater in 2015 as a result of fertilization according to the scenario 'policy'

Scenario results pertaining the nitrogen and phosphorus leaching from soils to surface water systems in The Netherlands are depicted in Figure 44 and Figure 45. To minimize the fluctuations caused by different meteorological conditions, the results are presented as a 'running' average over periods of 15 years.

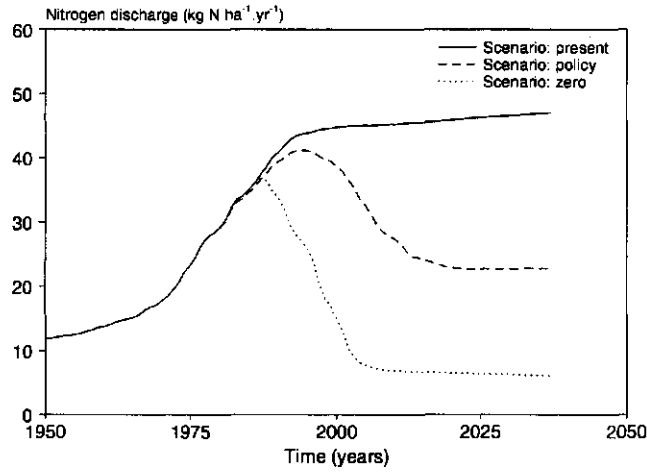


Fig. 44 Nitrogen leaching ($\text{kg ha}^{-1} \text{ a}^{-1} \text{ N}$) from soils of rural areas to surface water systems in The Netherlands as calculated for the scenarios: 'present', 'policy' and 'zero'

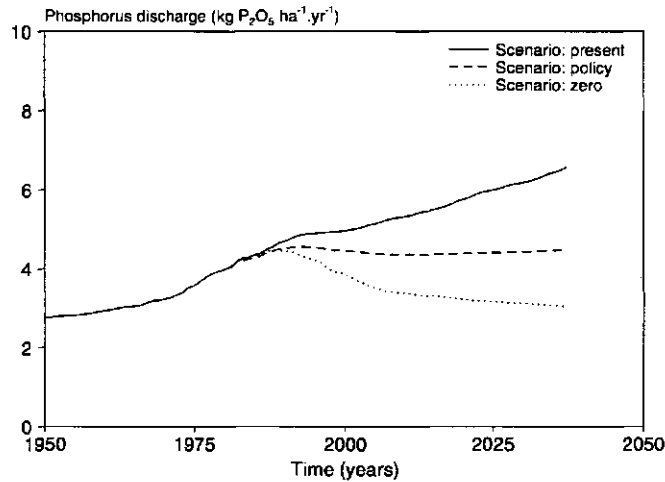


Fig. 45 Phosphorus leaching ($\text{kg ha}^{-1} \text{ a}^{-1} \text{ P}_2\text{O}_5$) from soils of rural areas to surface water systems in The Netherlands as calculated for the scenarios: 'present', 'policy' and 'zero'

The difference between the nitrogen results of the scenarios 'present' and 'zero' is large. Results from 'present' for the year 2045 show a leaching of nitrogen which is six times higher than the leaching from 'zero'. The same scenarios show that the leaching of phosphorus in the 'present' scenario is about twice as high as that of 'zero'. These scenario results indicate the maximum reduction that can be achieved if fertilization is stopped. In the year 2045, the scenario 'policy' resulted in a leaching of nitrogen of about 50% of the leaching that resulted from scenario 'present'. The phosphorus leaching from 'policy' is about 70% of the leaching from 'present'. The phosphorus leaching from the scenario 'policy' is almost constant from 1985 onward.

5.3 Simulation of phosphate leaching in catchments with phosphate saturated soils

5.3.1 Introduction

Some rural regions in The Netherlands show an intensive agricultural activity with very high livestock densities. Especially on sandy soils which are characterized by a small buffer capacity for phosphate, high doses of animal slurries and manure lead to substantial phosphate surpluses. As a result, present phosphate leaching in these area exceeds threshold values for surface water quality and adverse effects on the surface water quality occur. To investigate whether the phosphate leaching can be decreased by limiting the allowed P surplus, a modelling study was carried out to evaluate the effects of different fertilization scenario's (Groenenberg *et al.*, 1996).

5.3.2 Methodology

To estimate the phosphate leaching from soils in the area with sandy soils and a manure surplus in The Netherlands, simulations were carried out with dynamic models. The hydrology was simulated with the simple, two layer dynamic WATBAL model (Berghuis-van Dijk, 1985). Nutrient related processes were simulated with the ANIMO model. Computations were made for about 2100 units unique in soil chemistry, soil physics, hydrology, historic phosphate load and land use. After initialization of the models with the historic phosphate loads, two different scenario's were run for a period of 60 years.

The methodology and models were verified on the Schuitembeek catchment. In this catchment, measurements of phosphate leaching and phosphate concentrations were available for the period 1990-1993 which allow a comparison of simulated with measured values. Results of the verification show that the simulated phosphate saturation as a function of soil depth was within the range of measure values. Results, however, also indicate that the simulated phosphate front is sharper than the measured one which causes leaching and concentrations of phosphate that are somewhat lower than the measured data, especially for groundwater regime class V/V*. The comparison was hampered by the fact that the hydrologic years 1990-1993 were not in the meteorological data set used to compute the hydrology.

5.3.3 Results

In the first scenario, a phosphate surplus of $10 \text{ kg ha}^{-1} \text{ P}_2\text{O}_5$ was used whereas in the second scenario a surplus of $40 \text{ kg ha}^{-1} \text{ P}_2\text{O}_5$ was used. The effects of the scenario's was evaluated on some selected plots. From these plot calculations it can be concluded that leaching at the level of the average highest ground water level (GHG) tends to the level of the added surplus. Leaching fluxes towards surface waters increase with the $+40 \text{ kg}$ scenario, with the $+10 \text{ kg}$ scenario leaching fluxes are stabilized. Results of the scenario runs for the entire sandy area show that almost all evaluated units,

the units with groundwater regime classes I up to V*, have a phosphate saturation higher than 25% which means that these units are phosphate saturated. This is in accordance with results from Groenenberg *et al.*, (1996). Phosphate leaching and phosphate concentration for the +10 kg scenario hardly increased between year 20 and year 50 (Fig. 46) of the scenario run. For the +40 kg scenario, however, an increase in time for both concentration and leaching is simulated.

A first tentative assessment was made of the effects of a chemical treatment to reduce the leaching of phosphate, by assuming that this treatment was applied on all strongly P saturated soils in each catchment. In field experiments (Kruijne *et al.*, 1996) it was shown that this treatment reduces P leaching by about 70%. Results showed that such a measure can only reduce P leaching on catchment level if a scenario with a low P surplus for the other soils (with a P saturation < 75%) is used. In that case a reduction of maximal 20-30% in phosphate leaching was calculated. Higher reduction percentages are possibly only feasible in small (sub) catchments. In case of a larger surplus (40 kg), the positive effects of a chemical treatment for very strongly P saturated soils are diminished by an increased P leaching from other soils.

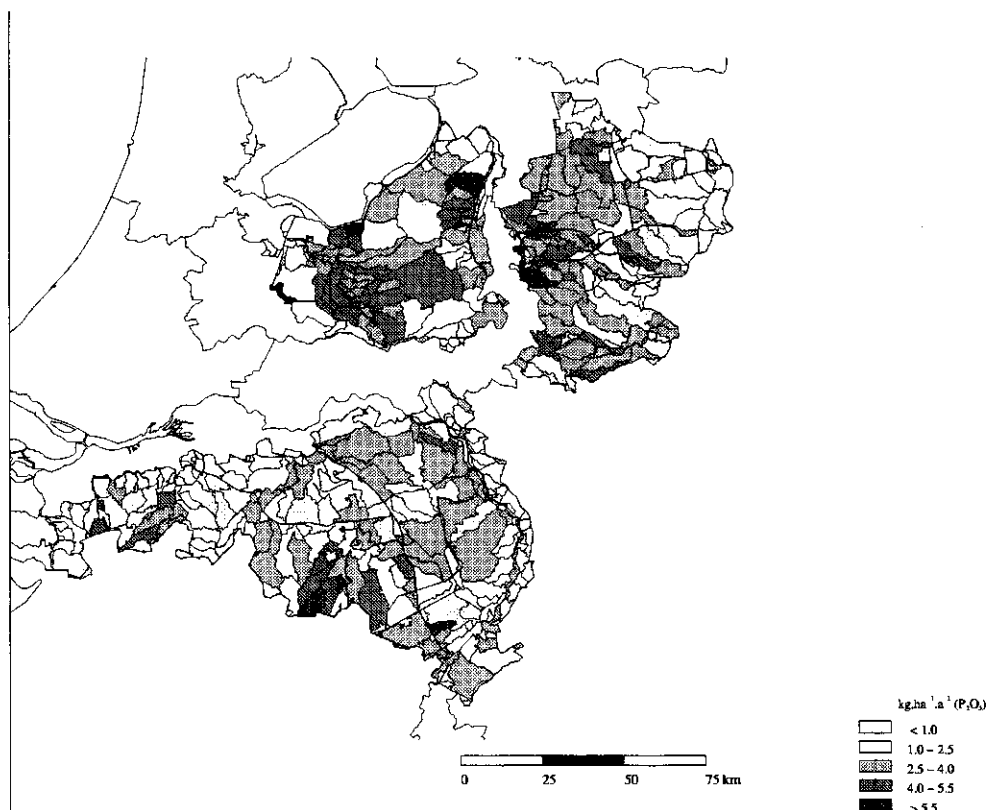


Fig. 46 Phosphate leaching ($\text{kg ha}^{-1} \text{a}^{-1} \text{P}_2\text{O}_5$) from sandy soils of rural areas to surface water systems as resulting from a scenario with 50 years of phosphate surplus of $10 \text{ kg ha}^{-1} \text{a}^{-1} \text{P}_2\text{O}_5$.

5.4 Beerze Reusel catchment

5.4.1 Introduction

Prohibition of groundwater withdrawal for sprinkling of grassland is considered as a combative measure to the regional lowering of groundwater levels. However, a rise of the water table possibly implies undesirable environmental impacts. Also, the raise of surface water levels which lead to swamp conditions are considered as possible measures to stimulate the evolution of former agricultural soils to wet nature areas. However, this type of water management can yield an undesirable increase of the nutrient leaching to surface water systems.

The study aimed at the quantification of the differences of nutrient discharges to groundwater and surface water as a consequence of the water management interference. In the framework of a regional study in the Beerze Reusel catchment in the southern part of The Netherlands, the impact of raised waterlevels were studied in the Beerze Reusel catchment in the Southern part of The Netherlands

5.4.2 Methodology

Nitrogen and phosphorous balances and nutrient loads on surface water systems were computed for different types of water management measures with integrated regional models for water management and groundwater flow. The regional groundwaterflow model SIMGRO (Querner and Van Bakel, 1988) was used to simulate the weekly water balances of 189 subregions for a meteorological series of 15 years. The SIMGRO model is an integrated hydrological model which comprises the unsaturated zone, the saturated zone and the surface water system. The saturated zone module consists of a quasi-three dimensional finite element model using an implicit calculation scheme. The saturated zone is subdivided into aquitards with vertical flow and aquifers with horizontal flow. In the top layers of the saturated zone different drainage systems can be introduced. The unsaturated zone is modelled as two reservoirs: one for the root zone and one for the subsoil. The storage of water in the root zone is considered along with extractions and inflows. From the subsoil waterbalance, the phreatic surface elevation is calculated using a storage coefficient. The unsaturated zone is related to land use on a sub-regional level. Subregions are chosen to have relative uniform soil properties and hydrologic conditions. The discharge from the saturated zone is influenced by the hydraulic properties of the surface water system by means of storage function and a discharge function which relates the drainage level to the discharge of a subregion.

In the Beerze-Reusel model, each sub-region was covered by maximal 10 types of land uses. The results of the SIMGRO model were verified with a limited number of groundwater elevation time series and estimated annual water discharges of some sub-catchments. A qualitative verification was conducted by a comparison of simulated and measured groundwater elevation maps for two points in time. The results were used as hydrological input to the ANIMO model.

Since the ANIMO model only describes the nutrient leaching as a local flow through a vertical column, the set of models was extended by a nutrient model simulating the transport of nutrients in deeper regional flow systems. Interactions between subregions via the groundwater system are accounted for by linking the ANIMO model to the model AQUIMIX (Fig. 47) which has been developed for the transport of N-compounds and phosphate in the aquifer system. It considers the reduction of the nitrate concentration in the aquifer oxidation of organic matter and pyrite. The AQUIMIX model calculates per nodal point and per layer the regional solute transport and the geochemical processes in the saturated zone with time steps of ½ to 1 years. The calculated concentrations in the top layer of AQUIMIX at the end of the time step are the input concentrations for upward seepage in the ANIMO model.

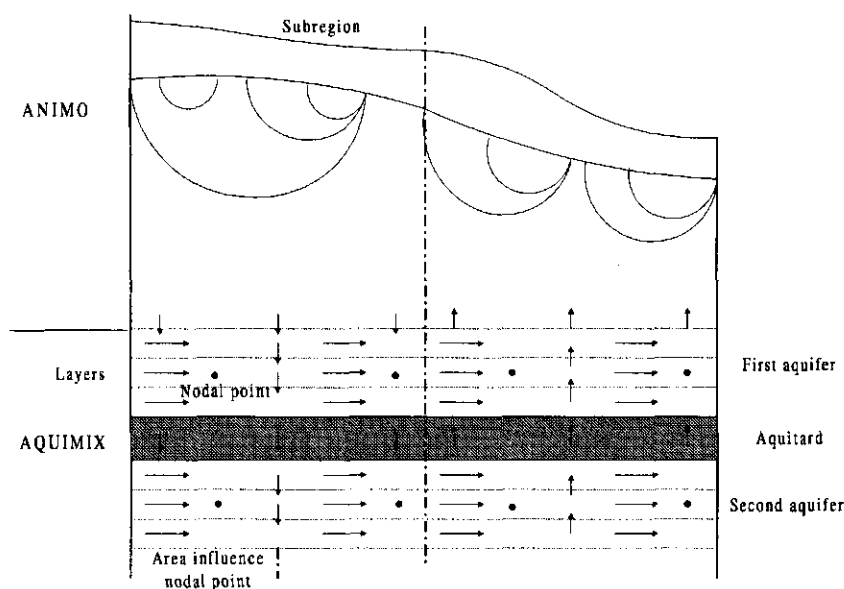


Fig. 47 Linking of the ANIMO model to a groundwater quality model AQUIMIX to account for regional interactions between infiltration areas and exfiltration areas

The historical and the future fertilizer applications were simulated by the SLAPP model (Van Walsum, 1988), which is based on linear programming principles and some assumptions with respect to the mineral requirement of crops and to the activity of nutrients in different types of manure.

This model configuration has been used to evaluate the environmental impacts with respect to reductions of permitted fertilization levels, the creation of new nature areas by the abolishment of fertilization (topic related to town and country planning), and water management strategies such as the prohibition of groundwater withdrawal for sprinkling purposes and the raise of the groundwater elevation to stimulate the generation of new nature areas. The research project was carried out in four phases:

1. Data-acquisition, schematization of the region and simulation of hydrology (Van der Bolt *et al.*, 1996a).
2. Estimation of fertilizer distribution and simulation of historical mineral charging of soils and present environmental pollution by nitrogen and phosphorus compounds (Van der Bolt *et al.*, 1996b).

3. Prediction of environmental impacts as caused by the reduction of fertilization levels. Effects of differentiated permitted fertilization levels with respect to land use types as defined by the town and country planning by national and provincial authorities were studied (Van der Bolt *et al.*, 1996c).
4. Prediction of the nutrient load on groundwater and surface water systems as influenced by a set of water management measures (Groenendijk and Van der Bolt, 1996).

5.4.3 Results

Results presented below are related to the fourth phase of the research project which studied the impact of hydrological interferences. One of the hydrological scenario's contained the prohibition of groundwater withdrawal for sprinkling purposes. In the reference situation, only dry sensitive pastures were irrigated during drought periods. On sandy soils which are sensitive to drought, the sprinkling prohibition results in a rise of the groundwater. A complete stop of sprinkling, whilst equal fertilization doses are applied, will lead to an increase of the average nitrate concentration in groundwater in areas characterized by a relative high sprinkling requirement (Table 13). The moisture deficit causes a decrease of crop dry matter production and as a consequence also a diminished mineral uptake by plant roots. The extra nitrogen surplus leaches to the groundwater zone and causes a slight increase of the nitrate concentration.

Table 13 Average nitrate concentration of groundwater in areas covered by grassland, classified by the average annual sprinkling requirement

Sprinkling requirement (mm a ⁻¹)	Nitrate concentration (mg.l ⁻¹ NO ₃ -N)	
	Sprinkled	Sprinkling prohibited
0 - 50	3.6	3.5
50 - 100	14.3	14.7
> 100	16.9	20.2

In the brook valleys with shallow groundwater levels, the nitrate concentrations were already low and change is expected. It was concluded that fine tuning of farm management and fertilization strategies on water management measures are necessary to avoid adverse environmental impacts.

Another water management scenario was defined to study the impacts of raising groundwater levels by water management. Within the future nature areas, the bottom of field ditches raised and in the agricultural areas water conservation measures were applied. Water conservation was assumed by weir management during the spring and the summer season. These types of hydrological interferences are relevant as a measure to prevent negative effects on ecology.

A special variant of this hydrological scenario comprised the restauration of the historical flow regime properties of semi-natural streams. The bottom of the streams were raised and the hydraulic resistances enlarged by an increased length of the stream

bed. Results of the simulated groundwater levels during spring time are depicted in Figure 48. Compared to the package of hydrological measures to raise groundwater elevations by less favourable drainage conditions, the restoration of the historical stream properties leads to an additional raise of groundwater levels. Conveyance of the precipitation surplus through the drainage system will be hampered and will lead to an additional raise of water levels in canals and field ditches.

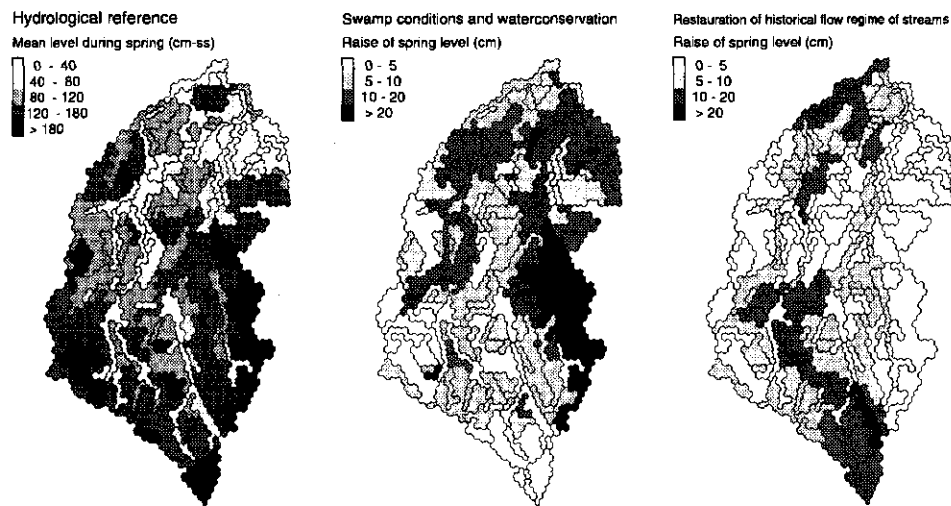


Fig. 48 Mean groundwater level during spring (left) raise of spring level resulted from the raise of third order drainage level and the weir management during summer (middle) and the additional raise of the spring level caused by the restauration of the historical flow regime of streams

The raise of groundwater levels induces wetter soil conditions which results in an increase of denitrification and to a decrease of mineralization. The additional increase of the groundwater elevation by the restauration of the historical flow regimes of natural streams leads to an additional decrease of nitrate concentrations (Fig. 49).

Based on the results of each sub-area, the results with respect to the P-leaching to surface water have been aggregated to sub-catchment level. All sub-catchments show an increase of P-discharge to surface water (Fig. 50). The phosphate load on surface water in these areas is 5 times as high as the P-discharge outside the stream valleys. The raise of water tables due to the nature oriented water management will lead to a considerable increase of P-discharge in the future nature areas. Higher groundwater elevations lead to an increase of shallow water discharge through phosphate rich soil layers. The raise of groundwater generates adverse conditions from the point of view from eutrofication by phosphates. The additional raise of the groundwater elevation which is accompanied by the retardation of surface water discharge leads in some sub-catchments to a slight decrease of phosphate leaching, compared to the phosphate discharge which results from the water management package without the adjustment of the flow regime of the streams, while in other sub-catchments a slight increase will occur. The average P-load on surface water systems shows an increase from $1.0 \text{ kg ha}^{-1} \text{ a}^{-1}$ to $1.4 \text{ kg ha}^{-1} \text{ a}^{-1}$ as a result from the water management measures, while the additional raise of groundwater elevations causes a counter balancing effect and the average P-load amounts to $1.2 \text{ kg ha}^{-1} \text{ a}^{-1}$.

Effects of increased mobilization of dissolved phosphate compounds induced by soil chemical reactions which will occur under these anaerobic circumstances have not been taken into account. Therefore, the calculated increase of phosphate leaching has to be considered as a prudent prediction.

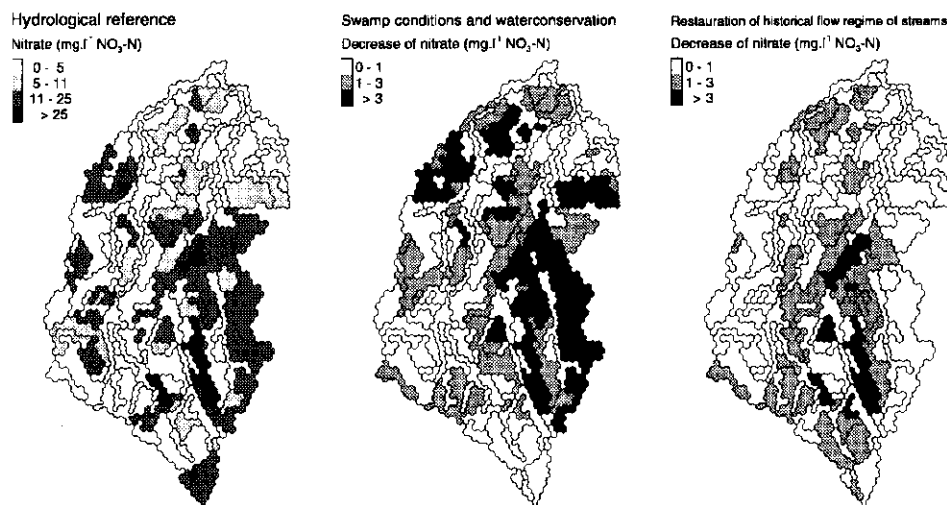


Fig. 49 Nitrate concentration in the reference situation predicted for areas covered by grassland (left) decrease of nitrate concentration as resulted from the raise of third order drainage level and the weir management during summer (middle) and the additional decrease of the nitrate concentration caused by the restauration of the historical flow regime of streams (right)

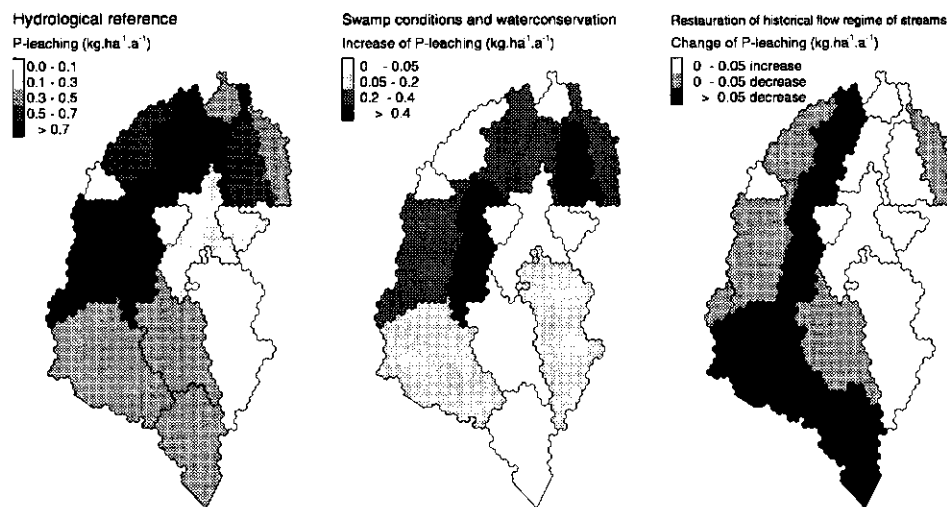


Fig. 50 P-leaching to surface water in the reference situation (left), P-discharge as resulted from the raise of third order drainage level and the weir management during summer (middle) and the additional raise of the spring level caused by the restauration of the historical flow regime of streams (right)

References

Abrahamse, A.H., G. Baars and E. van Beek, 1982. Policy analysis of water management for the Netherlands. Model for regional hydrology, agricultural water demands and damage from drought and salinity. Vol. XII. RAND corporation, Delft Hydraulics Laboratory, Delft.

Appelo, C.A.J., 1988. The retardation of pollutants in aquifers by ion exchange and adsorption. Institute of Earth Science, Free University, Amsterdam. Lecture notes for a course on Applied Modelling of Groundwater Pollution, IGWMC, Delft.

Bakker, J.W., F.R. Boone and P. Boekel, 1987. Diffusie van gassen in grond en zuurstofdiffusiecoëfficiënten in Nederlandse akkerbouwgronden. Rapport 20. Instituut voor Cultuurtechniek en Waterhuishouding. Wageningen.

Belmans, C., J.G. Wesseling and R.A. Feddes, 1983. Simulation model of the water balance of a cropped soil: SWATRE. *Journal of Hydrology* 63, 3/4: 271-286.

Berghuijs-van Dijk, J.T., 1985. WATBAL: a simple water balance model for an unsaturated/saturated soil profile. Nota 1670. Institute for Land and Water Management Research, Wageningen.

Berghuijs-van Dijk, J.T., P.E. Rijtema and C.W.J. Roest, 1985. ANIMO: agricultural nitrogen model. Nota 1671. Institute for Land and Water Management Research, Wageningen.

Boers, P.C.M., H.L. Boogaard, J. Hoogeveen, J.G. Kroes, I.G.A.M. Noij, C.W.J. Roest, E.F.W. Ruijgh and J.A.P.H. Vermulst, 1997. Present and future fertilizer loads on surface waters (published in Dutch as: 'Huidige en toekomstige belasting van het oppervlaktewater met stikstof en fosfaat vanuit de landbouw'). Report 97.013, RIZA, Lelystad.

Boesten, J.J.T.I., 1986. Behaviour of herbicides in soil: simulation and experimental assessment. Thesis Agricultural University, Wageningen: 263 pp.

Bolt, F.J.E. van der, J. Pankow, C.W.J. Roest and A. van den Toorn, 1990. De invloed van de stikstofhuishouding in de bodem op de grondwaterkwaliteit in waterwingebied 't Klooster. Rapport 31. DLO-Winand Staring Centrum, Wageningen.

Bolt, F.J.E. van der, P.E.V. van Walsum and P. Groenendijk, 1996a. Nutriëntenbelasting van grond- en oppervlaktewater in de stroomgebieden van de Beerze, de Reusel en de Rosep. Simulatie van de regionale hydrologie. Rapport 306.1. DLO-Winand Staring Centrum, Wageningen.

Bolt, F.J.E. van der, P. Groenendijk and H.P. Oosterom, 1996b. Nutriëntenbelasting van grond- en oppervlaktewater in de stroomgebieden van de Beerze, de Reusel en de Rosep. Simulatie van de nutriëntenhuishouding. Rapport 306.2. DLO-Winand Staring Centrum, Wageningen.

Bolt, F.J.E. van der, P. Groenendijk, and H.P. Oosterom, 1996c. Nutriëntenbelasting van grond- en oppervlaktewater in de stroomgebieden van de Beerze, de Reusel en de Rosep. Effecten van bemestingsmaatregelen. Rapport 306.3. DLO Winand Staring Centrum, Wageningen.

Bruggenwert, M.G.M. and A. Kamphorst, 1982. Survey of experimental information on cation exchange in soil systems. In: G.H. Bolt (ed.) Soil chemistry B. Physico-chemical models. Developments in soil science 5B. Elsevier, Amsterdam. pp.141-203.

Davis, G.B. and R.B. Salama, 1996. Modelling point sources of groundwater contamination: a review and case study. In: Adriano, D.C. et al. (eds.), Contamination of groundwaters. pp. 111-140. Advances in Environmental Science. Science reviews.

De Wit, C.T., 1965. Photosynthesis of leaf canopies. Agric. Res. Reports 663: 1-57.

Drent, J., J.G. Kroes and P.E. Rijtema, 1988. Nitraatbelasting van het grondwater in het zuidoosten van Noord-Brabant. Rapport 26. Instituut voor Cultuurtechniek en Waterhuishouding, Wageningen.

Dijk van, W., J. Schröder, L. ten Holte and W.J.M. de Groot, 1995. Effecten van wintergewassen op verliezen en benutting van stikstof bij de teelt van snijmais, Verslag van onderzoek op ROC Aver-Heino tussen voorjaar 1991 en najaar 1994. Verslag nr. 201. PAGV, Lelystad.

Dijkstra J.P. and M.J.D. Hack-ten Broeke, 1995. Simulation of different management options within integrated arable farming affecting nitrate leaching. In: J.F.Th.Schoute, P.A.Finke, F.R.Veeneklaas, H.P.Wolfert (eds.), Scenario studies for the rural environment, proceedings of Symposium held in Wageningen, 12-15 Sept.1994. Published by Kluwer Academic Publishers as: Environment & Policy volume 5, Dordrecht.

Dijkstra, J.P., P. Groenendijk, J.J.T.I. Boesten and J. Roelsma, 1996. Emissies van bestrijdingsmiddelen en nutriënten in de bloembollenteelt. Modelonderzoek naar de uitspoeling van bestrijdingsmiddelen en nutriënten. Rapport 376.5. DLO Winand Staring Centrum, Wageningen.

Enfield, C.G., T. Phan, D.M. Walters and R. Ellis Jr., 1981. Kinetic model for phosphate transport and transformation in calcareous soils: I. Kinetics of transformation. Soil Sci. Soc. Am. J. 45: 1059-1064.

Ernst, L.F., 1973. De bepaling van de transporttijd van het grondwater bij stroming in de verzadigde zone. Nota 755. Instituut voor Waterhuishouding en Cultuurtechniek, Wageningen.

Ernst, L.F., 1978. Drainage of undulating sandy soils with high groundwater tables. I. A drainage formula based on a constant hydraulic head ratio. *Journal of Hydrology*, 39: 1-30.

Feddes, R.A., P.J. Kowalik and H. Zaradny, 1978. Simulation of field water use and crop yield. PUDOC, Simulation Monographs, Wageningen. 189 pp.

Fonck, H., 1986a. Stikstofconcentraties in bodemvocht en grondwater onder grasland op zandgrond in afhankelijkheid van runderdrijfmest- en kunstmestdosering (3e onderzoeksjaar 1982/1983). Nota 1707. Instituut voor Waterhuishouding en Cultuurtechniek, Wageningen.

Fonck, H., 1986c. Stikstofconcentraties in bodemvocht en grondwater onder grasland op zandgrond in afhankelijkheid van runderdrijfmest- en kunstmestdosering (5e onderzoeksjaar 1984/1985). Nota 1690. Instituut voor Waterhuishouding en Cultuurtechniek, Wageningen.

Fonck, H., 1982b. Stikstofconcentraties in bodemvocht en grondwater onder grasland op zandgrond in afhankelijkheid van runderdrijfmest- en kunstmestdosering (2e onderzoeksjaar 1981/1982). Nota 1407. Instituut voor Waterhuishouding en Cultuurtechniek, Wageningen.

Fonck, H., 1982a. Stikstofconcentraties in bodemvocht en grondwater onder grasland op zandgrond in afhankelijkheid van runderdrijfmest- en kunstmeststikstofdosering. Nota 1337. Instituut voor Waterhuishouding en Cultuurtechniek, Wageningen.

Fonck, H., 1986b. Stikstofconcentraties in bodemvocht en grondwater onder grasland op zandgrond in afhankelijkheid van runderdrijfmest- en kunstmestdosering (4e onderzoeksjaar 1983/1984). Nota 1685. Instituut voor Waterhuishouding en Cultuurtechniek, Wageningen.

Gliński, J. and W. Stepniewski, 1985. Soil aeration and its role for plants. CRC Press, Boca Raton.

Groenenberg, J.E., G.J. Reinds and A. Breeuwsma, 1996. Simulation of phosphate leaching in catchments with phosphate saturated soils in the Netherlands. Report 116. DLO Winand Staring Centre, Wageningen.

Groenenberg, J.E., C. van der Salm, E. Westein and P. Groenendijk, 1999. Gevoeligheidsanalyse en beperkte onzekerheidsanalyse van het model ANIMO. Rapport 446. DLO Winand Staring Centrum, Wageningen (in press).

Groenendijk, P., *in prep.* Modelling the influence of sorption and precipitation processes on the availability and leaching of chemical substances in soil. Report 76. DLO Winand Staring Centrum, Wageningen (in press).

Groenendijk, P. and F.J.E. van der Bolt, 1996. Nutriënten belasting van grond- en oppervlaktewater in de stroomgebieden van de Beerze, de Reusel en de Rosep. Effecten van waterhuishoudkundige ingrepen. Rapport 306.4. DLO Winand Staring Centrum, Wageningen.

Groot J.J.R., P. de Willigen and E.L.J. Verberne, 1990. Data-set. Workshop 5-6 June 1990. Nitrogen turnover in the soil crop ecosystem: modelling of biological transformations, transport of nitrogen and nitrogen use efficiency. Institute for Soil Fertility, Haren. 97 pp.

Hack-ten Broeke, M.J.D, and J.P. Dijkstra, 1995. Effects of different management options for grazing cattle within dairy farming. In: J.F.Th.Schoute, P.A.Finke, F.R.Veeneklaas, H.P.Wolfert (eds.), Scenario studies for the rural environment, proceedings of Symposium held in Wageningen, 12-15 Sept.1994. Published by Kluwer Academic Publishers as: Environment & Policy volume 5, Dordrecht.

Hansen, S., H.E. Jensen, N.E. Nielsen and H. Svendsen, 1990. Daisy; a soil plant system model. The Royal Veterinary and Agricultural University, Dept. agric. Sci., Section Soil and Water and Plant Nutrition. Copenhagen.

Hendriks, R.F.A., J.W.H. van der Kolk and H.P. Oosterom, 1994. Effecten van beheersmaatregelen op de nutriëntenconcentraties in het oppervlaktewater van peilgebied Bergambacht; Een modelstudie. Rapport 272. DLO-Staring Centrum, Wageningen.

Hoeks, J., D. Beker and R.J. Borst, 1979. Soil column experiments with leachate from a waste tip. II. Behaviour of leachate components in soil and groundwater. Nota 1131. Institute for Land and Water Management Research, Wageningen.

Jansen, E.J. 1991a. Results of simulations with ANIMO for several field situations, in Comm. Eur. Communities, Soil and Groundwater Research Report II: Nitrate in soils, pp. 269-280.

Jansen, E.J., 1991b. Nitrate leaching from non-grazed grassland on a sandy soil: experimental data for testing of simulation models. Report 26, DLO Winand Staring Centre, Wageningen.

Janssen, B.H., 1986. Een één-parametermodel voor de berekening van de decompositie van organisch materiaal. Vakblad voor biologen 76:297-304.

Kolenbrander, G.J., 1969. De bepaling van de waarde van verschillende soorten organische stof ten aanzien van hun effect op het humusgehalte bij bouwland. C 6988 Instituut voor Bodemvruchtbaarheid, Haren.

Kroes, J.G., 1988. ANIMO version 2.0, User's guide. Nota 1848. Institute for Land and Water Management Research, Wageningen.

- Kroes, J.G., C.W.J. Roest, P.E. Rijtema and L.J. Locht, 1990. De invloed van enige bemestingsscenario's op de afvoer van stikstof en fosfor naar het oppervlaktewater in Nederland. Rapport 55. DLO Winand Staring Centrum, Wageningen.
- Kroes, J.G., W.J.M. de Groot, J.Pankow and A. van den Toorn, 1996. Resultaten van onderzoek naar de kwantificering van de nitraatuitspoeling bij landbouwgronden. Rapport 440. DLO Winand Staring Centrum, Wageningen. 77pp.
- Kroes, J.G. and J. Roelsma, 1998. User's guide for the ANIMO version 3.5 nutrient leaching model. Technical Document 46. DLO-Winand Staring Centre, Wageningen.
- Kruijne, R. and O.F. Schoumans, 1995. Onderzoek naar maatregelen ter vermindering van de fosfaatuitspoeling uit landbouwgronden. Meting van de fosfaatuitspoeling uit fosfaatverzadigde zandgrond met en zonder een hydrologische maatregel. Rapport 374.1. DLO Winand Staring Centrum, Wageningen.
- Kruijne, R., J.G. Wesseling and O.F. Schoumans, 1996. Onderzoek naar maatregelen ter vermindering van de fosfaatuitspoeling uit landbouwgronden. Rapport 374.4. Ontwikkeling en toepassing van één- en tweedimensionale modellen. DLO Winand Staring Centrum, Wageningen.
- Mansell, R.S., H.M. Selim, P. Kanchanasut, J.M. Davidson and J.G.A. Fiskell, 1977. Experimental and simulated transport of phosphorus through sandy soils. *Water Resour. Res.* 13: 189-194.
- Noordwijk, P. van, P. de Willigen, P.A.I. Ehlert and W.J. Chardon, 1990. A simple model of P uptake by crops as a possible basis for P fertilizer recommendations. *Netherlands Journal of Agricultural Science* 38: 317-332.
- Ommen, H.C. van, 1985. The 'mixing-cell' concept applied to transport of reactive components in soil and groundwater. *Journal of Hydrology* 78: 201-213.
- Pignatello, J.J., 1989. Sorption dynamics of organic compounds in soils and sediments. In: B.L. Shawney & K. Brown (eds.). *Reaction and movement of organic chemicals in soils*, SSSA Spec. Publ. 22. SSSA and ASA, Madison, WI. pp 45-80.
- Querner, E.P. and P.J.T. van Bakel, 1989. Description of the regional groundwater flow model SIMGRO. Report 7. DLO Winand Staring Centre, Wageningen.
- Reiniger, P, J. Hutson, H. Jansen, J. Kragt, H. Piehler, M. Swarts and H. Vereecken, 1990. Evaluation and testing of models describing nitrogen transport in soil: a European project. In: *Transaction of 14th ICSS, Kyoto, Japan, August 12-18, 1990. Volume I: 56-61.*
- Roest, C.W.J. and P.E. Rijtema, 1983. Analysis of a model for transport, adsorption and decomposition of solutes in the soil. Nota 1404. Institute for Land and Water Management Research, Wageningen.

Rijtema, P.E. and J.G. Kroes, 1991. Some results of nitrogen simulations with the model ANIMO. *Fertilizer Research* 27: 189-198.

Rijtema, P.E., P. Groenendijk and J.G. Kroes, 1999. Environmental impact of land use in rural regions. The development, validation and application of model tools for management and policy analysis. Series on environmental science and management, vol. 1. Imperial College Press, London.

Schils, R.L.M., 1994. Nitrate losses from grazed grassland and grass/clover pasture on clay soil. In: *Meststoffen*: 78-84.

Schoumans, O.F., 1995. Beschrijving en validatie van de procesformulering van de abiotische fosfaatreacties in kalkloze zandgronden. Rapport 381. DLO Winand Staring Centrum, Wageningen.

Schoumans, O.F. and R. Kruijne, 1995. Onderzoek naar maatregelen ter vermindering van de fosfaatuitspoeling uit landbouwgronden. Eindrapport. Rapport 374. DLO Winand Staring Centre, Wageningen.

Schoumans, O.F. and P. Lepelaar, 1995. Emissies van bestrijdingsmiddelen en nutriënten in de bloembollenteelt. Procesbeschrijving van het gedrag van anorganisch fosfaat in kalkrijke zandgronden. Rapport 374. DLO Winand Staring Centrum, Wageningen.

Schröder, J., L. ten Holte, W. van Dijk, W.J.M. de Groot, W.A. de Boer and E.J. Jansen. 1992. Effecten van wintergewassen op de uitspoeling van stikstof bij de teelt van snijmaïs. Verslag nr. 148. PAGV, Lelystad.

Selim, H.M. and M.C. Amacher, 1988. A second-order kinetic approach for modeling solute retention and transport in soils. *Water Resour. Res.* 24: 2061-2075.

Steenvoorden, J.H.A.M., 1983. Nitraatbelasting van het grondwater in zandgebieden; denitrificatie in de ondergrond. Nota 1435. Instituut voor Cultuurtechniek en Waterhuishouding. Wageningen.

Steenvoorden, J.H.A.M., J.W.H. van der Kolk, R. Rondaij, O.F. Schoumans and R.W. de Waal, 1990. Bestrijdingsmiddelen en eutrofiërende stoffen in bodem en water. Verkenning van de problematiek in het landinrichtingsgebied Bergen-Schoorl. Rapport 78. DLO-Staring Centrum, Wageningen.

Todini, E., 1996. Evaluation of pollutant transport in rivers and coastal waters. In: P.E. Rijtema and V. Elias (eds.), *Regional Approaches to Water Pollution in the Environment*, 195-225. Kluwer Academic Publishers. The Netherlands.

Uunk, E.J.B., 1991. Eutrophication of surface waters and the contribution of agriculture. Proceedings no. 303, read before the Fertiliser Society in London on 11 April 1991. Greenhill House, Thorpe Wood Peterborough PE3 6GF. The Fertiliser Society.

Van Dam, J.C., J. Huygen, J.G. Wesseling, R.A. Feddes, P. Kabat, P.E.V. van Walsum, P. Groenendijk and C.A. van Diepen, 1997. Simulation of water flow, solute transport and plant growth in the Soil-Water-Atmosphere-Plant environment. Technical Document 45. DLO Winand Staring Centre, Wageningen.

Vanclouster, M., P. Viaene, J. Diels and K. Christiaens, 1994. WAVE, a mathematical model for simulating water and agrochemicals in the soil and the vadose environment. Reference & user's manual (release 2.0). Institute for land and water management, Leuven.

Van den Toorn, A., J. Pankow and O.M. Hooyer, 1994. Nitraatuitspoeling van gras-klaverpercelen op proefbedrijf de Waiboerhoeve in de Flevopolder. Veldonderzoek in de periode 1993-1994. Interne Mededeling 314. DLO Winand Staring Centrum, Wageningen.

Wadman, W.P. and C.M.J. Sluysmans, 1992. Mestinjectie op grasland. De betekenis voor de bodemvruchtbaarheid en risico's voor de nitraatuitspoeling; Ruurlo 1980-1984. Instituut voor Bodemvruchtbaarheid, Haren.

Wagenet, R.J. and J.L. Hutson, 1992. LEACHM, Leaching Estimation And Chemistry Model. A process-based model of water and solute movement, transformations, plant uptake and chemical reactions in the unsaturated zone. Version 3. Research Series No. 92-3. New York State College of Agriculture and Life Sciences, Cornell University, Ithaca, New York.

Walsum, P.E.V. van, 1988. SLAPP: een rekenprogramma voor het genereren van bemestingsscenario's (betreffende dierlijke mest and stikstofkunstmest) ten behoeve van milieu-effectonderzoek, versie 1.0. Nota 1920. Instituut voor Cultuurtechniek en Waterhuishouding, Wageningen.

Wösten, J.H.M., G.J. Veerman and J. Stolte, 1994. Waterretentie- en doorlatendheids-karakteristieken van boven- en ondergronden in Nederland: de Staringreeks. Vernieuwde uitgave 1994. DLO Winand Staring Centrum, Wageningen.

Zee, S.E.A.T.M. van der, 1988. Transport of reactive contaminants in heterogeneous soil systems. Ph.D. Thesis. Agricultural University, Wageningen. 283 pp.

Zee, S.E.A.T.M. van der and G.H. Bolt, 1991. Deterministic and stochastic modeling of reactive solute transport. *Journal of Contaminant Hydrology* 7: 75-93.

Zee, S.E.A.T.M. van der and W.H. van Riemsdijk, 1991. Model for the reaction kinetics of phosphate with oxides and soil. In: G.H. Bolt et al. (eds.). *Interactions at the Soil Colloid - Soil Solution Interface*, pp. 205-239.

Annex 1 List of symbols

a	assimilation efficiency (-)
A	constant in the numerical solution of the convection dispersion equation (d^{-1})
B	constant in the numerical solution of the convection dispersion equation ($kg\ m^{-3}\ d^{-1}$)
A_{ae}	aerated area (m^2)
A_0	annual temperature amplitude ($^{\circ}C$)
C_h	differential heat capacity of the soil ($J\ m^{-3}\ ^{\circ}C^{-1}$)
c_{eq}	phosphate liquid concentration equilibrium (buffer concentration) ($kg\ m^{-3}$)
c_w	dissolved oxygen concentration in the saturated soil phase ($kg\ m^{-3}$)
c_{we}	dissolved oxygen concentration at equilibrium with oxygen in soil gas phase ($kg\ m^{-3}$)
c^*	content of a substance ($kg\ m^{-3}$)
c_{eq}^*	hypothetical equilibrium concentration for computation of phosphate distribution over rate dependent sorption sites ($kg\ m^{-3}$)
c_0	liquid concentration in the surficial reservoir ($kg\ m^{-3}$)
c_1	liquid concentration in the first soil layer ($kg\ m^{-3}$)
c_p	liquid concentration in precipitation water ($kg\ m^{-3}$)
c_{pt}	liquid concentration in plant tissues ($kg\ m^{-3}$)
$c_{opt,1}; c_{opt,2}$	optimal concentrations in the transpiration flux ($kg\ m^{-3}$)
c_{OM}	liquid concentration of dissolved organic matter ($kg\ m^{-3}$)
c_{ON}	liquid concentration of dissolved organic nitrogen ($kg\ m^{-3}$)
c_{NH4}	liquid concentration of NH_4-N ($kg\ m^{-3}$)
c_{NO3}	liquid concentration of NO_3-N ($kg\ m^{-3}$)
c_{OP}	liquid concentration of dissolved organic phosphorus ($kg\ m^{-3}$)
c_{PO4}	liquid concentration of PO_4-P ($kg\ m^{-3}$)
c_{i-1}	liquid concentration in an adjacent upstream soil layer ($kg\ m^{-3}$)
$i-1$	time averaged liquid concentration in an adjacent upstream soil layer ($kg\ m^{-3}$)
c_i	liquid concentration in soil layer i ($kg\ m^{-3}$)
i	time averaged liquid concentration in soil layer i ($kg\ m^{-3}$)
c_g	oxygen concentration in soil gas phase ($kg\ m^{-3}$)
C/N	carbon nitrogen weight ratio of organic compounds (-)
C/P	carbon phosphorus weight ratio of organic compounds (-)
D_g	oxygen diffusion coefficient in the soil gas phase ($m^2\ d^{-1}$)
D_0	oxygen diffusion coefficient in free atmosphere ($m^2\ d^{-1}$)
D_w	oxygen diffusion coefficient in water ($m^2\ d^{-1}$)
D_m	damping depth of heat transport in soil ($m^2\ d^{-1}$)
D_n	coefficient expressing the numerical dispersion ($m^2\ d^{-1}$)
D_h	heat diffusivity ($m^2\ d^{-1}$)
D_{dd}	apparent dispersion coefficient ($m^2\ d^{-1}$)
D_{dis}	natural dispersion coefficient ($m^2\ d^{-1}$)
D_{df}	diffusion coefficient ($m^2\ d^{-1}$)
E_i	error propagation factor according to Von Neumann-method (-)
EX	content of root exudates ($kg\ m^{-3}$)
$E_{t, re}$	real transpiration ($m\ d^{-1}$)
$E_{t, pot}$	potential transpiration ($m\ d^{-1}$)
f_{ae}	multiplication factor for the influence of limited soil aeration (-)
f_T	multiplication factor for the influence of temperature (-)
f_b	multiplication factor for the influence of drought stress (-)
f_{pH}	multiplication factor for the influence of pH (-)
f_0	fraction of the runoff that passes the surficial reservoir (-)
f_1	fraction of the runoff that passes the first model compartment (-)
$f_{i,fn}$	weight fraction of organic material i attributed to class fn (-)
k_{fn}	first order rate coefficient for decomposition of organic class fn (-)
$f_{i,fn}^*$	weight fraction of dissolved organic matter of applied organic material i attributed to class fn (-)
f_i^O	organic fraction of the applied material i (-)
f_h	fraction of fresh organic matter which is not subject to solubilization (-)

f_{netero}	ratio between organic transformation rate when only nitrate-oxygen is available and the transformation rate under fully aerated circumstances (-)
f_{NO3}	weight fraction of NO_3 -N of the applied material (-)
$f_{N,fn}$	nitrogen weight fraction of organic material assigned to class fn (-)
f_{NH4}	weight fraction of NH_4 -N of the applied material (-)
f_v	volatilization fraction of ammonium (-)
$f_{N,r,min}$	minimum nitrogen weight fraction of grass roots dry matter (-)
$f_{N,s,min}$	minimum nitrogen weight fraction of grass shoots dry matter (-)
$f_{N,s,max}$	maximum nitrogen weight fraction of grass shoots dry matter (-)
$f_{pl,NO3}$	nitrate-N weight fraction of grass shoots dry matter (-)
$f_{pl,Ntot}$	total-N weight fraction of grass shoots dry matter (-)
f_{NP}	reduction factor for limited dry matter production due to lack of nutrients (-)
f_{cl}	cloudiness factor (-)
f_{sh}	shoot fraction (-)
f_{ds}	dry matter weight fraction of biomass (-)
$f_{gr,loss}$	fraction of grazing losses (-)
$f_{ha,loss}$	fraction of harvest losses (-)
$f_{def,max}$	nutrient stress tolerance factor (fraction of cumulative uptake below which nutrient shortage results in unrecoverable crop damage) (-)
$f_n()$	apparent adsorption isotherm, used in the non-linear kinetic sorption formulation of phosphates ($kg\ kg^{-1}$)
fr_N	nitrogen weight fraction of dry matter of productive parts of arable crops (-)
fr_P	phosphorus weight fraction of dry matter of productive parts of arable crops (-)
$f_{P,fn}$	phosphorus weight fraction of organic material assigned to class fn (-)
$f_{P,s,min}$	minimum phosphorus weight fraction of grass shoots dry matter (-)
$f_{P,r,min}$	minimum phosphorus weight fraction of grass roots dry matter (-)
h_d	drainage level (m)
h	height of the phreatic groundwater level at half of the drain distance (m)
$h_{d,i}$	height of the water level in drain system i (m)
h_{gw}	phreatic groundwater level (m)
H	thickness of the homogeneous soil layer (m)
HU	content of organic material present in humus/biomass pool ($kg\ m^{-3}$)
i	counter (-)
$J_{s,r}$	runoff solute flux ($kg\ m^{-2}\ d^{-1}$)
J_s	vertical solute flux ($kg\ m^{-2}\ d^{-1}$)
$J_{s,ON}$	flux of dissolved organic nitrogen ($kg\ m^{-2}\ d^{-1}$)
$J_{s,NH4}$	flux of ammonium-N in the liquid phase ($kg\ m^{-2}\ d^{-1}$)
$J_{s,NO3}$	flux of nitrate ($kg\ m^{-2}\ d^{-1}$)
$J_{s,OP}$	flux of dissolved organic phosphorus ($kg\ m^{-2}\ d^{-1}$)
$J_{s,PO4}$	flux of phosphate-P in the liquid phase ($kg\ m^{-2}\ d^{-1}$)
J_w	water flux ($m\ d^{-1}$)
$(kH)_i$	transmissivity ($m^2\ d^{-1}$)
k	counter (-)
k_{ref}	reference value of first order rate constants (d^{-1})
K_L	Langmuir sorption coefficient ($m^3\ kg^{-1}$)
K_F	Freundlich sorption coefficient (...)
$K_{d,i}^{ap}$	apparent linear sorption coefficient ($m^3\ kg^{-1}$)
k_{ads}	first order rate constant of adsorption (d^{-1})
k_{des}	first order rate constant of desorption (d^{-1})
k_d	drainage rate ($m^3\ m^{-3}\ d^{-1}$)
k_s	first order rate constant of decomposition of dissolved organic compounds (d^{-1})
k_{ex}	first order rate constant of decomposition of exudates (d^{-1})
K_d	linear adsorption coefficient ($m^3\ kg^{-1}$)
k_1	first order rate coefficient of decomposition (d^{-1})
k_0	zero order production term ($kg\ m^{-3}\ d^{-1}$)
$k_{gr,dif}$	rate constant accounting for nitrogen diffusion to grass roots (d^{-1})
$k_{gr,death}$	first order rate constant for death rate of grass roots (d^{-1})
k_{nif}	first order rate constant for nitrification (d^{-1})
L_i	drain distance (m)

M_{st}	release of material from the surficial reservoir during the time increment (kg m^{-2})
M	dose of material application (kg m^{-2})
N_{lse}	number of live stock units (-)
N_{por}	number of soil pores in a unit volume (-)
N_{dr}	total number of drain systems present (-)
N_r	number of compartments in the root zone (-)
$M_i(t)$	dry matter weight of material i (kg m^{-2})
$Om_{fn}(t)$	dry matter content of organic class fn (kg m^{-3})
$ON_{fn}(t)$	dry matter content of organic nitrogen assigned to class fn (kg m^{-3})
$OP_{fn}(t)$	dry matter content of organic phosphorus assigned to class fn (kg m^{-3})
Δp	pressure difference between air phase and water phase in a soil pore (Pa)
P_1, P_2	parameters of the function describing the diffusion coefficient as a function of volumetric gas content (-)
P_{tot}	total phosphor content (kg m^{-3})
$P_{st}(t)$	standard dry matter accumulation (kg m^{-3})
q_{neu}	net precipitation excess ($\text{m}^3 \text{m}^{-2} \text{d}^{-1}$)
q	water flux ($\text{m}^3 \text{m}^{-2} \text{d}^{-1}$)
q_p	precipitation ($\text{m}^3 \text{m}^{-2} \text{d}^{-1}$)
q_t	transpiration ($\text{m}^3 \text{m}^{-2} \text{d}^{-1}$)
$q_{e,s}$	soil evaporation ($\text{m}^3 \text{m}^{-2} \text{d}^{-1}$)
q_r	surface runoff ($\text{m}^3 \text{m}^{-2} \text{d}^{-1}$)
q_v	vertical percolation ($\text{m}^3 \text{m}^{-2} \text{d}^{-1}$)
q_l	leaching ($\text{m}^3 \text{m}^{-2} \text{d}^{-1}$)
$q_{d,1}, q_{d,2}, q_{d,3}$	drainage flux to first, second and third order drainage system ($\text{m}^3 \text{m}^{-2} \text{d}^{-1}$)
q_z	waterflux in the z -direction ($\text{m}^3 \text{m}^{-2} \text{d}^{-1}$)
q_x	waterflux in the x -direction ($\text{m}^3 \text{m}^{-2} \text{d}^{-1}$)
$q_{d,r}$	regional drainage flux ($\text{m}^3 \text{m}^{-2} \text{d}^{-1}$)
$q_{d,t}$	drainage water flux ($\text{m}^3 \text{m}^{-2} \text{d}^{-1}$)
q_i	vertical water flux in soil compartment ($\text{m}^3 \text{m}^{-2} \text{d}^{-1}$)
q_{i-2}	water flux, inflow from adjacent upstream soil compartment ($\text{m}^3 \text{m}^{-2} \text{d}^{-1}$)
q_{i+2}	water flux, outflow to adjacent downstream compartment ($\text{m}^3 \text{m}^{-2} \text{d}^{-1}$)
$\Delta Q_{s,gr}$	accumulated dry matter grass shoots in the time interval (kg m^{-2})
$\Delta Q_{r,gr}$	accumulated dry matter grass roots in the time interval (kg m^{-2})
Σq_{tr}	expected cumulative transpiration flow within the time span (m)
$Q_s(t)$	dry matter accumulation of grass shoots (kg m^{-2})
$Q_{s,ref}$	reference value of dry matter accumulation, related to light absorption coefficient κ (kg m^{-2})
$Q_r(t)$	dry matter accumulation of grass roots (kg m^{-2})
r_{por}	average radius of an air filled soil pore (m)
r_{aer}	radius of the aerobic zone (m)
R_{gas}	gas constant ($\text{J mol}^{-1} \text{°K}$)
R_p	production rate ($\text{kg m}^{-3} \text{d}^{-1}$)
R_d	decomposition rate ($\text{kg m}^{-3} \text{d}^{-1}$)
R_u	uptake rate ($\text{kg m}^{-3} \text{d}^{-1}$)
R_x	lateral outflow rate ($\text{kg m}^{-3} \text{d}^{-1}$)
$RO(t_0 + \Delta t)$	dry matter quantity of crop roots at the end of a time interval (kg m^{-2})
$RO(t_0)$	dry matter quantity of crop roots at the beginning of a time interval (kg m^{-2})
t_{res}	residence time (d)
t_p	planting time (day number) (-)
t_c	transition between both growing periods (day number) (-)
t_h	harvesting date (day number) (-)
Δt	time increment (d)
T	temperature ($^{\circ}\text{C}$)
T_{ref}	reference temperature ($^{\circ}\text{C}$)
T_a	annual average temperature ($^{\circ}\text{C}$)
u_{tr}	transpiration rate (d^{-1})
$U(t)$	cumulative nutrient uptake (kg m^{-2})
$U^*_j; U^*_2$	expected optimal cumulative uptake within the time span (kg m^{-2})
ΔV	change in areic water volume during a time increment ($\text{m}^3 \text{m}^{-2}$)

W	sink function for uptake by grazing ($\text{kg m}^{-2} \text{d}^{-1}$)
x	distance relative to the water divide between 2 drains (m)
X_e	quantity of substance sorbed to equilibrium sorption sites (kg kg^{-1})
X_n	quantity of substance sorbed to non-equilibrium sorption sites (kg kg^{-1})
X_p	precipitated quantity of a substance (kg kg^{-1})
$X_{e,NH4}$	quantity of ammonium-N sorbed to equilibrium sorption sites (kg kg^{-1})
$X_{e,PO4}$	quantity of phosphate-P sorbed to equilibrium sorption sites (kg kg^{-1})
$X_{n,PO4}$	quantity of phosphate-P sorbed to non-equilibrium sorption sites (kg kg^{-1})
$X_{p,PO4}$	precipitated quantity of a substance (kg kg^{-1})
$X_{e,max}$	maximum sorption capacity of equilibrium sorption sites (kg kg^{-1})
Δz	thickness of soil compartment (m)
z	depth below the soil surface (m)
Z_{surf}	thickness of surficial material reservoir (m)
α_B	Bunsen's coefficient of solubility ($\text{m}^3 \text{m}^{-3}$)
β	frequency of the error (m^{-1})
γ	number of the timestep since the beginning of the simulation (-)
δ	layer number (-)
ϵ	porosity ($\text{m}^3 \text{m}^{-3}$)
θ	actual volumetric moisture fraction (-)
θ_{sat}	volumetric moisture fraction at saturation (-)
θ_g	volumetric soil air content (-)
$\Delta\theta$	soil moisture difference between actual value and value at air entry point (-)
ϕ	change of volumetric moisture content (-)
Φ	phase shift (rad)
Φ_{NO3}	nitrate availability (kg m^{-2})
Φ_{NH4}	ammonium availability (kg m^{-2})
Φ_{PO4}	phosphate availability for plant uptake (kg m^{-2})
Θ	amplification factor (-)
χ	efficiency factor for dry matter production of grass shoots (-)
$\xi_1(t), \xi_2(t)$	time dependent functions for computation of the resulting liquid concentration used in the numerical solution of the convection dispersion equation (-), (d)
$\zeta_1(t); \zeta_2(t)$	time dependent functions for computation of the average liquid concentration during the time interval used in the numerical solution of the CDE (-), (d)
κ	light absorption coefficient (-)
λ_h	thermal heat conductivity ($\text{J m}^{-1} \text{d}^{-1} \text{°C}^{-1}$)
λ_r	tortuosity factor for diffusion in saturated soil particles ($m_w m_s^{-1}$)
λ_v	factor accounting for the tortuosity of air-filled pores (m m^{-1})
μ	molar activation energy (J mol^{-1})
ρ_d	dry bulk density (kg m^{-3})
η	surface tension of water (N m^{-1})
σ	selectivity coefficient for plant uptake (-)
σ_{NO3}	selectivity factor for nitrate uptake (-)
σ_{NH4}	selectivity factor for ammonium uptake (-)
$\sigma_{N,max}$	maximum value of selectivity factors for nitrogen uptake (-)
σ_P	selectivity factor for phosphate-P uptake (-)
$\sigma_{P,max}$	maximum value of selectivity factor for phosphate-P uptake (-)
τ	infinite small time increment (d)
ω	frequency of temperature wave (d^{-1})
Ω_N	uptake requirement (kg m^{-2})
$\Omega_{N,max}$	maximum uptake requirement (kg m^{-2})
$\Omega_{N,mean}$	mean uptake requirement (kg m^{-2})
$\Omega_{N,def}$	nitrogen demand to recover from nitrogen deficiency (kg m^{-2})
$\Omega_{N,gr}$	nitrogen demand for growth and maintenance (kg m^{-2})
$\Omega_{N,lux}$	nitrogen demand for luxurious consumption and accumulation (kg m^{-2})
$\Omega_{N,def,max}$	maximum value of nitrogen uptake deficit (kg m^{-2})
Ω_P	phosphate uptake requirement (kg m^{-2})
$\Omega_{P,gr}$	phosphate uptake requirement for plant growth (kg m^{-2})
$\Omega_{P,def}$	phosphorus demand to recover from phosphorus deficiency (kg m^{-2})

$\Omega_{p,gr}$	phosphorus demand for growth and maintenance (kg m^{-2})
$\Omega_{p,lux}$	phosphorus demand for luxurious consumption and accumulation (kg m^{-2})
$\Omega_{p,def,max}$	maximum value of phosphorus uptake deficit (kg m^{-2})
Ω_{ox}	demand for atmospheric oxygen ($\text{kg m}^{-3} \text{d}^{-1}$)
$\Psi(x,z)$	stream function Ψ ($\text{m}^3 \text{m}^{-1} \text{d}^{-1}$)
ψ	soil moisture suction (cm)
ψ_a	soil moisture suction at air entry point (cm)
Y_d	drainage resistance of an open field drain or a tile drainage system (d)
Y_i	drainage resistance of drainage system i (d)

Annex 2 The coefficients $\xi_1(t)$ and $\xi_2(t)$, $\zeta_1(t)$ and $\zeta_2(t)$ in the equations to compute the resulting and the average concentration (Par. 2.2.3)

If $\varphi \neq 0$ and $A \neq 0$:

$$\xi_1(c,t) = \left(\frac{\theta(t_0) + \rho_d \bar{k}_a(c) + \varphi t}{\theta(t_0) + \rho_d \bar{k}_a(c)} \right)^{-\frac{A}{\varphi}} \quad \text{and} \quad \xi_2(c,t) = \frac{1 - \xi_1(c,t)}{A} \quad (\text{A1})$$

If $\varphi \neq 0$ and $A \neq 0$ and $\varphi \neq A$:

$$\zeta_1(c,t) = \frac{\theta(t_0) + \rho_d \bar{k}_a(c)}{t(\varphi - A)} \left[\left(\frac{\theta(t_0) + \rho_d \bar{k}_a(c) + \varphi t}{\theta(t_0) + \rho_d \bar{k}_a(c)} \right)^{\frac{\varphi - A}{\varphi}} - 1 \right] \quad (\text{A2})$$

$$\text{and} \quad \zeta_2(c,t) = \frac{1 - \zeta_1(c,t)}{A}$$

If $\varphi \neq 0$ and $A \neq 0$ and $\varphi = A$:

$$\zeta_1(c,t) = \frac{\theta(t_0) + \rho_d \bar{k}_a(c)}{\varphi t} \ln \left(\frac{\theta(t_0) + \rho_d \bar{k}_a(c) + \varphi t}{\theta(t_0) + \rho_d \bar{k}_a(c)} \right) \quad (\text{A3})$$

$$\text{and} \quad \zeta_2(c,t) = \frac{1 - \zeta_1(c,t)}{A}$$

If $\varphi = 0$ and $A \neq 0$:

$$\xi_1(c,t) = e^{-\frac{A}{\theta(t_0) + \rho_d \bar{k}_a(c)} t} \quad \text{and} \quad \xi_2(c,t) = \frac{1 - \xi_1(c,t)}{A} \quad (\text{A4})$$

$$\zeta_1(c,t) = \frac{\theta(t_0) + \rho_d \bar{k}_a(c)}{A t} \left(1 - e^{-\frac{A}{\theta(t_0) + \rho_d \bar{k}_a(c)} t} \right) \quad (\text{A5})$$

$$\text{and} \quad \zeta_2(c,t) = \frac{1 - \zeta_1(c,t)}{A}$$

If $\varphi \neq 0$ and $A = 0$:

$$\xi_1(c,t) = 1 \quad \text{and} \quad \xi_2(c,t) = \frac{1}{\varphi} \ln \left(\frac{\theta(t_0) + \rho_d \bar{k}_a(c) + \varphi t}{\theta(t_0) + \rho_d \bar{k}_a(c)} \right) \quad (\text{A6})$$

$$\zeta_1(c,t) = 1 \quad \text{and}$$

$$\zeta_2(c,t) = \frac{1}{\varphi} \left[\left(\frac{\theta(t_0) + \rho_d \bar{k}_a(c) + \varphi t}{\varphi t} \right) \ln \left(\frac{\theta(t_0) + \rho_d \bar{k}_a(c) + \varphi t}{\theta(t_0) + \rho_d \bar{k}_a(c)} \right) - 1 \right] \quad (\text{A7})$$

If $\varphi = 0$ and $A = 0$:

$$\xi_1(c,t) = 1 \quad \text{and} \quad \xi_2(c,t) = \frac{1}{\theta(t_0) + \rho_d \bar{k}_a(c)} t \quad (\text{A8})$$

$$\zeta_1(c,t) = 1 \quad \text{and} \quad \zeta_2(c,t) = \frac{1}{2(\theta(t_0) + \rho_d \bar{k}_a(c))} t \quad (\text{A9})$$